Alkimos Hydrodynamic Modelling

Calibration Report

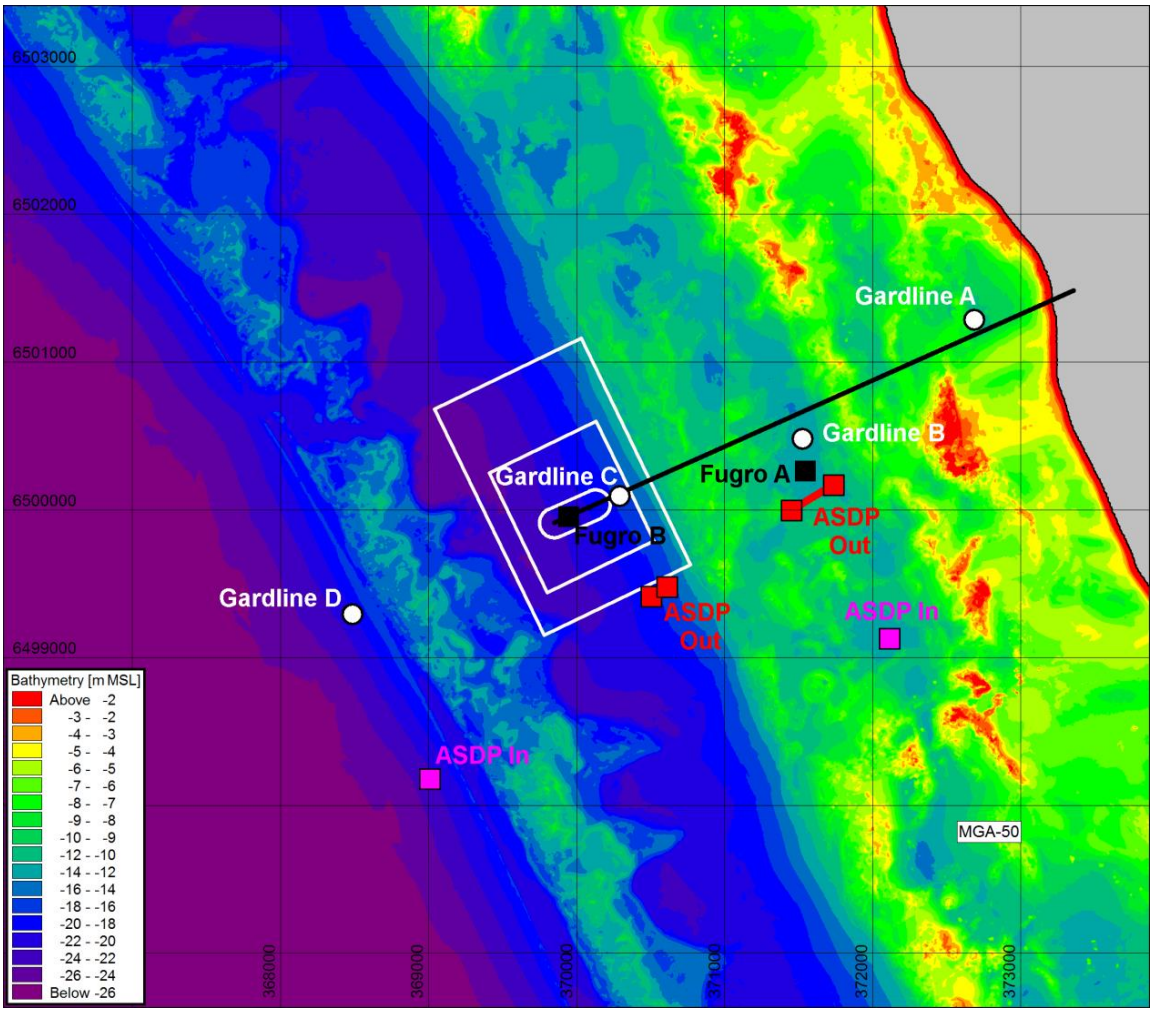

Water Corporation

Calibration Report

January 2019

This report has been prepared under the DHI Business Management System certified by Bureau Veritas to comply with ISO 9001 (Quality Management)

Alkimos Hydrodynamic Modelling

Calibration Report

Prepared for	Water Corporation
Represented by	Bree Atkinson

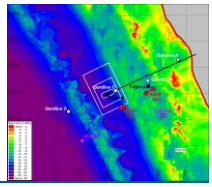

Alkimos Reef and Infrastructure

Project manager	Jason Antenucci
Author	Andrew Driscoll
Quality supervisor	Jason Antenucci

Project number	43802755
Approval date	16 January 2019
Revision	Rev. C
Classification	Confidential

DHI Water & Environment Pty Ltd • Suite 146, Equus Centre • 580 Hay Street • 6000 Perth • Australia
Telephone: +61 8 9225 4622 • dhi@dhigroup.com

CONTENTS

FIGURES

TABLES

GLOSSARY

2DV	Two Dimensional, in Vertical plane
ABSLMP	Australian Baseline Sea Level Monitoring Project
ADCP	Acoustic Doppler Current Profiler (TRDI Branded wave/current meter)
AHD	Australian Height Datum
AHS	Australian Hydrographic Service
ANTT	Australian National Tide Tables
ASDP	Alkimos Seawater Desalination Plant
AWAC	Acoustic Wave and Current Profiler (Nortek branded wave/current meter)
BoM	Australian Bureau of Meteorology
CD	Chart Datum
CFSR	Climate Forecast System Reanalysis (NOAA gridded met fields)
C-MAP	Commercial package of digital navigation charting by Jeppesen
CTD	Conductivity Temperature Depth instrument
DoT	Western Australia Dept. of Transport
DTU	Danish Technical University
GEBCO	GEneralized Bathmetric Chart of the Oceans
HYCOM	Hybrid Coordinate Ocean Model
IoA	Index of Agreement
IMOS	Integrated Marine Observing System
LAT	Lowest Astronomical Tide
LIDAR	Light Detection and Ranging
MAE	Mean Absolute Error
MSL	Mean Sea Level
NOAA	US National Oceanographic and Atmospheric Administration
PRP	(Alkimos) Peer Review Panel
RMSE	Root Mean Square Error
UNESCO	United Nations Educational, Scientific and Cultural Organization
WP	WorleyParsons
WWTP	(Alkimos) Wastewater Treatment Plant

1 Introduction

1.1 Background

DHI Water and Environment (DHI) has been contracted by the Water Corporation to perform a numerical modelling assessment of hydrodynamics, plume transport and dilution for the discharge of brine effluent from the proposed Alkimos Seawater Desalination Plant (ASDP). The intake and outfall systems of the ASDP will be located amidst or offshore of a highly complex reef system which is exposed to energetic swell waves for much of the year.

The proposed ASDP will be co-located with the existing Alkimos Wastewater Treatment Plant, which was commissioned in 2010 and discharges buoyant greywater effluent from a linear offshore diffuser. A previous modelling study (WP, 2005) was prepared in support of submittals for regulatory approval of the WWTP. The marine monitoring program has found the WWTP plant to be compliant to date in relation to the marine discharge and there is no indication of any adverse marine impacts.

The minimisation of potential impacts to the reef system is a priority for the development of the ASDP, as is the maintenance of the level of dilution which has already been permitted for the existing WWTP.

The present report documents the setup and calibration of the hydrodynamic and wave models established to describe the dynamics of the ASDP and WWTP effluent plumes. The models reported here address ambient hydrodynamics prior to the introduction of wastewater plumes.

1.2 Model Updates of Note

A number of notable updates have been performed to the model systems subsequent to that reported in Rev A of this report, both in response to comments from the Peer Review Panel (PRP) and through DHI initiated improvements. Specifically:

- The models now incorporates bathymetric LIDAR data from the 2016 DoT acquisition campaign. Rev. A mis-cited the 2016 data, but that applied in the model originated from an earlier 2009 DoT LIDAR campaign.
- The innermost region of 50m nominal mesh resolution has been expanded significantly.
- The Local 3D Model now incorporates spatially and temporally variable ambient salinity and temperature, as well as incorporating full heat exchange and associated evaporation. The calibration of salinity and temperature response within the Local 3D Model is limited by data inavailability. Salinity and temperature response within the Local 3D Model is effectively uncalibrated.
- The Local 3D Model Flather boundaries, previously prescribed as depth-integrated lines of (water level, u and v) based upon extracted values from the Regional 3D Model, are now applied as lines of water level in combination with 2DV fields of (u and v).

- Local 3D Model wind forcing, previously provided via CFSR fields for consistency with the Regional 3D Model, is now applied using measured winds from Ocean Reef.

- The Rev. A model applied wave forcing (via radiation stresses) when waves at the WWTP outfall exceeded a critical value. The models reported here include a comparative parallel application of the above approach along with an application where wave forcing is fully omitted. The model arrangement excluding wave forcings is ultimately recommended for the screening of design options, though it is also recommended to consider confirming the final candidate with waves included if the candidate includes intakes or outfalls located inshore of the existing WWTP.

- Rev. A of this report featured a primary calibration period within Apr-Jun 2017, with a validation period of May-Jun 2005 (the latter utilizing the calibration data and period applied in WP (2005)). In order to incorporate seasonal variability, the following revised calibration / validation periods are applied:

    - Autumn 2017 (Primary Calibration): 16 Apr – 15 May 2017
    - Autumn 2005 Validation: 30 Apr – 28 May 2005
    - Winter 2017 Validation: 23 Jun – 22 Jul 2017
    - Summer 2017 Validation: 17 Nov – 16 Dec 2017

  where it is noted that the above 30-day periods from 2017 are also applied for seasonal design screening, while the 2005 period aligns with the calibration period applied in WP (2005).

The net result of the above updates is a modest improvement in model skill, as well as an expanded validation exercise relative to that reported in Rev. A of this document.

1.3 Report Structure

The remainder of the report is structured as follows:

- Section 2 describes a scope overview and a high level site characterisation
- Section 3 describes the available field measurements as a whole in terms of moorings, originators of various datasets, and general data handling.
- Section 4 presents the construction and calibration of the Regional 2D/3D Hydrodynamic Model
- Section 5 describes the construction and calibration of the Local Wave and Local 3D Hydrodynamic Model
- Section 6 provides a list of references cited.

1.4 Conventions

Unless otherwise stated, the following conventions prevail within the report:

- The local models have been constructed and reported using horizontal positioning in the MGA-50 projection using the GDA94 coordinate datum.

- The regional models described were necessarily constructed in latitude/longitude and are presented as such.
- The models have been constructed using a vertical datum of mean sea level (MSL), and this is used throughout except where otherwise noted.
- Wind and wave directions are reported as "from", while current directions are "to".
- Except where noted, time references denote Greenwich Mean Time (GMT).

2 Project Overview

2.1 High-Level Site Characterisation

The study area features weak, dominantly diurnal tidal forcing with a mean daily range on the order of 0.7m. Wind driven processes predominate, particular in summer due to land-sea breeze cycles commonly reaching speeds greater than 15 m/s. Wind stresses are at their lowest typically in late Autumn (Apr/May). Median depth-averaged current speeds range from 9.9 cm/s in 21m water depth immediately offshore of the outer reef to 7.8 cm/s at the existing WWTP outfall to 4.3 cm/s at 10m depth within the inshore reef.

The broader-scale circulation in the region is dominated by the Leeuwin Current, a warm boundary current flowing southwards along the edge of the continental shelf. Inshore of the Leeuwin Current, the Capes Current flows northward as a result of upwelling and northward wind stresses, and is thus strongest in spring and summer months. Owing to its location on the inner coastal shelf, as well as proximity to the Leewin Current and the inshore Capes Current, nontidal residual flows contribute to the current energy on the shelf near the Alkimos site. Continental shelf waves induce long-period modulations in water level which can reach the same order of magnitude as the tide. Further details can be found in Gallop et al (2012), Mihanovic et al (2016), and references therein.

The area is exposed to persistently high swell conditions, despite some sheltering to swell originating in the Southern Ocean from Rottnest Island. Annual mean wave conditions approaching the outer reef have been measured at a significant wave height of Hs=1.8m with an associated peak period of Tp=12.2s.

Offshore dominant mechanisms are a combination of meteorological and oceanographic (non-tidal) flows. Over the inner reef, wave-driven currents become important when waves are large. Due to the complexity of the reef structure, wave effects on mean flows tend to be manifested primarily as shoreward-directed flow over shallow areas and offshore-directed return flows in locally deeper areas.

2.2 Overview of Modelling Approach

The overall objective is to develop a local validated model that will support the design process, environmental approvals, and stakeholder engagement. The modelling uses a downscaled model ecosystem approach to meet these objectives, in the manner described in Figure 2-1.

The top tier models shown in Figure 2-1 are global in scale. DHI's Global Wave Model is a mature application of the MIKE21 SW Spectral Wave modelling system which is run in both operational and hindcast modes in support of projects worldwide. The output of the DTU-Space Global Tidal Model (Cheng and Andersen, 2010), allows for the generation of tidal level boundary data at a resolution of 0.125°, and is used to provide the tidal forcing component of the Regional Hydrodynamic Model. HYCOM (HYCOM, 2016) is a widely used 3D global oceanographic model which is utilized to supply residual boundary inputs (nontidal water level and velocities over the vertical plane) as well as the vertical distribution of salinity and temperature for the DHI Regional Hydrodynamic Model.

The middle tier models shown in Figure 2-1 are regional in scale, and are project-tailored derivatives of versions originally developed by DHI for the Australian Maritime Safety Authority. These models are applied purely for the purpose of generating boundary data to force the Local Wave Model and Local Hydrodynamic Model.

The bottom tier models shown in Figure 2-1 were developed specifically for this project, with the Local 3D Hydrodynamic Model being the vehicle applied for the ASDP and WWTP plume assessments. The Local Wave Model is required in order to supply the direct forcing by waves onto the mean flow (via radiation stresses) as well as providing input for the increased effective roughness acting on the mean flow over the reef as a result of wave action.

The Global and Regional Wave Model boxes are shaded gray, and connected to the the Local Wave Model via a dotted line, as the calibration simulations were ultimately performed using a version of the Local Wave Model forced directly from measurements. The reasoning behind this decision is discussed in Section 5.5.1.

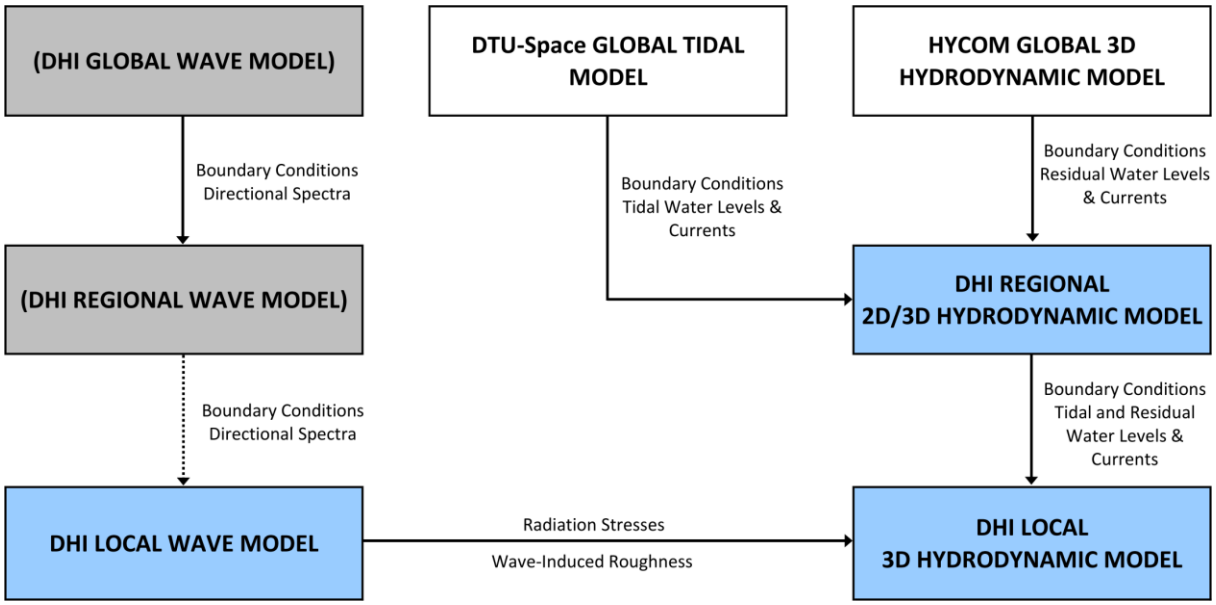

Figure 2-1 Flowchart of models applied in the present work.

3 Site Characterisation and Field Data

3.1 Introduction

DHI has carried out a review and analysis of field data provided by Water Corporation and third party suppliers. This data includes measurements of ambient environmental conditions as well as hindcasts from other (mostly regional/global) modelling products.

A site plan indicating key infrastructure and mooring locations is provided in Figure 3-1. A summary of the ambient environmental datasets measured in the vicinity of the ASDP/WWTP site using fixed instrumentation is provided Table 3-1.

Section 3.2 describes the data sources in terms of moorings, originators of various datasets, and general data handling details.

Sections 3.3 through 3.6 present ambient environmental data by category.

3.2 Data Sources

The data applied in the present work originates from a range of sources. Those sources are, in brief:

Water Corporation
The proposed site development details have originated from Water Corporation. The majority of monitoring information has originated from third party contractors to Water Corporation. Various minor inputs and details have been provided / clarified by Water Corporation directly, and are noted where appropriate in the text.

BMT
BMT are a standing supplier of environmental services to Water Corporation, and have facilitated many of the data transfers which have occurred in support of the present work. BMT have also specifically provided a draft version of a reef classification map generated via groundtruthed satellite imagery (BMT, 2018) which underpins the characteristic roughness regions applied to describe the Alkimos reef within the wave and hydrodynamic models. BMT have also provided three years of summer synoptic CTD monitoring at the site. While this latter effort primarily targets compliance of the existing WWTP, it also provides valuable baseline data on water column character away from the WWTP oufall.

Fugro
Fugro was the originator of the monitoring campaign supporting the 2005 modelling effort for the permitting of the WWTP (WP, 2005); (Fugro, 2005). This included instrumentation of two fixed moorings (Fugro A and B) as described in Table 3-1 and Figure 3-1. The Fugro datasets were provided as post-processed ASCII files which have been used despite retaining a note of “preliminary” status in the file headers. Several items which would have been recorded by some of the instruments (water temperature and pressure) were not provided in the final dataset. Wave data measured at Fugro B is available only in terms of bulk spectral parameters, without a sea/swell split.

Gardline
Gardline was responsible for the execution of a year-long campaign, in four phased delpoyments, to instrument the Alkimos site in support of the ASDP development. This campaign featured four bottom-mounted, wave-enabled Nortek AWAC instruments

installed along a cross-shore profile close to the alignment of the existing WWTP diffuser pipe (Figure 3-1).

Each of the four instruments measured directional currents as well as directional waves, near-bottom water temperature, and pressure (from which water levels can be derived). Wave data measured at all stations is available only in terms of bulk spectral parameters, without a sea/swell split.

The four deployment periods executed as part of the Gardline campaign are:

- Deployment 1: 02 Apr 2017– 28 Jun 2017
- Deployment 2: 02 Jul 2017– 09 Oct 2017
- Deployment 3: 09 Oct 2017 – 31 Jan 2018
- Deployment 4: 02 Feb 2018 – 22 Mar 2018

No data report has been provided to DHI, and it is unclear what QC steps may have been implemented prior to data handover. There was no data return from Gardline A during Deployment 4. Gardline D has been discarded for currents and temperatures in Deployment 3, owing to a drastic increase in noise levels relative to the other deployments. Gardline D also exhibits periods with high noise levels and clearly erroneous returns in the upper water column, particularly toward the end of Deployment 1. In such cases the upper water column measurements have been discarded, as have depth-integrated values which are in part derived from the upper water column, but near-bottom currents and temperature data have been retained.

NOAA

Regional scale atmospheric (wind, pressure, air temperature, relative humidity and cloud cover fields) as well as coarse regional scale nontidal 3D flow model data (water level, flow, salinity, temperature fields) were sourced from the US National Oceanic and Atmospheric Administration (NOAA). These datasets, specifically CFSR atmospheric products (Saha et al., 2011) and HYCOM oceanographic hindcast products (HYCOM Consortium, 2016) are further described in subsequent sections.

BoM

The Australian Bureau of Meteorology (BoM) supplied time series of meteorological parameters from three stations surrounding the Alkimos site. Those sites, as indicated on Figure 4-2, are Rottnest Island, Swanbourne and Ocean Reef. This data has been used in the calibration phase of the hydrodynamic modelling in terms of confirming the viability of regional CFSR fields, as well as directly providing wind forcing of the Local 3D Model.

AHS

The Australian Hydrographic Service supplied tidal constituents throughout the region, which was used to validate the tidal performance of the regional hydrodynamic models.

DoT

The WA Department of Transport (DoT, 2016) supplied high resolution bathymetric LIDAR data covering the inshore region of interest. A previous DoT LIDAR survey dating from 2009 was also provided via BMT, which extends slightly further offshore from shore to roughly the -25m contour (DoT, 2009).

DoT also provided data from two additional inshore AWAC instruments deployed in 2008 support of the WWTP construction, though these have not to date been utilized for the present work.

UNESCO

Bathymetric information in deep water (roughly 100m or deeper) was provided through global GEBCO data (UNESCO, 2014) for the regional hydrodynamic model.

Jeppesen

Bathymetric information in shallow water (roughly 100m or shallower) not already covered by project surveys was provided through C-MAP digital navigational charting data (Jeppesen, 2014).

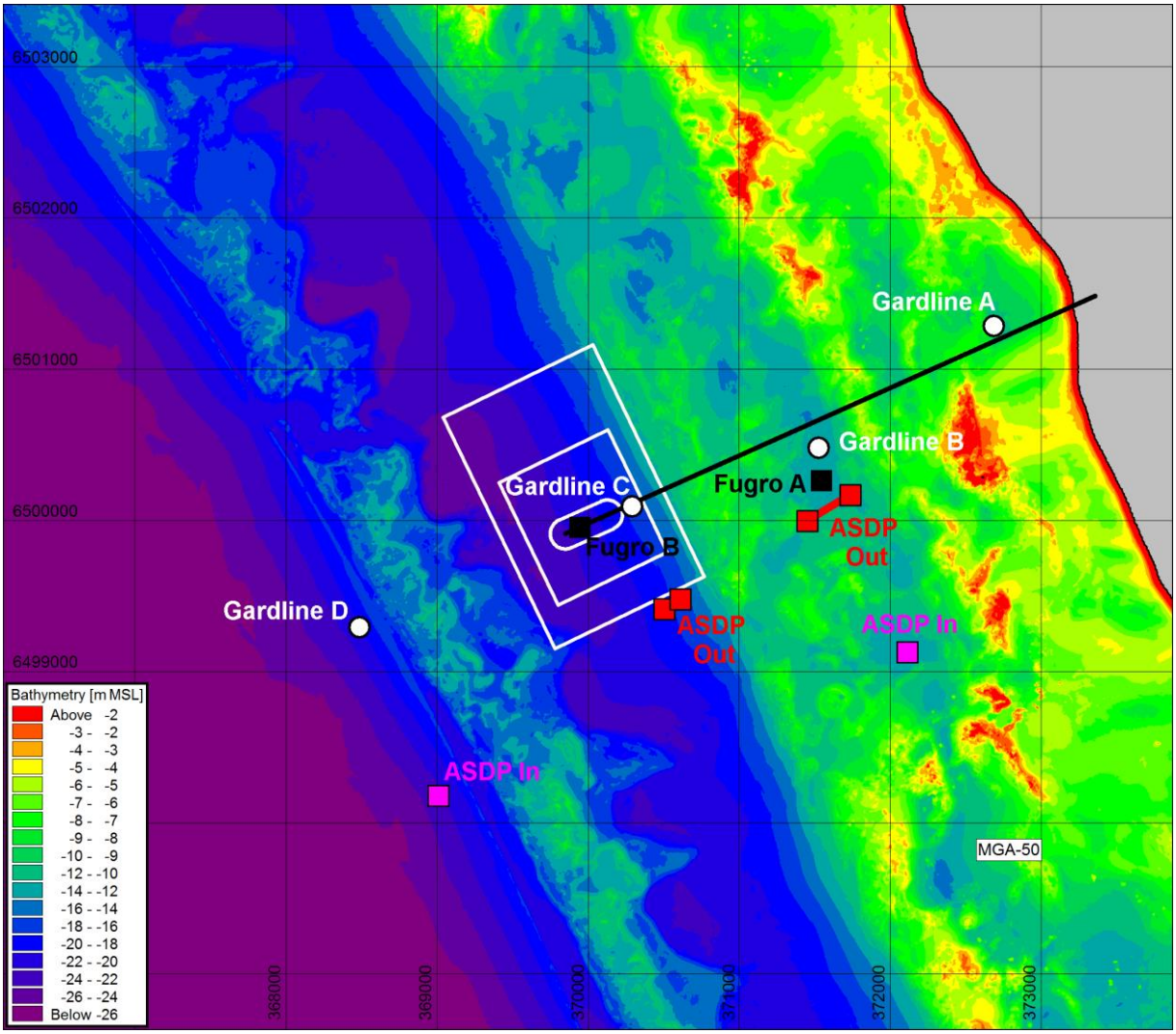

Figure 3-1 Map indicating locations of Fugro (2005) and Gardline (2017-2018) instrumentation installed on behalf of Water Corp. WWTP diffuser, and WWTP regulatory zones and candidate ASDP intake and outfall locations also shown. Bathymetry shown is 5m resolution to align with the native 5m gridded resolution of the DoT (2016) and DoT (2009) bathymetric LIDAR datasets.

Table 3-1 Details of dedicated fixed instrumentation established at the Alkimos WWTP/ASDP site, as locations indicated in Figure 3-1. Gardline particulars as shown pertain specifically to Deployment 1. Minor shifts to positioning, ambient depth and vertical bin elevations are seen between deployments.

Station	Coordinates		MGA50		Instrument Type(s)	Ambient Depth (m MSL)	bin thickness	"Bottom" Data m MSL (m ASB)	"Surface" Data m MSL (m ASB)	Provided Items	Output Time Step
	Long	Lat	E(m)	N(m)							
Fugro A*[1]	115.64558	-31.62563	371,545	6,500,263	Aanderaa RCM9 Aanderaa RCM7	12m	n/a	-9.0m MSL (+3.0m ASB)	-3.0m MSL (+9.0m ASB)	Directional currents*[2]	10min
Fugro B	115.62857	-31.62832	369,936	6,499,945	Wave-enabled 300 kHz RDI Workhorse ADCP	20m	2m	-15.5m MSL (+4.5m ASB)	-3.5m MSL (+16.5m ASB)	Directional currents, Temperature, Bulk wave parameters*[3]	10min (flow) 3hrs (waves)
Gardline A (Deployment 1)	115.65881	-31.61653	372,788	6,501,287	Nortek AWAC	9.5m	1m	-8.1m MSL (+1.4m ASB)	-2.1m MSL (+7.4m ASB)	Directional currents, Temperature, Pressure, Depth (derived), Bulk wave parameters	10min (flow, pressure, water temp) 2hrs (waves)
Gardline B (Deployment 1)	115.64580	-31.62347	371,563	6,500,503	Nortek AWAC	12.7m	1m	-11.3m MSL (+1.4m ASB)	-3.3m MSL (+9.4m ASB)	Directional currents, Temperature, Pressure, Depth (derived), Bulk wave parameters	10min (flow, pressure, water temp) 2hrs (waves)
Gardline C (Deployment 1)	115.63203	-31.62755	370,263	6,500,034	Nortek AWAC	17.9m	1m	-16.5m MSL (+1.4m ASB)	-3.5m MSL (+14.4m ASB)	Directional currents, Temperature, Pressure, Depth (derived), Bulk wave parameters	10min (flow, pressure, water temp) 2hrs (waves)
Gardline D (Deployment 1)	115.61307	-31.63455	368,474	6,499,235	Nortek AWAC	20.7m	1m	-19.3m MSL (+1.4m ASB)	-4.3m MSL (+16.4m ASB)	Directional currents, Temperature, Pressure, Depth (derived), Bulk wave parameters	10min (flow, pressure, water temp) 2hrs (waves)

*[1] Instrument was moved by a third party to approx. 120m WNW of this location sometime between 28 May and 26 Jun 2005.

*[2] Water temperature provided for provisionally processed versions of both instruments, but not included in final deliverable and some data clearly erroneous. Omitted from present work.

*[3] Instrument also records pressure, but this information was not included in data provided to DHI.

3.3 Meteorology

3.3.1 Wind and Pressure

Wind is a significant contributor to residual flows on the inner shelf near Alkimos. Wind and pressure is available from a range of sources for the project:

- Fixed BoM ground stations. Long-term data was acquired from BoM for the stations of most relevance (Rottnest, Swanbourne, Ocean Reef and Hillarys per Figure 4-2).
- An anemometer mounted at the WWTP facility. As this is not considered representative of over-water conditions, it has not been used.
- CFSR wind and pressure fields, which are used to drive DHI's regional 3D model of the South-West. Similar products (Access-G, Access-R) are also available through BoM and other providers.

CFSR data offers complete temporal coverage over all periods of interest, as well as having the advantage of capturing spatial variations over the entirety of the DHI Regional Hydrodynamic Model area. CFSR fields have been applied to drive the Regional Hydrodynamic Models.

Measured winds from the BoM Ocean Reef station have been applied to drive the Local 3D Model.

Figure 3-2 describes the local wind climate in terms of monthly wind roses from 18 years of measurements at Ocean Reef. The data presents a strong seasonal character, with summers showing strong seabreezes and a net direction from south of shore-normal. Winterr months are directionally more variable, and punctuated by storms. The highest median winds occur in January, with the weakest typically occurring in April / May.

3.3.2 Ancillary Meteorological Items Required for Heat Exchange

Additional meteorological inputs are required to support detailed heat exchange calculations. Air temperature, relative humidity and cloud cover are prescribed from CFSR (Saha et al, 2011) fields to drive the heat exchange calculations, in combination with the CFSR and Ocean Reef winds for the Regional and Local 3D Hydrodynamic Models, respectively.

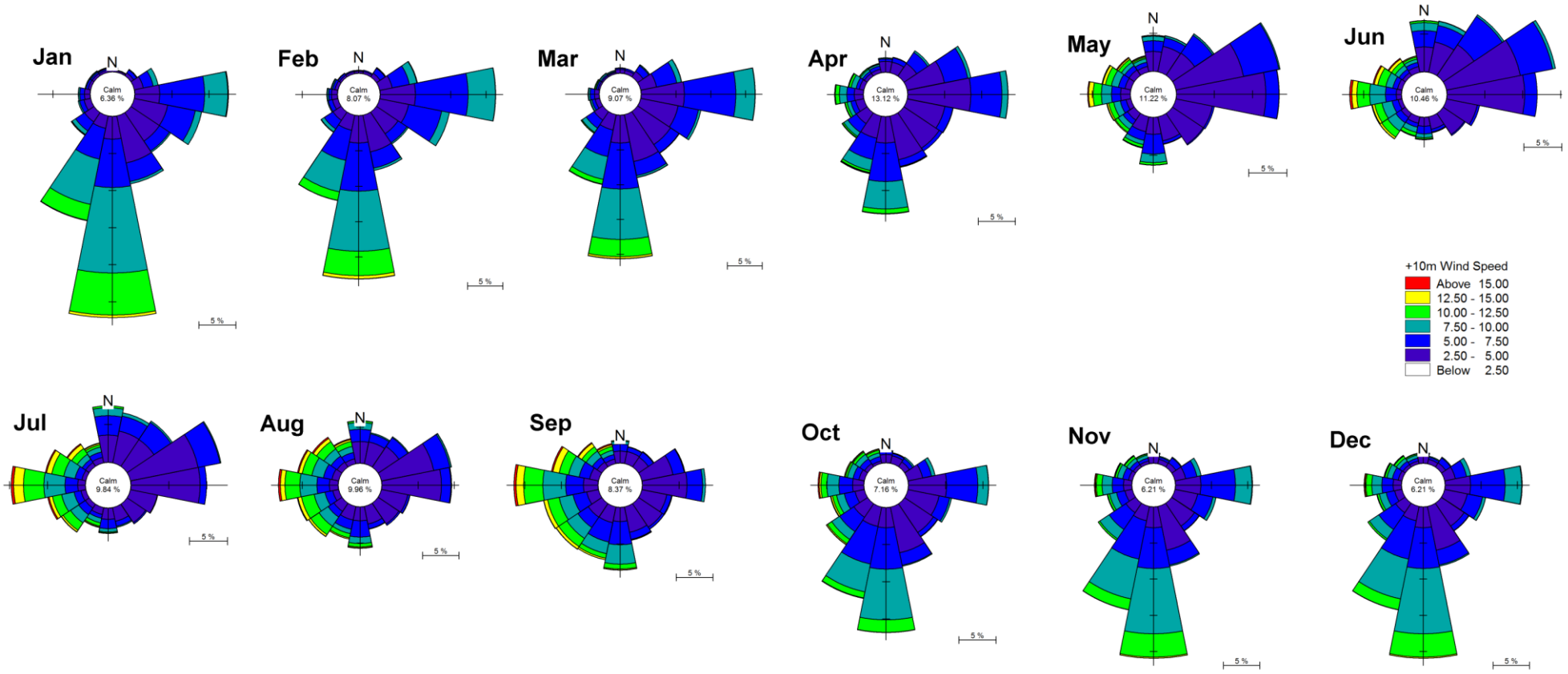

Figure 3-2 Long-term monthly wind roses from 18 years of measurements at BoM Ocean Reef station (2000-2017).

3.4 Water Levels

The tidal planes for ANTT stations close to the site are provided in Table 3-2, noting that the tide at Alkimos is strongly diurnal in character.

Water levels at the site are driven by a weak diurnal tidal signal superimposed upon strong nontidal residuals induced by a range of forcing mechanisms on the regional and local scales. Such effects are readily apparent in the one year measured record from the Hillarys ABSLMP station (Figure 3-3), where it is clear that the nontidal contribution is commonly on the same order as the tide. This is also clearly visible in the measured current signals from the Alkimos area, for which the predominant energy is nontidal. It is thus essential that a regional numerical modelling exercise seeking to capture currents be capable of incorporating offshore stratification and complex shelf effects.

Figure 3-4 shows the persistent medium-term modulation of water levels in the region north of Perth, where the pressure signals from the AWAC instruments have been simplistically zeroed relative to the record means and superimposed upon the Hillarys record.

Table 3-2 Tidal planes for ANTT stations adjacent to the Alkimos site (AHS, 2018), in metres relative to LAT.

Tidal Plane	Hillarys	Two Rocks
Highest Astronomical Tide (HAT)	1.2	1.2
Mean Higher High Water (MHHW)	0.9	0.9
Mean Lower High Water (MLHW)	0.8	0.8
Mean Sea Level (MSL)	0.56	0.55
Mean Higher Low Water (MHLW)	0.3	0.3
Mean Lower Low Water (MHHW)	0.2	0.2
Lowest Astronomical Tide (LAT)	0.0	0.0

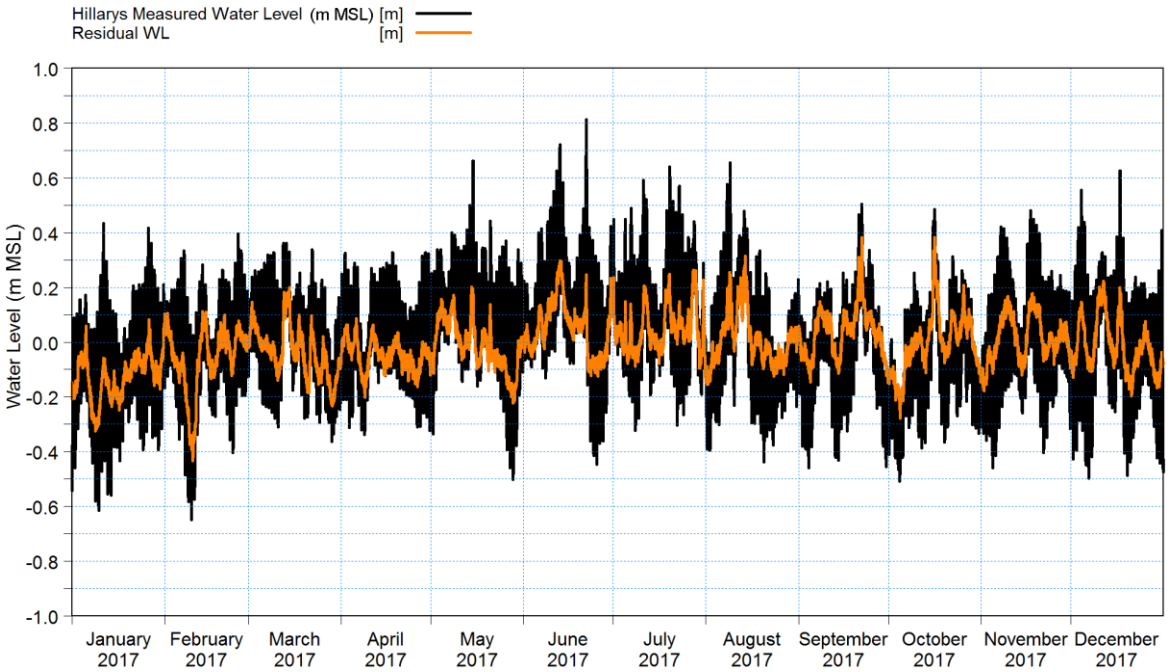

Figure 3-3 Annual tidal record from Hillarys ABSLMP station, showing total measured water level as well as the nontidal residual.

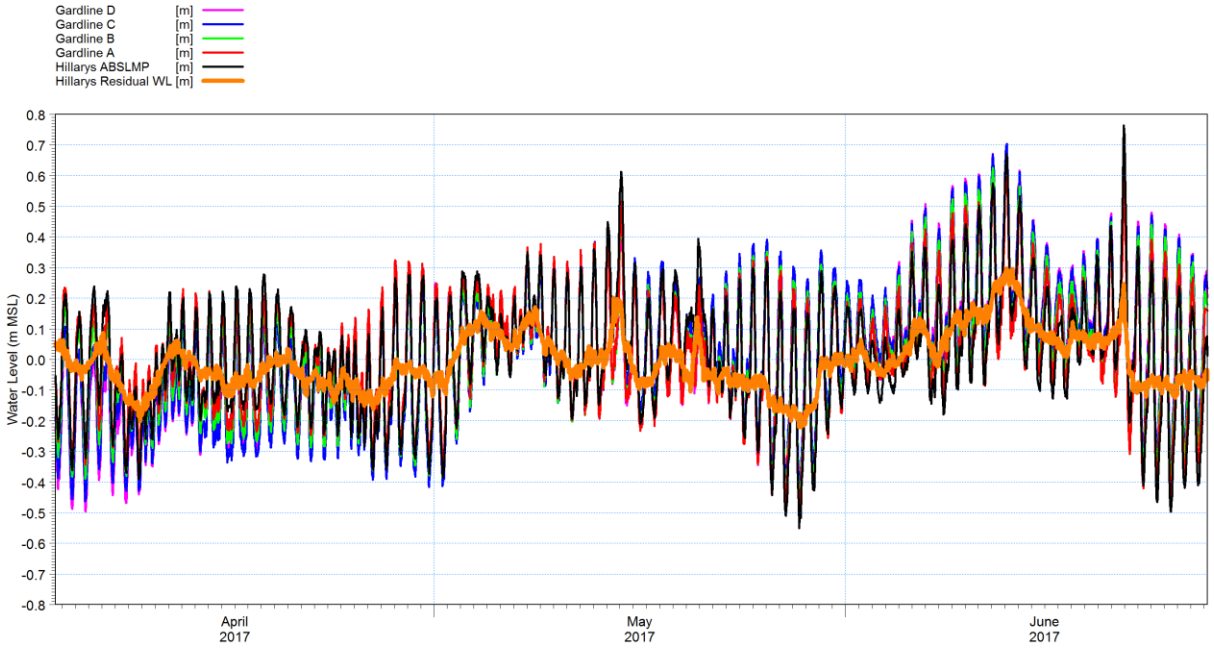

Figure 3-4 Water levels from the four Gardline AWACs, superimposed upon the measured record from the Hillarys ABSLMP station as associated nontidal residual.

3.5 Currents

Currents in the vicinity of the Alkimos WWTP / ASDP facility have been measured in 2005 at two moorings by Fugro and in 2017 at four locations by Gardline.

Figure 3-5 shows the measured percentiles of current speed from all instruments in the 2005 campaign, while Figure 3-8 provides current roses of the depth-integrated currents from the same stations. The trends exhibited in terms of current intensity are fully intuitive, with larger current speeds offshore (Fugro B) and larger currents at the surface. The directionality of the depth-averaged currents are effectively aligned with the bathymetric features at Fugro B, and are considerably more scattered on the reef at Fugro A.

Figure 3-6 shows the measured percentiles of current speed from all instruments in Deployment 1 of the the 2017 campaign. The trends exhibited in terms of current intensity are also intuitive, with larger current speeds offshore (Gardline C/D) and larger currents at the surface. One observation of note is the increased strength of bottom currents at Gardline D relative to the other locations. The directionality of the depth-averaged currents are effectively aligned with the bathymetric features at Gardline C and D, while Gardline B resembles that from the nearby Fugro A. Gardline A experiences a significant change in orientation relative to other stations, presumably due in part to wave effects.

Figure 3-7 provides a matrix of depth-integrated current roses for the four Gardline instruments (columns) and for different time periods (rows). The seasonal nature of currents is prominent, with strongly northward flows in Summer and a southward trend in Winter. The Autumn calibration period is seen to have a balance of northward and southward flows.

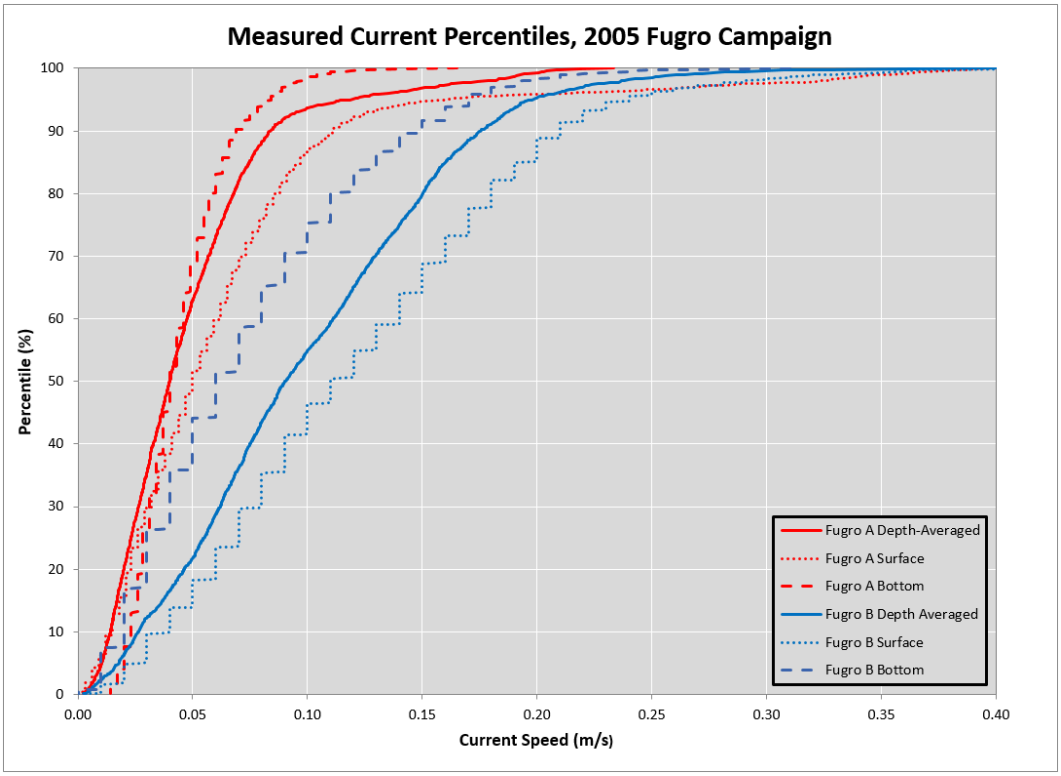

Figure 3-5 Percentile plot of depth-averaged, surface and bottom current speeds from the 2005 Fugro campaign.

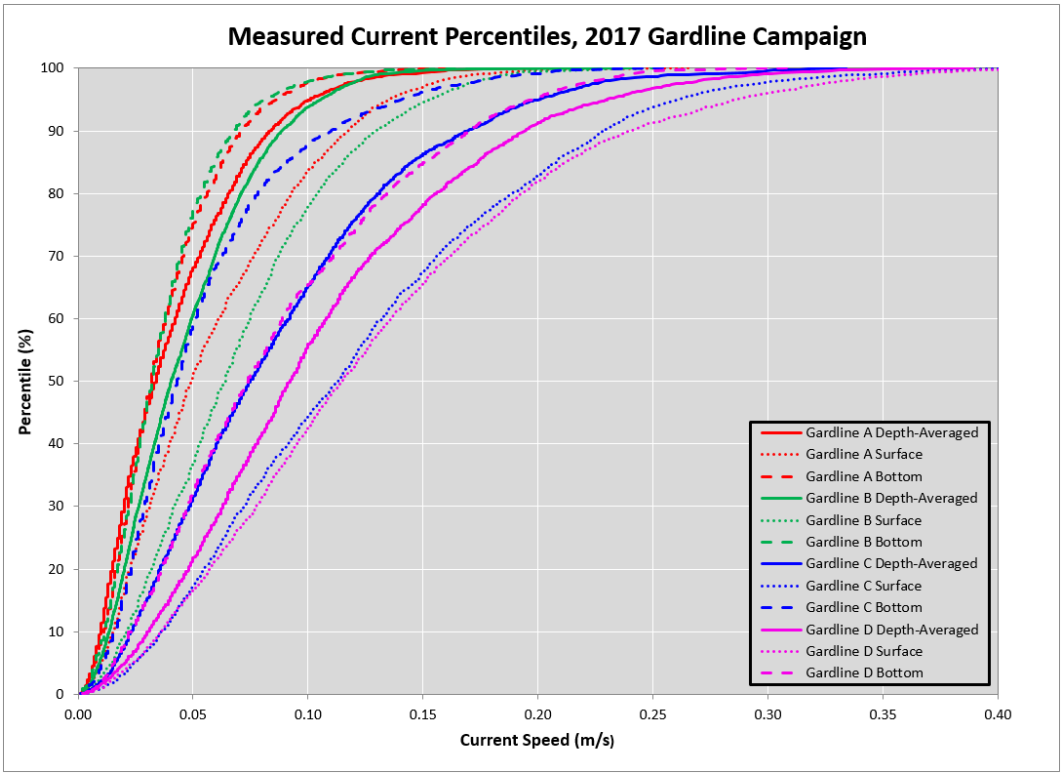

Figure 3-6 Percentile plot of depth-averaged, surface and bottom current speeds from Deployment 1 of the 2017 Gardline campaign.

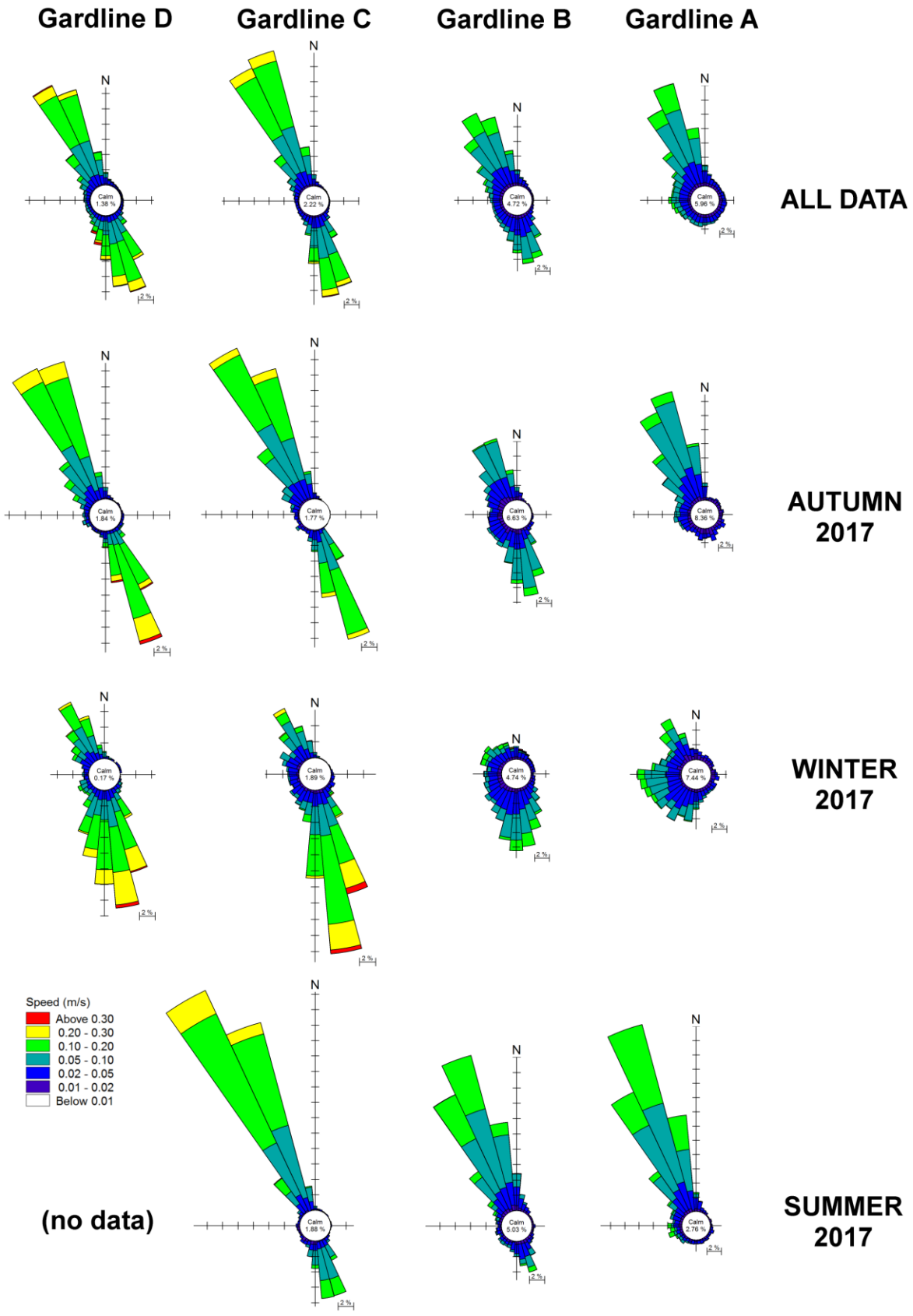

Figure 3-7 Matrix of depth-integrated current roses for the four Gardline instruments (columns) and for different time periods (rows). Note that "All Data" differs by instrument, with Gardline D missing Deployment 3 and Gardline A missing Deployment 4. Autumn, Winter and Summer refer to the 30 day simulation periods as described in Section 1.2.

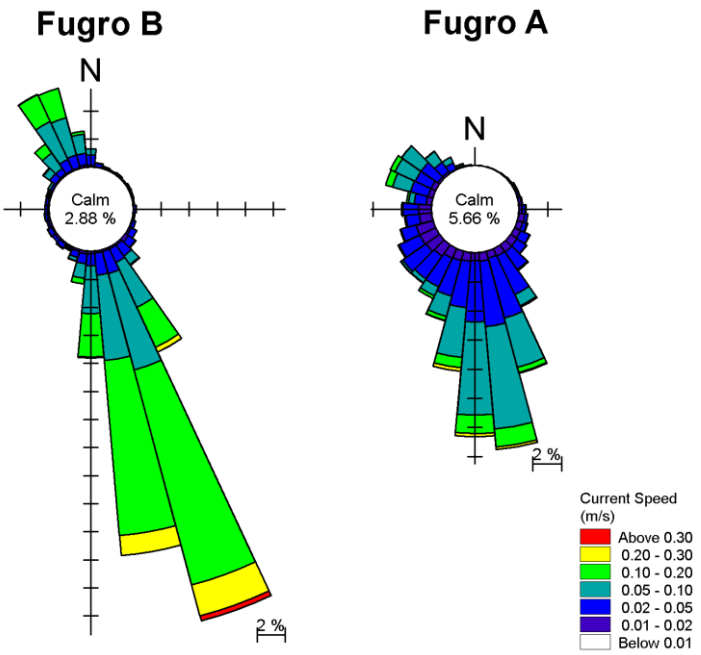

Figure 3-8 Current roses showing depth-integrated currents at the Fugro moorings in Apr-Jun 2005.

3.6 Ambient Salinity and Temperature

3.6.1 Introduction

Salinity and temperature defines the density distribution within the water column, which can have a profound effect on both ambient circulation patterns and in particular on the behaviour of discharge plumes. Density differences between the effluent and the receiving water play a key role in defining the near-field behaviour, while variable density (stratification) in the ambient receiving water can affect both near-field and far-field plume characteristics.

Based on the shallow inner shelf location, the degree of wave exposure at the Alkimos site and the lack of notable runoff sources, there a reasonable expectation that ambient stratification is minimal. A review of available instrumentation confirms this assumption. Synoptic CTD profiling of salinity and temperature performed in support of WWTP permit compliance is presented in Section 0. Fixed instrumentation of temperature is presented in Section 3.6.3.

For reference, the constant values shown in Table 3-3 were applied in WP(2005) for modelling in support of WWTP permitting.

Table 3-3 Representative salinity and temperature conditions as applied for previous modelling of the Alkimos WWTP in WP (2005).

Water Property	Summer	Autumn
Temperature (°C)	23.0	19.0
Salinity (ppt)	36.5	35.3

3.6.2 Synoptic CTD Profiles

BMT perform compliance monitoring for the WWTP twice per month during the period of December to March. Each survey consists of a minimum of four reference stations as well as five mobile stations targeting the plume centreline at fixed distances from the WWTP diffuser. The mobile stations are aligned on-site with a drogue released from the diffuser location, which is assumed to remain within the plume.

Sample synoptic temperature and salinity profiles are shown in Figure 3-9 through Figure 3-12 for the 2016-2017 monitoring period. The locations of the profiles (indicated as AWR1 through AWR4) are located within the shore-parallel channel at which the WWTP diffuser is located. The specific profile locations are not repeated from survey to survey but typically lie within 3km of the WWTP outfall in comparable water depth.

The salinity varies from 35.7 to 36.6 ppt, but (aside from a few instances of instrument noise) the vertical gradient does not exceed 0.1 ppt within any given set of four profiles for a given deployment.

The temperature varies from 20.7 to 22.7°C, but the vertical gradient does not exceed 1.1°C within any given set of four profiles for a given deployment. When weak temperature-induced stratification is measurable, the largest gradient is seen in 7-10m water depth.

The profiles as measured thus confirm a water column with a character varying between being well-mixed and weaky stratified.

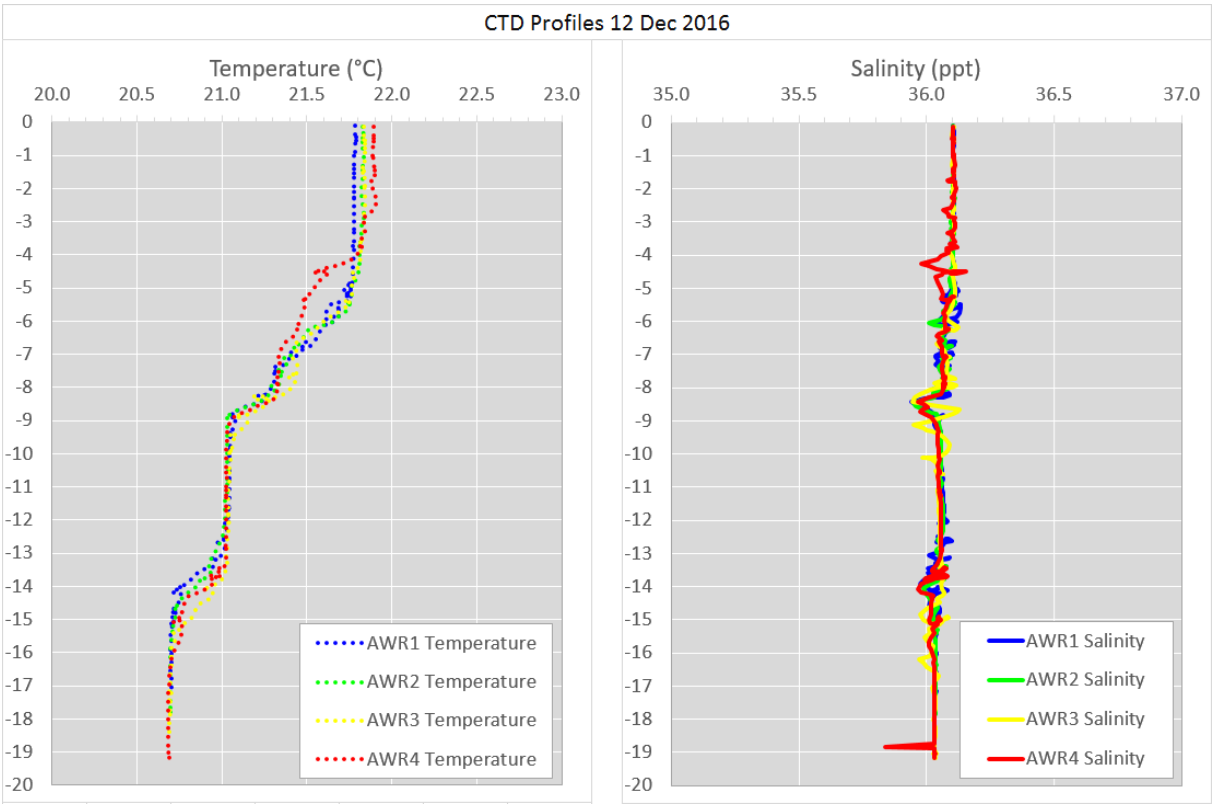

Figure 3-9 Synoptic CTD profiles taken in connection with WWTP compliance, 12 Dec 2016.

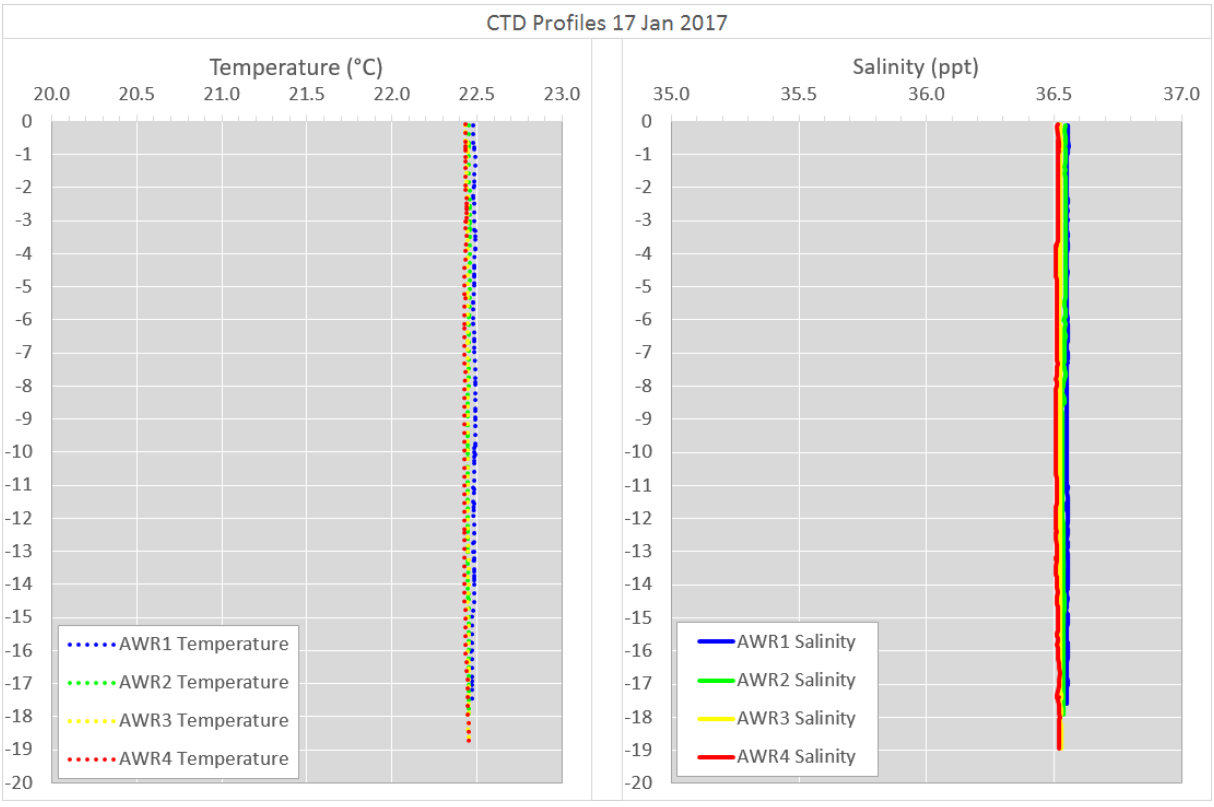

Figure 3-10 Synoptic CTD profiles taken in connection with WWTP compliance, 17 Jan 2017.

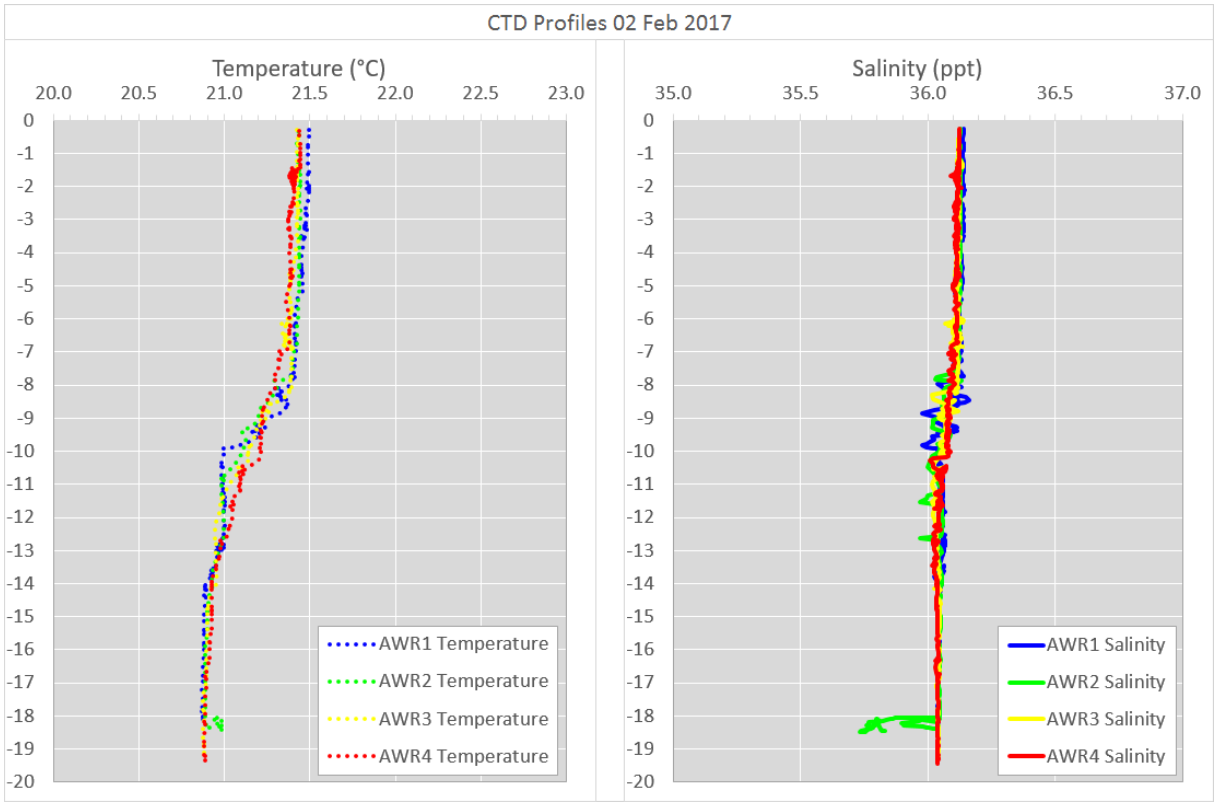

Figure 3-11 Synoptic CTD profiles taken in connection with WWTP compliance, 02 Feb 2017.

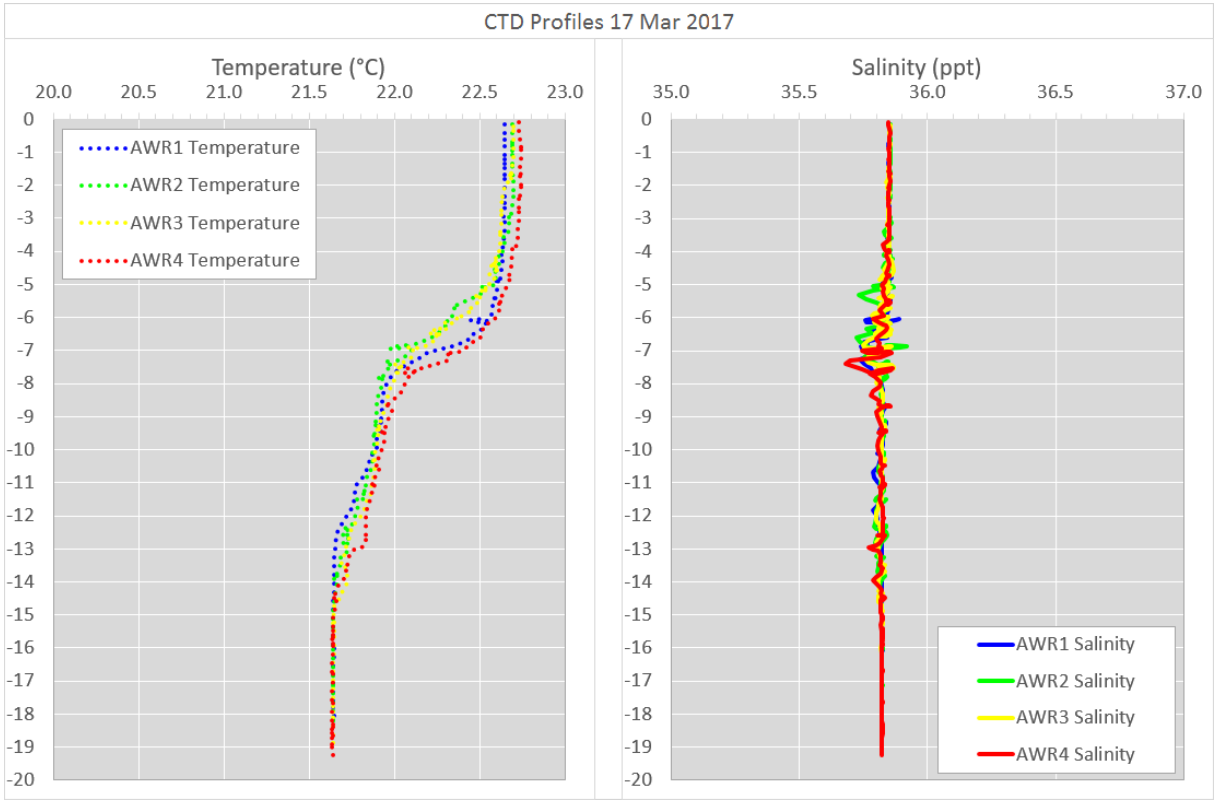

Figure 3-12 Synoptic CTD profiles taken in connection with WWTP compliance, 17 Mar 2017.

In the context of ambient salinity and temperature, the issue of greatest interest with respect to outfall behaviour is the vertical density gradient. This has been quantified through the processing of a large number of the available CTD profiles, which are located primarily in the shore-parallel channel within which the existing WWTP outfall is sited. The bulk of the reference stations are located in on the inshore shoulder of the channel, in water depth that is too shallow (<15m depth) to be representative of the outfall channel itself. As such, statistics have been derived using CTD profiles both from the reference stations and also from mobile stations in order to act on a far larger body of profiles. This inherently captures some degree of the existing WWTP plume along with the desired ambient salinity and temperature. However, the effluent flow out of the WWTP outfall is on the order of 10% (~8ML/day) of the design flow and efficiently diffused with an intermediate capping arrangement. As such, its signature on the ambient water column is generally small.

The percentile distribution of the vertical density difference measured via 143 CTD profiles is shown in Figure 3-13. It is again noted that the statistic visualised in Figure 3-13 represents both ambient stratification as well as that induced by the existing WWTP plume, and that the profiles applied were acquired almost exclusively during the summer months.

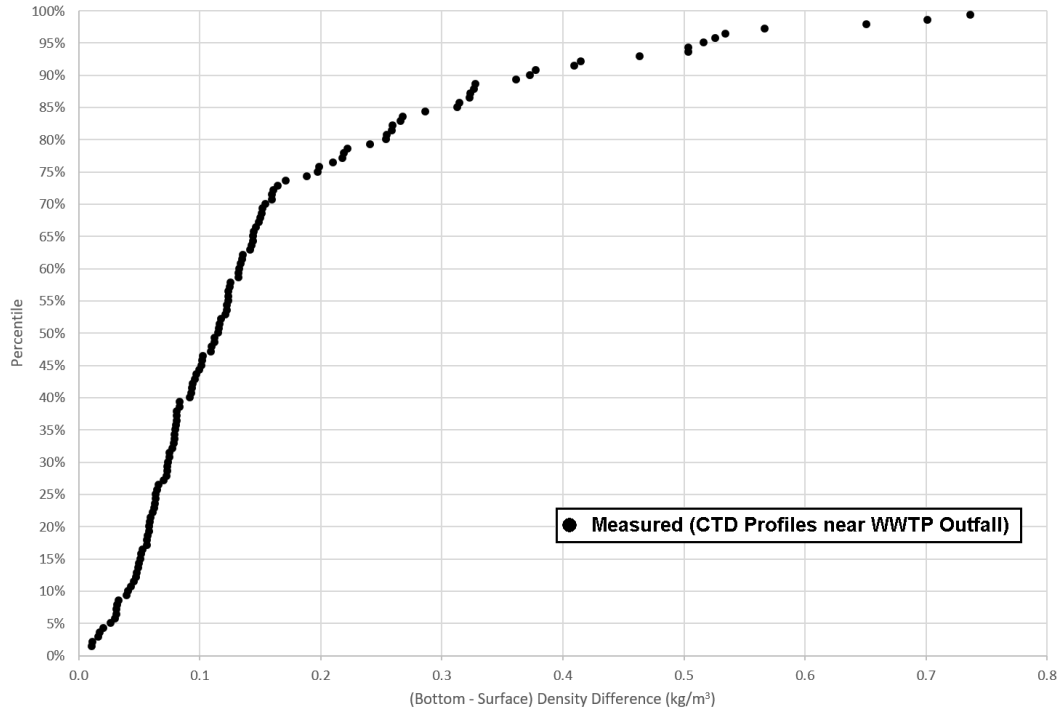

Figure 3-13 Summer vertical density difference over water column as measured by 143 CTD profiles in the vicinity of existing WWTP outfall (nominally 21m water depth).

3.6.3 Fixed Instrumentation

As seen in Table 3-1, near-bottom temperatures were measured by the four Gardline AWAC instruments. Figure 3-14 compares the measured near-bottom temperatures over a full annual cycle as measured by the four instruments, as well as with the Hillarys ABSLMP station, duly noting that the Hillarys station is located within a semi-enclosed harbour. With the exception of late autumn and winter (say Oct-Mar), the shallow AWAC locations (Gardline A and B) align closely with each other and with the Hillarys station. The outer Gardine D lags the inshore stations seasonally, both cooling and heating more slowly as would be expected.

No fixed salinity measurements were acquired in either the 2005 or 2017 campaigns established to support the Alkimos site development. Information is available from the innermost Stn A of the three CSIRO Two Rocks moorings independently maintained during 2004-2005. Figure 3-15 shows one year of salinity and temperature data captured from the historical inshore mooring at Two Rocks Stn A, which featured instruments at both bottom and mid-depth. This data is of interest as it is both long-term and is located (Figure 5-1) within the same shore-parallel channel occupied by the WWTP outfall as well as the Fugro B and Gardline C moorings. As such, it is a reasonable proxy for conditions near the existing WWTP outfall.

Figure 3-15 shows that the temperature at mid-depth (10m) is slightly warmer (mean 0.18°) than that at the bottom. The salinity record is more difficult to interpret with confidence as, owing to the challenges of long-term conductivity measurements, there is lower data return and portions of the records appear to be affected by biofouling. The mid-depth record is consistently more saline than the bottom record. While the CTD profiles do on occasion show small salinity inversions, the Two Rocks data shows this as a prominent and virtually permanent feature which is at odds with the Alkimos CTD profiles. Consequently the Two Rocks Stn A salinity record has not been explicitly applied, though it is useful in the context of illustrating the annual trend of ambient salinity within the area of interest which is otherwise lacking.

The Gardline AWAC records shown in Figure 3-14 capture the annual heating and cooling cycle in a manner which is outwardly reasonable, but upon close inspection exhibit some counterintuitive behaviour:

- During Deployment 1, the lowest AWAC temperatures are recorded at Gardline A, which is consistent with rapid seasonal cooling occurring most strongly in shallow water close to shore. However, after the instruments are replaced at the start of Deployment 2, the lowest temperatures are recorded at Gardline B. It is difficult to explain this abrupt trend reversal, as it would be reasonable to expect the lowest temperatures to remain at Gardline A through to the point of the annual minimum. There are no synoptic profiles available to cross-check these records.

- Another abrupt transition occurs between Deployments 2 and 3, at which time the temperature at Gardline C increases by 2°, and markedly deviates from Gardline D with a trend that appears to be non-physical. Perplexingly, this new trend is then maintained from Deployment 3 into Deployment 4. Cross-checking the Gardline C and D fixed moorings with synoptic profiles taken by BMT on 11 Dec 2017 and 31 Jan 2018, in both cases the bottom temperatures from the profiles align well with far lower bottom temperatures from the Gardline D mooring. Further, the trend of Gardline C being far warmer than Hillarys during summer 2017 is opposite to the trend seen for Two Rocks StnA (a proxy for Gardline C) which was consistently cooler than Hillarys in the Summer months of 2005 (Figure 3-15). The Gardline C temperatures for Deployments 3 and 4 are thus taken to be erroneous and are subsequently discarded for model calibration/validation.

- There are a number of less prominent periods during which the cross-shore gradient in near-bottom temperature takes on a character which is outwardly counterintuitive. During the month of April, the highest water temperatures occur persistently at Gardline B. Conversely, for the entirety of Deployment 2, Gardline B has the lowest temperature of the four AWACs.

The annual water temperature record as measured at Hillarys Boat Harbour (BoM, 2018b) is seen to align well with the representative seasonal values in Table 3-3 as applied in WP (2005).

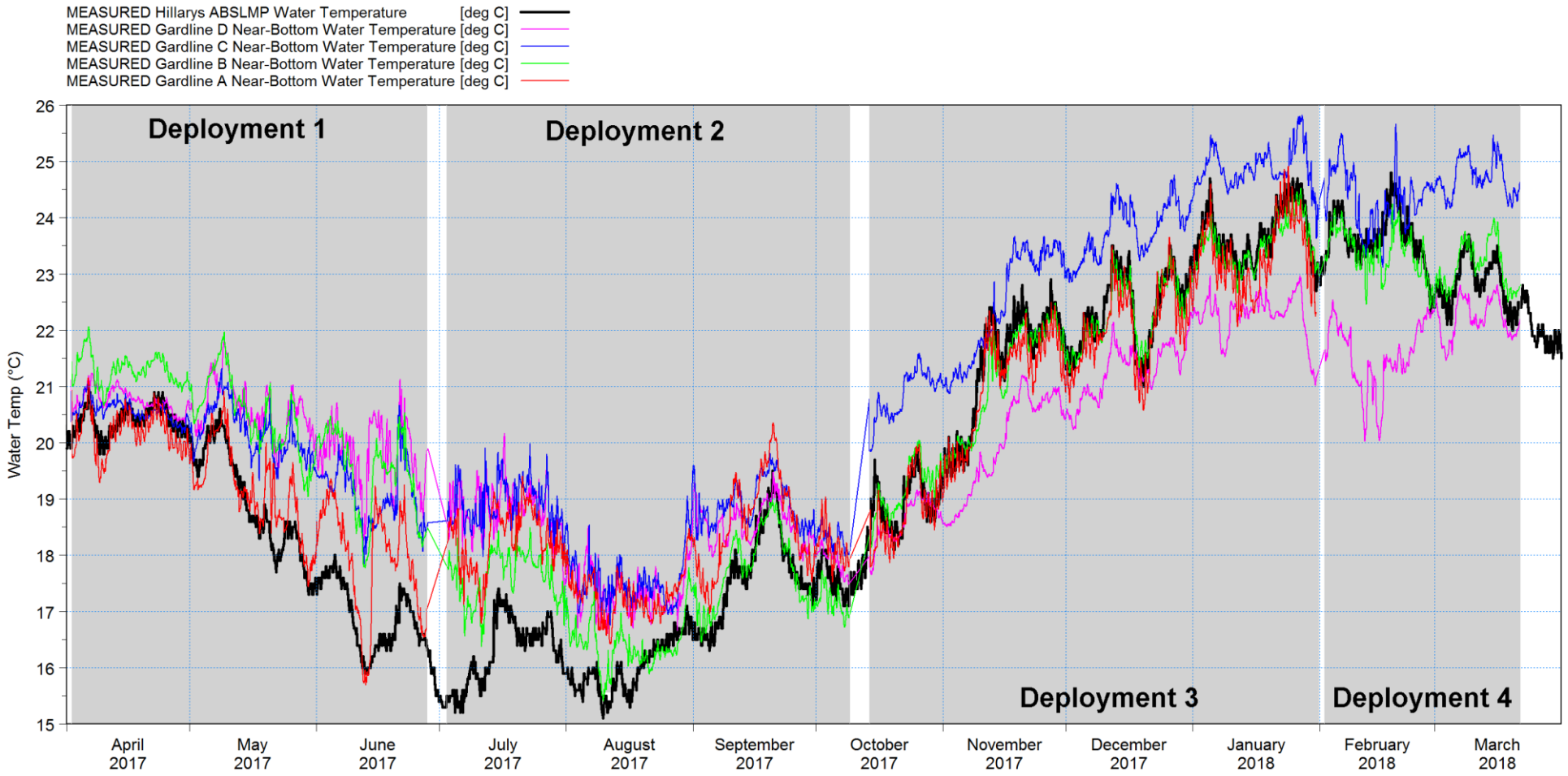

Figure 3-14 Near-bottom water temperatures as measured by the four AWACs of the four Gardline deployments, as well as at the Hillarys ABSLMP station (BoM, 2018b).

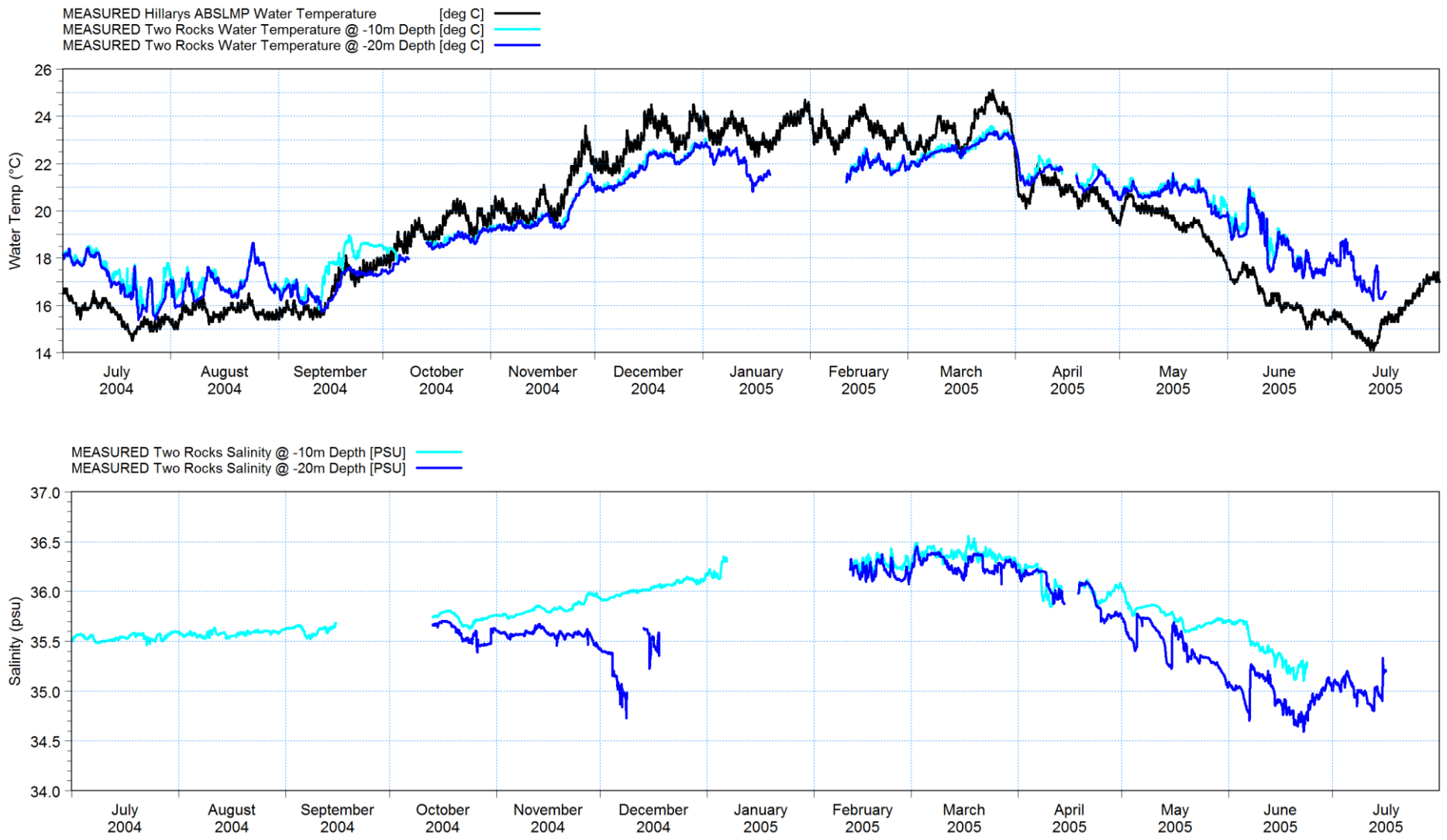

Figure 3-15 Long-term measured temperature and salinity at bottom and mid-depth from Two Rocks Stn A mooring (CSIRO, 2006).

4 Regional 2D/3D Hydrodynamic Model

4.1 Introduction

The Regional Hydrodynamic Model plays the role of a facilitator for the present work, as it provides no answers itself but provides critical forcing data to drive the Local 3D Hydrodynamic Model. The Regional Hydrodynamic Model incorporates both tidal and nontidal forcing, as well as describing the fully stratified water column offshore of southwest WA. This ensures that the complex mechanisms which dominate medium-term water levels and flows on the shelf are present in the boundary data which are then fed into the Local 3D Hydrodynamic Model as a one-way nesting.

4.2 Model System

MIKE 3 FMHD solves the time-dependent conservation equations of mass and momentum in three dimensions, the Reynolds-averaged Navier-Stokes equations. The flow field and pressure variation are computed in response to a variety of forcing functions, when provided with the bathymetry, bed resistance, hydrographic boundary conditions, etc. The conservation equations for heat and salt are also included. MIKE 3 uses the UNESCO equation for the state of sea-water (1980) as the relation between salinity, temperature and density. The hydrodynamic phenomena included in the equations are:

- Effects of buoyancy and stratification
- Turbulent (shear) diffusion, entrainment and dispersion
- Coriolis forces
- Barometric pressure gradients
- Wind stress
- Variable bathymetry and bed resistance
- Hydrodynamic effects of rivers, outfalls and sediment
- Sources and sinks (both mass and momentum)
- Heat exchange with the atmosphere including evaporation and precipitation
- Wave forcing via radiation stresses

MIKE 3 FM has an advection - diffusion equation solver that simulates the transport of heat and of dissolved and suspended substances subject to the transport processes described by the hydrodynamics. A full heat balance is included in MIKE 3 for the calculation of water temperature.

MIKE 3 FM is based on an unstructured flexible mesh and uses a finite volume solution technique based on linear triangular or quadrilateral elements. This approach allows for a variation of the horizontal resolution of the model grid mesh within the model area to allow for a finer resolution of selected sub-areas.

The vertical dimension in MIKE 3 FM can discretised either using a sigma grid or a sigma-z grid. This allows for maximum flexibility in model construction depending on the nature of the problem at hand and the simulation domain.

The MIKE 3 FM model allows for consideration of wave radiations stresses, tidal potential, and an array of structures (eg weirs, culverts, piers, gates, turbines). The commercial basis of the model and the large global user base means that new updates are regularly available with additional features and integration with other MIKE models. For the present application, integration between MIKE3 FMHD and MIKE21 SW is a key feature, as the

wave action affects mean flows in terms of direct forcing (via radiation stresses) as well as via additional effective roughness (wave-induced roughness calculations).

The model is available in hydrostatic and non-hydrostatic versions, however is applied in this case in hydrostatic mode.

4.3 Regional 3D Model

4.3.1 Model Setup

The spatial extent of the Regional 3D Hydrodynamic Model is shown in Figure 4-1, with intermediate and fine details shown in Figure 4-2. Basic details of the model construction are summarized below:

- Constructed in DHI's MIKE3 FMHD system, in spherical (lat/long) coordinates.
- Bathymetric data compiled from:
    - GEBCO bathymetric database in regions deeper than 100m
    - C-MAP (digital navigation charting) data for the remainder of the domain
    - DoT (2016) LIDAR surveys are applied wherever available.
    - All bathymetry has been reduced to mean sea level through the generation of a regional map describing the MSL-CD offset.
- Boundary forcing is based upon predicted water levels from a global tidal model (Cheng and Andersen, 2010), in combination with nontidal level and flow boundary forcing from HYCOM reanalysis version GLBu0.08 (1/12°, 40 z-levels) simulations for 2005 and analysis version GLBa0.08 (1/12°, 33 z-levels) simulations for 2017.
- Incorporates tidal potential forcing within body of model.
- Meteorological forcing is applied as hourly spatial wind and pressure fields from NOAA CFSR data at a spatial resolution of 0.31° for the 2005 validation period, and NOAA CFSRv2 data, at a spatial resolution of 0.2° for the 2017 validation period (both being the best CFSR resolutions available for those respective years).
- 36 vertical layers, including 13 sigma layers (61m depth and above) and 23 z-layers (below 61m depth).
- Initial salinity and temperature fields are also applied from the above HYCOM simulations.
- Previously calibration against 14 tidal stations, records from 8 IMOS ADCPs and proprietary datasets. For present purposes model has been revalidated against six ANTT tidal stations specifically for the 2005 and 2017 validation periods, and has also been compared against the outer Gardline / Fugro stations at Alkimos in terms of depth-integrated currents.

Key model specifications for both Regional and Local 3D Models are provided in Table 4-1:

Table 4-1 Summary of Regional and Local MIKE3 hydrodynamic model configurations as applied.

Property	Regional 3D Model	Local 3D Model
Model System	MIKE3FM HD	MIKE3FM HD
Nominal Mesh Resolution	9km → 500m	750m → 50m
Coordinate System	Long/Lat	MGA-50
Bathymetry	GEBCO, C-MAP, DoT LIDAR	C-MAP, DoT LIDAR
Vertical Grid	36 layers (13 σ in top 61m, then 23 z)	13 σ layers of variable relative thickness, enhanced at surface (5%) and bottom (2.5%)
Time step	dynamic	dynamic
Hydrodynamic Boundary Conditions	Flather Boundaries, as a hybrid of a Global Tidal Model and non-tidal components from HYCOM	Flather Boundaries, water level + 2DV fields of u,v as extracted from Regional 3D Model
Salinity and Temperature Boundary Conditions	HYCOM	2DV fields of S,T as extracted from Regional 3D Model
Initial 3D Salinity & Temperature Fields	HYCOM	Interpolated from results of Regional 3D Model
Met Forcing	CFSR fields of wind, pressure, rel. humidity, net precipitation, cloud cover	BoM-measured winds at Ocean Reef
Atm. Heat Exchange and Evaporation	Included	Included
Wind Friction	w_{fc} = 0.0026	w_{fc} = 0.00125
Tidal Potential	Included	Omitted
Roughness	5mm	Variable, with wave-induced roughness when waves included
Eddy Viscosity	Smagorinsky (horiz) / k-ε (vertical)	Smagorinsky (horiz) / k-ε (vertical)
Dispersion Factor	1.0 (Horizontal) / 0.1 (Vertical)	1.0 (Horizontal) / 0.1 (Vertical)

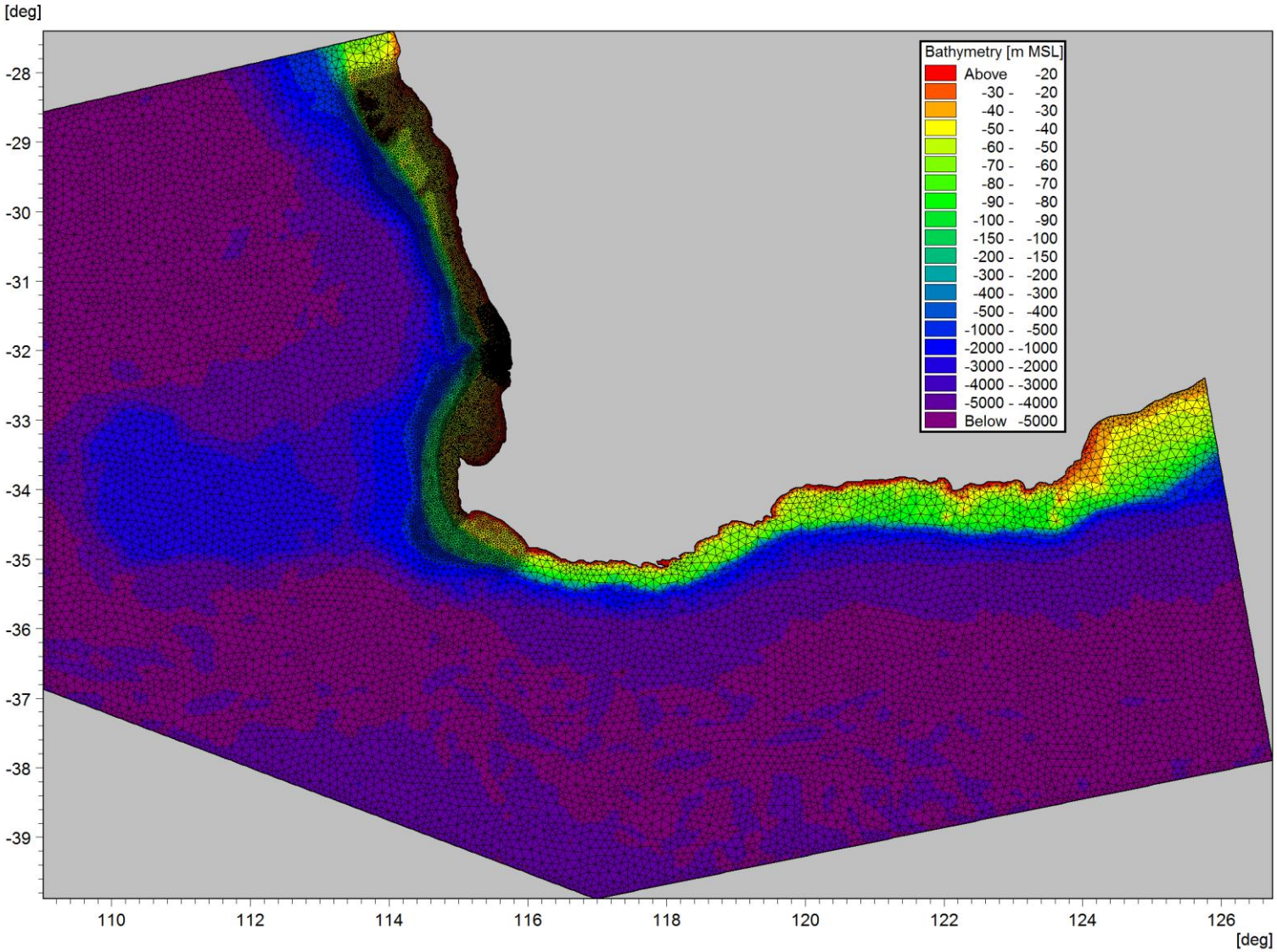

Figure 4-1 Unstructured mesh of the Regional 3D Hydrodynamic Model (full area).

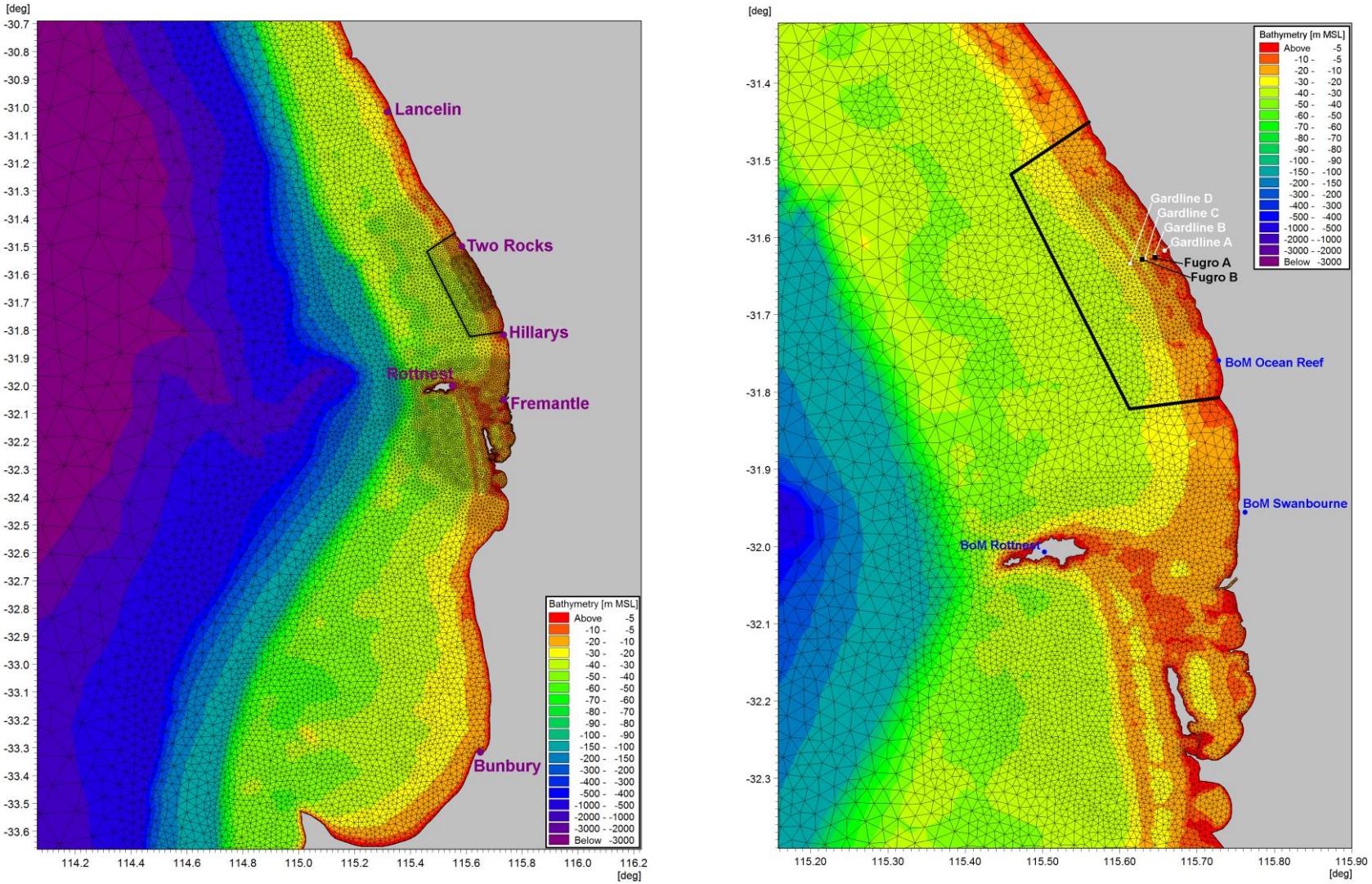

Figure 4-2 Left: Unstructured mesh of the Regional 3D Hydrodynamic Model (intermediate detail, indicating ANTT tidal calibration stations).
Right: Detail indicating Alkimos instrumentation stations and BoM met stations. Black line indicates extend of Local Wave and 3D Hydrodynamic Models.

4.4 Calibration Results and Discussion

The Regional Hydrodynamic Model was executed in both 2D and 3D for a range of mesh arrangements and meteorological forcing scenarios. Ultimately the Regional 3D Hydrodynamic Model provided the best overall performance and was retained for production, in combination with CFSR winds and a high constant wind drag coefficient of 0.0026.

The model was calibrated previously to tidal stations throughout the domain, as well as available current meters. Validation of the model was performed in stages, first confirming tidal performance in the absence of other forcing. Time series comparisons of these tests are provided in Figure 4-3 and Figure 4-4.

Residual (non-tidal) forcing is active in the model through a range of mechanisms, with the primary drivers being oceanic flows entering via the HYCOM contributions at the Regional Hydrodynamic Model open boundaries, as well as wind and atmospheric pressure acting within the body of the model, and local baroclinic forcing. The non-tidal response of the Regional Hydrodynamic Model is compared against measured and third party modelled data in Figure 4-5 and Figure 4-6.

Figure 4-5 shows a comparison of filtered water level gradients from the Regional 3D Hydrodynamic Model vs. those derived from measurements between Hillarys and Fremantle Fishing Boat Harbour, which provide an indication of the forcing in place to drive the longshore component of non-tidal flows. The model is shown to respond very well qualitatively, but to overall show less variability than measured, in particular for the largest events.

Figure 4-6 shows the non-tidal response of the regional model vs. filtered and unfiltered water level measurements at Hillarys, as well as showing the corresponding water level response predicted by the global HYCOM model from which the non-tidal boundary contributions of the Regional Hydrodynamic Model are derived. The figure shows that there is a reasonable agreement between the modelled and measured residual water levels, with both the HYCOM and MIKE3 models responding to medium-term water level perturbations observed at Hillarys. The HYCOM signal, being an instantaneous once-daily value, is naturally less smooth.

A large battery of tests were performed which addressed various permutations of roughness, meteorological forcing and mesh resolution (as well as tests in 2D and 3D setups) to arrive at the best predictive performance against the most offshore of the Alkimos moorings (Fugro B in 2005 and Gardline D in 2017). As the regional model is necessarily coarse, no effort was made to describe the inshore reef conditions with this model. A sample set of calibration curves for the Regional 3D Hydrodynamic Model vs. Gardline D measurements is shown in Figure 4-7.

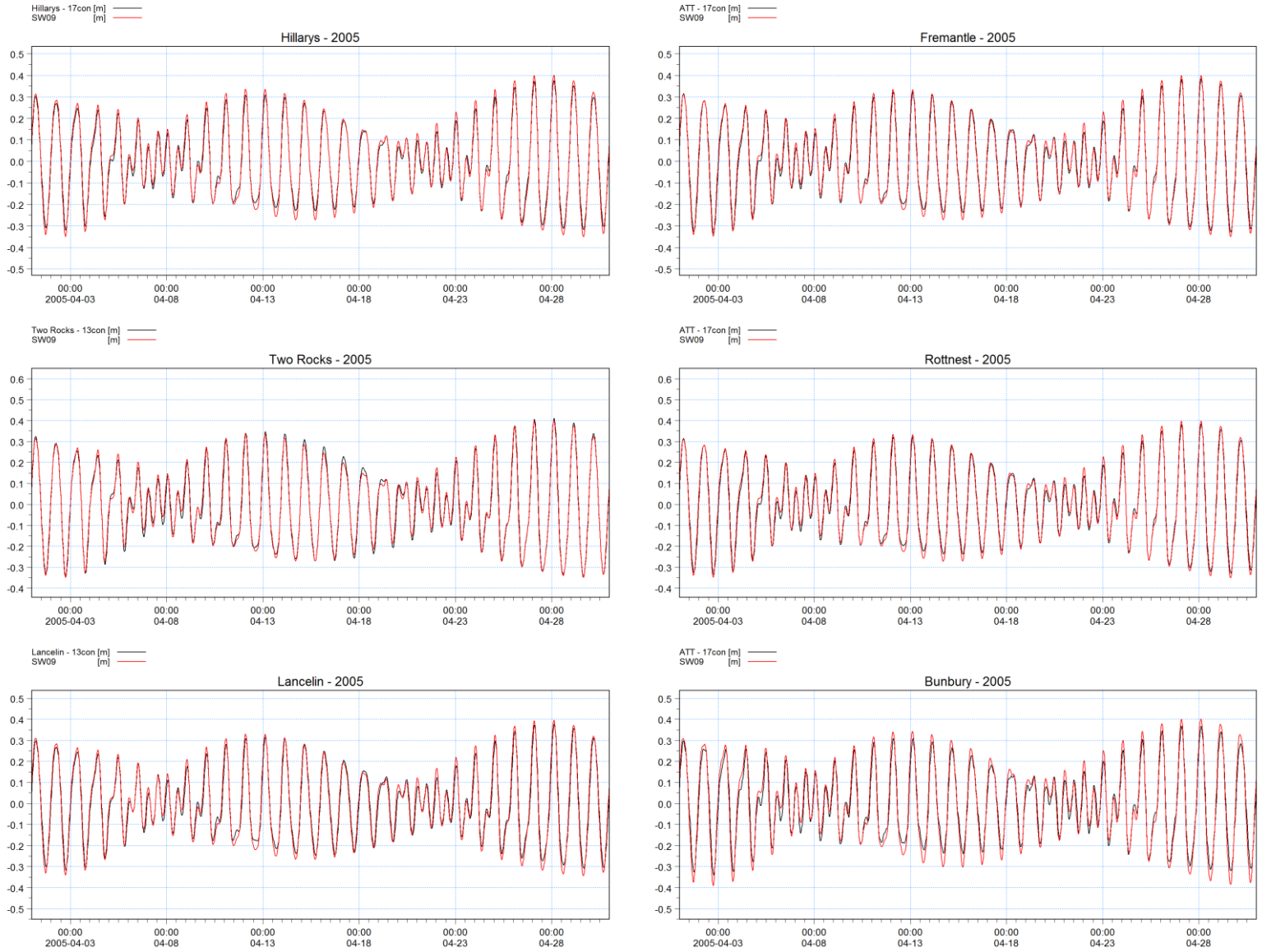

Figure 4-3 Regional Hydrodynamc Model validation for pure tidal forcing (red) vs. the ANTT stations shown in left pane of Figure 4-2 for 2005 (black).

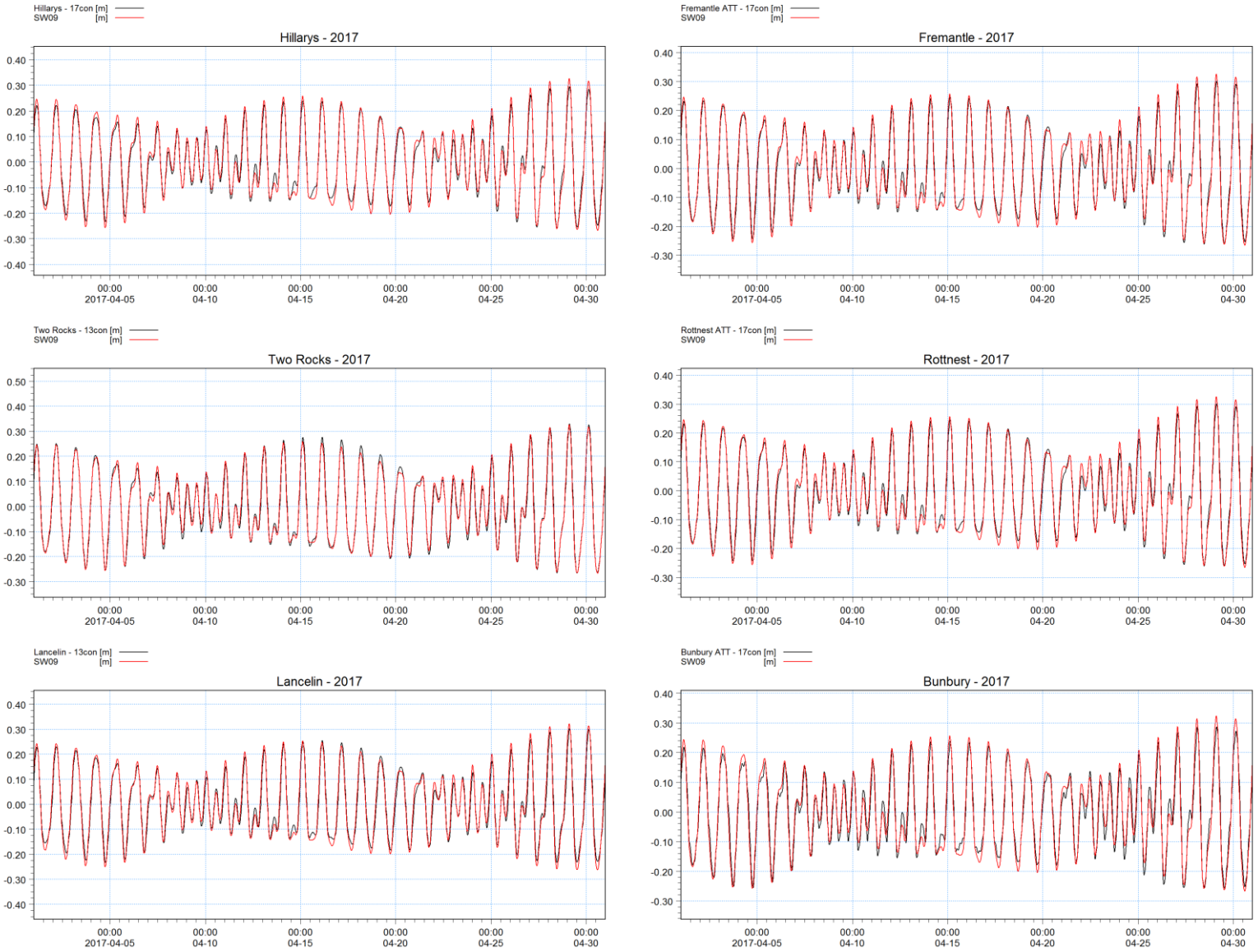

Figure 4-4 Regional Hydrodynamc Model validation for pure tidal forcing (red) vs. the ANTT stations shown in left pane of Figure 4-2 for 2017 (black).

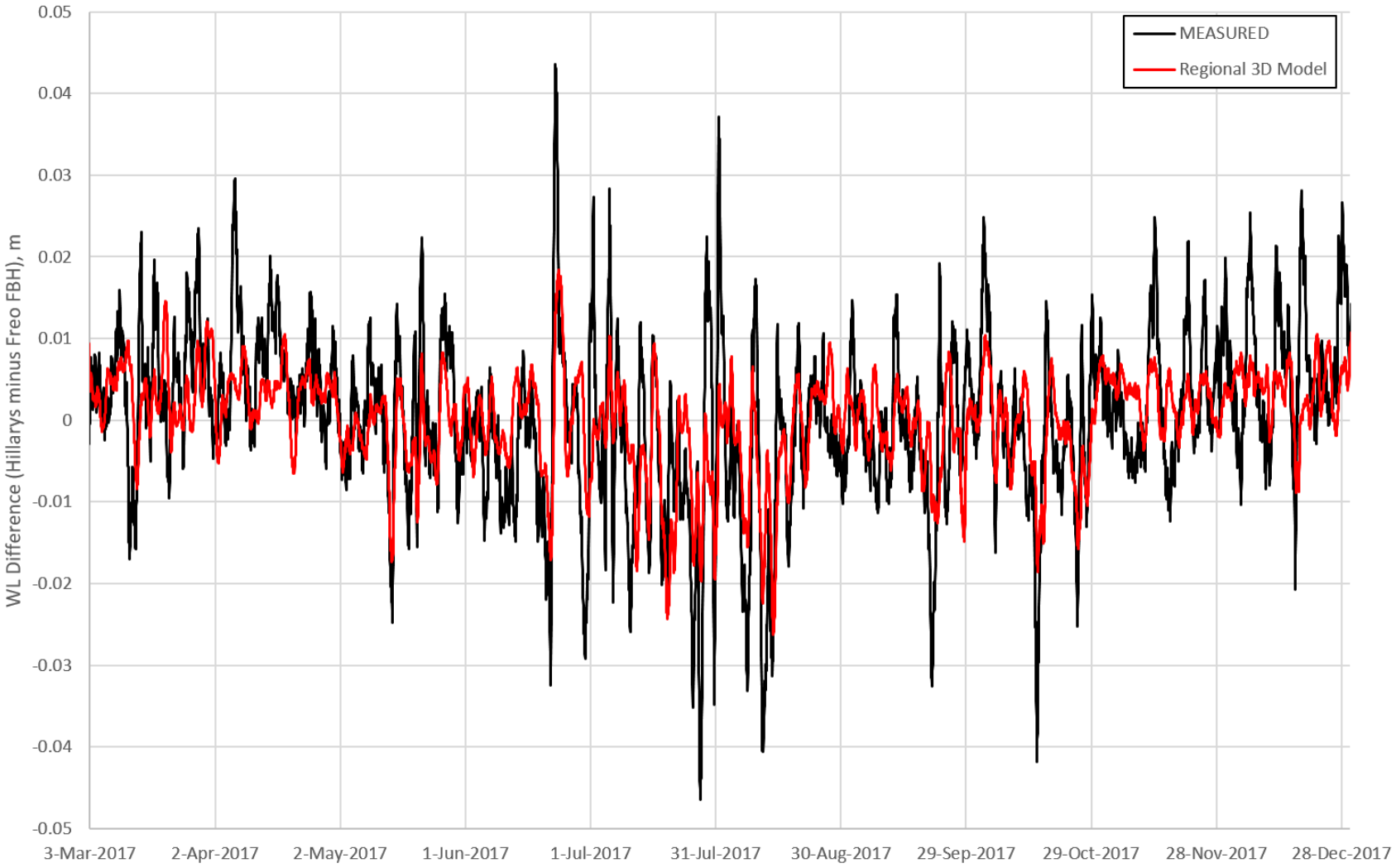

Figure 4-5 Comparison of filtered water level gradients from the Regional 3D Hydrodynamic Model vs. those derived from measurements between Hillarys and Fremantle Fishing Boat Harbour.

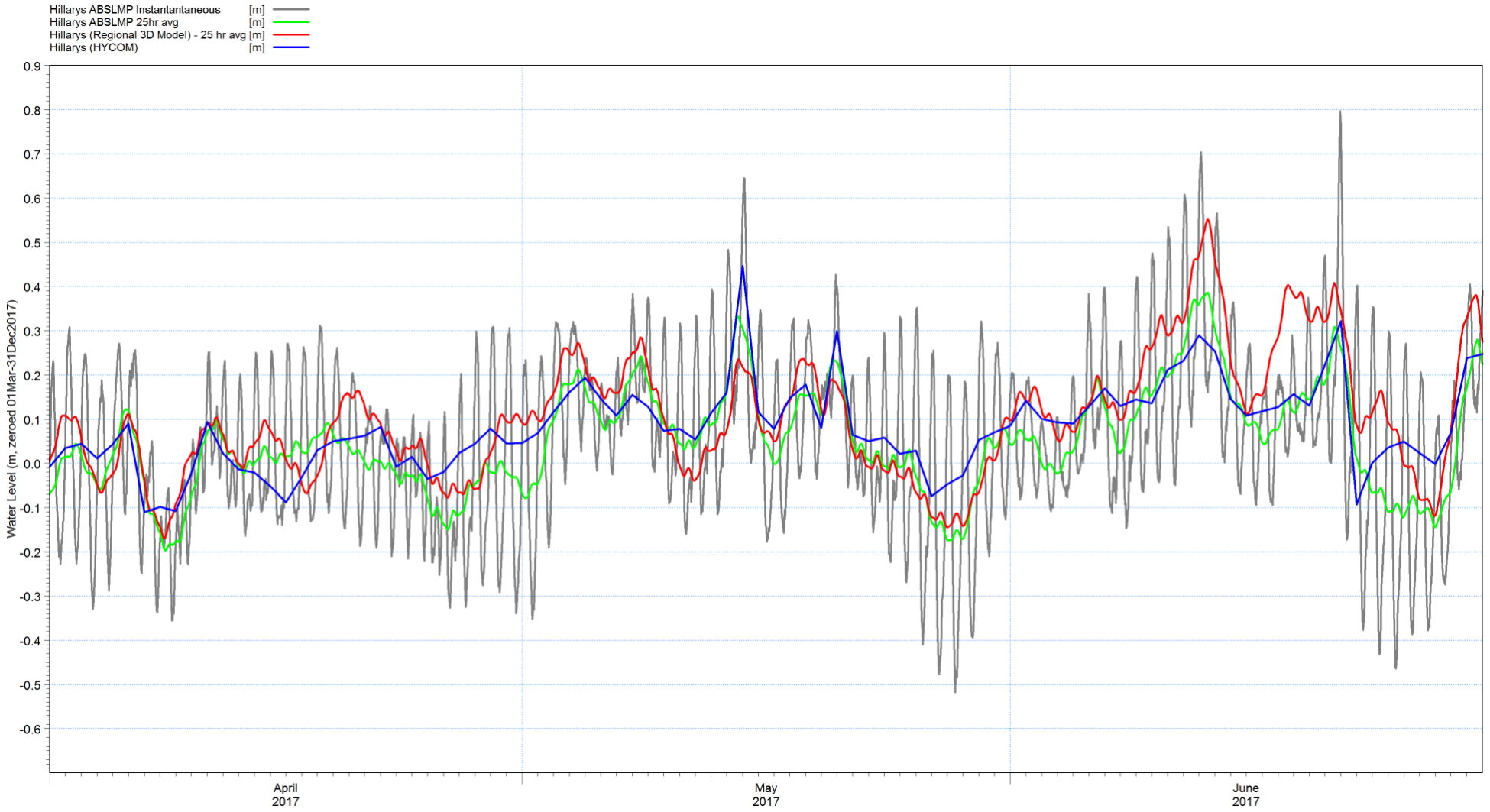

Figure 4-6 Instantaneous (grey) and associated residual (green) water level measurements at Hillarys, with simulated residual water level signals originating from the global HYCOM model (blue) and the Regional 3D Hydrodynamic Model as applied in present project (red).

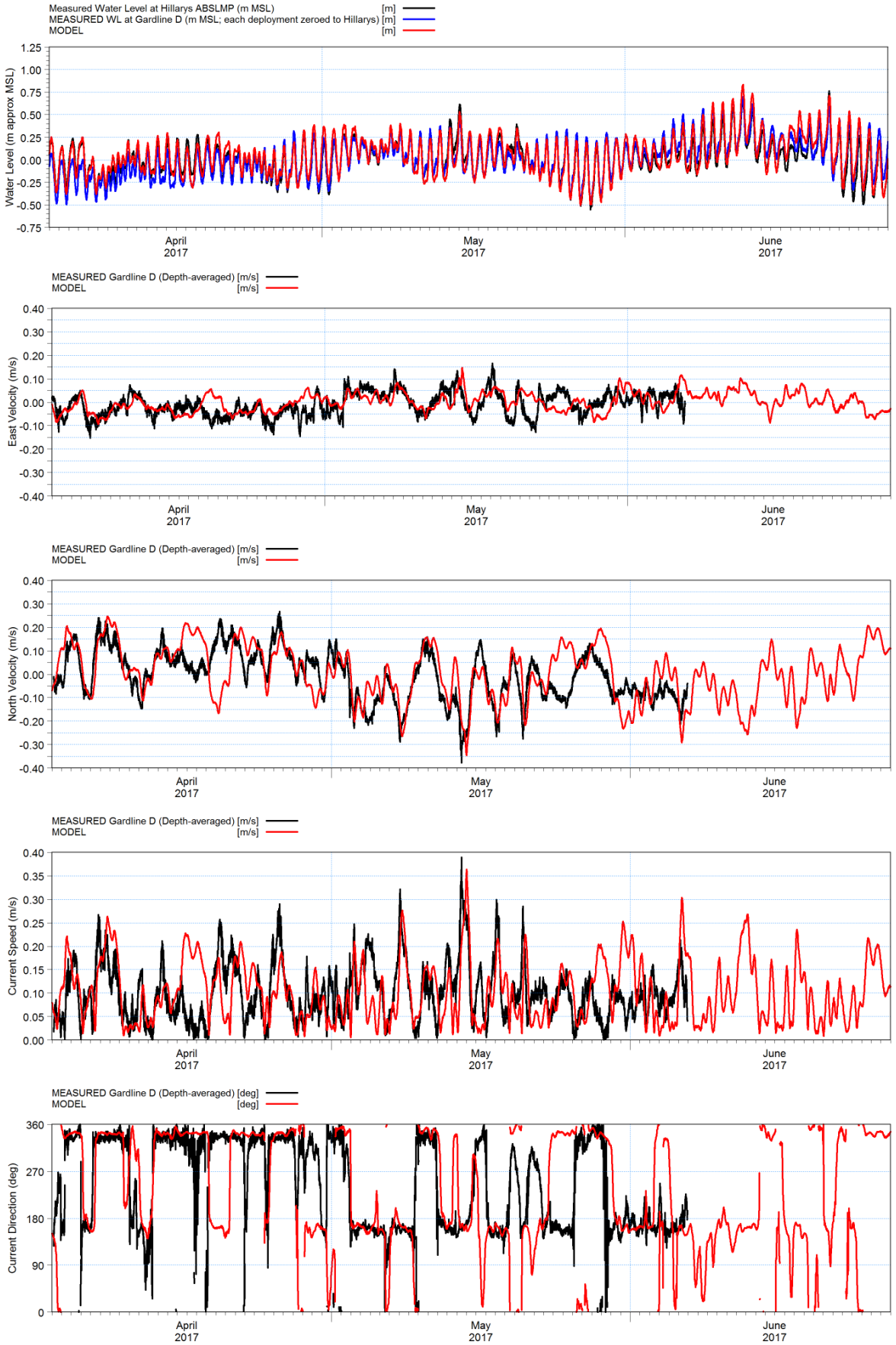

Figure 4-7 Calibration results from the Regional 3D Hydrodynamic Model vs. depth-integrated measurements at Gardline D AWAC, 2017.

5 Local Wave and 2D/3D Hydrodynamic Model

5.1 Introduction

The Local 3D Hydrodynamic Model is the decision making tool for ASDP intake/outfall assessments, and as such the bulk of the calibration effort has focussed on this portion of the model workflow.

Wave forcing plays a role in driving circulation within the inner portion of the reef when waves are large, but are of minimal importance when waves are smaller. A spectral wave model has been established for the purposes of a) providing direct forcing onto the mean flow via radiation stresses and b) modifying the effective bed roughness felt by the hydrodynamic model via wave-induced roughness calculations.

Extensive testing has been performed both with and without wave forcing, and both variants are presented here. The inclusion of wave forcing tends to result in modest improvements relative to measurements in the inshore stations, but to reduce model skill in deeper water.

Given the additional complexity associated with including wave forcing, the primary model arrangement proposed for ASDP scenario screening omits wave forcing. In the event that one of the inshore solutions for the ASDP intake or outfall (see Figure 3-1) is proposed to be carried forward for implementation, it is recommended that the design be confirmed with a simulation in which wave forcing is are enabled.

The Local Hydrodynamic Model is thus driven by both boundary data from the Regional Hydrodynamic Model, as well as (when enabled) by wave forcing from the Local Wave Model as indicated by the flowchart in Figure 2-1.

5.2 Model Systems

The Local 3D Hydrodynamic Model applies the s MIKE3 FM HD code which was described in Section 4.2 for the Regional 3D Hydrodynamic Model.

The Local Wave Model applies DHI's state-of-the-art third generation unstructured mesh spectral wave model MIKE21 SW. The MIKE21 SW model includes all relevant physical phenomena of interest including important shallow/coastal water wave transformation processes such as non-linear wave-wave interactions, wave-current interactions, dissipation due to depth-induce wave breaking and bottom friction.

MIKE21 SW applies a cell-centred finite volume and unstructured (flexible) mesh method for discretisation of the governing equations in geographic and spectral space. This approach provides significant advantages over contemporary fixed and fixed nested grid models by enabling the model resolution to be varied spatially within the model domain to provide very high resolution results at particular areas of interest, whilst enabling computational overhead to be limited in areas of lower interest or where wave transformation processes are varying slowly.

Similar to MIKE3, the MIKE21 SW computational engine supports parallelisation in either OpenMP or MPI memory architecture, enabling simulations to be undertaken on High Performance Computers (HPC) or on standard workstations as required.

5.3 Local Model Mesh

A common calibration mesh is applied in both the Local Wave Model and the Local 3D Hydrodynamic Model, which is shown in full in Figure 5-1 and as a detail in Figure 5-2. The bathymetry implemented within the mesh is generated in a manner which is wholly consistent with that applied in the Regional Hydrodynamic Model. It is noted that the mesh applied is specifically for calibration. Additional mesh structure is applied at the active source locations for scenario testing with active WWTP and ASDP discharges.

A range of nominal mesh resolutions have been evaluated as part of the setup and testing phase of the Local Hydrodynamic Model. Ultimately the vast majority of calibration was performed using a nominal mesh resolution of 50m within the area of interest, coarsening to roughly 400m at the open boundaries. As with any numerical model study, the choice here is driven by seeking a manageable balance between the spatial resolution which would ideally be applied and that which is practicable from the perspectives of runtime and cost. Fundamental to this decision is the question of the dominant spatial scales which must be resolved to describe both ambient processes and those most important with respect to the assessment of ASDP plume behaviour. Appendix E documents a series of tests performed on an analogous model to address the sufficiency of the 50m nominal mesh resolution to describe the ASDP plume behaviour.

When the model is ultimately applied for plume characterisation, any waste constituents in the water column which exit the Local Hydrodynamic Model domain will be lost from the simulation. As such, it is also critical that the model domain is sufficiently large that it comfortably encompasses the potential impact area of the plume as well as ensuring that the character of the ASDP and WWTP plumes are not contaminated by boundary interactions. Based upon Water Corporation (2018) specifications, the requirements of the model will be met if it its extent is able to comfortably describe the 1:100 dilution contours for the ASDP plume and the 1:1000 dilution contours for the WWTP plume. Testing performed in connection with the setup of the Local Hydrodynamic Model with diagnostic plume releases indicated that these conditions would be comfortably met within the model domain shown in Figure 5-1. Formal simulations performed in connection with the Alkimos Scenarios Report (DHI, 2018) confirm this conclusion, with the above specified minimum dilution targets for both discharges being met at least 5km before reaching the model open boundaries, even considering instantaneous minimum dilution over the full water column.

5.4 Local Model Reef Map

As is evident from the graphics presented, the reef structure surrounding the project site is highly complex. The project is fortunate to have access to 5m resolution gridded LIDAR data from DoT (2016), though even such resolution (which is beyond that practical for the present application in terms of computational burden) is insufficient to resolve all detail on the irregular reef crests. This presents a range of challenges for accurate modelling, in terms of resolving geometry as well as parameterizing the energy losses and associated transformations which occur as waves and flow pass over the complex submerged features.

As a result of these complexities, the calibration process is involved and requires spatially if not also temporally variable roughness to mimic observed behaviour. In this process, it is preferable to distribute roughness in a manner which has as much physical basis as possible, which requires an accurate reef classification map.

The present work has relied upon a provisional reef characterisation map provided by BMT in Jan 2018, which is based upon image classification of satellite imagery in combination with surveyed ground truthing. The provisional map covers an area of roughly 10km

longshore x 5km crosshore, centred upon the WWTP ouffall. Three reef classes were delineated:

- Vegetated (macroalgal and seagrass habitats over reef or sand)
- Unvegetated (bare sand only)
- Exposed Reef (areas of the reef exposed at the time of image capture based on visual assessment of the image)

This large-scale provisional map was cross-checked against a more detailed, but spatially limited, benthic classification performed previously along the outfall corridor (Oceanica, 2006) shown in Figure 5-3. It was found that close alignment within the overlap area of the two maps was found if each was grouped into a simple binary mapping of “sand” and “all else”. As an additional cross-check, the provisional map was draped over a 3D rendering of the DoT LIDAR data (Figure 5-4), which confirmed that locally low-relief areas of the bathymetric map aligned well with those regions of the provisional reef map which were classified as “sand”.

As the 10 km x 5km coverage of the BMT provisional reef map is too small to the Local Model area, additional coverage was added through simple digitization of sand area from Google Earth imagery. The final reef map defined in the manner described is shown in Figure 5-5.

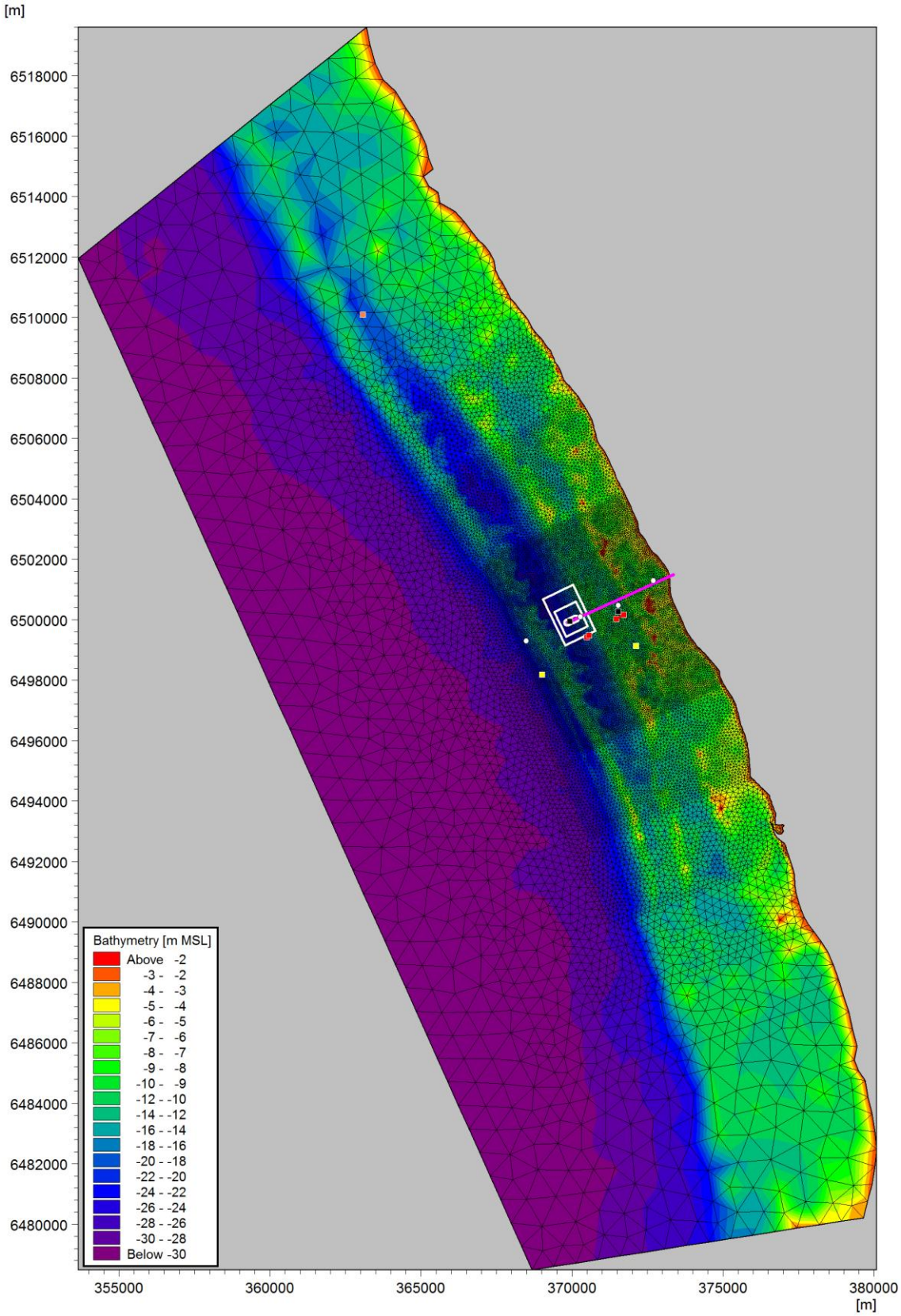

Figure 5-1 Unstructured mesh applied for the Local Wave Model and Local 3D Hydrodynamic Model (full area). White dots = Gardline AWACs, black squares = Fugro stations, orange square = Two Rocks Stn A mooring, magenta line = WWTP outfall pipe, yellow squares = candidate ASDP intakes, red squares = candidate ASDP outfalls.

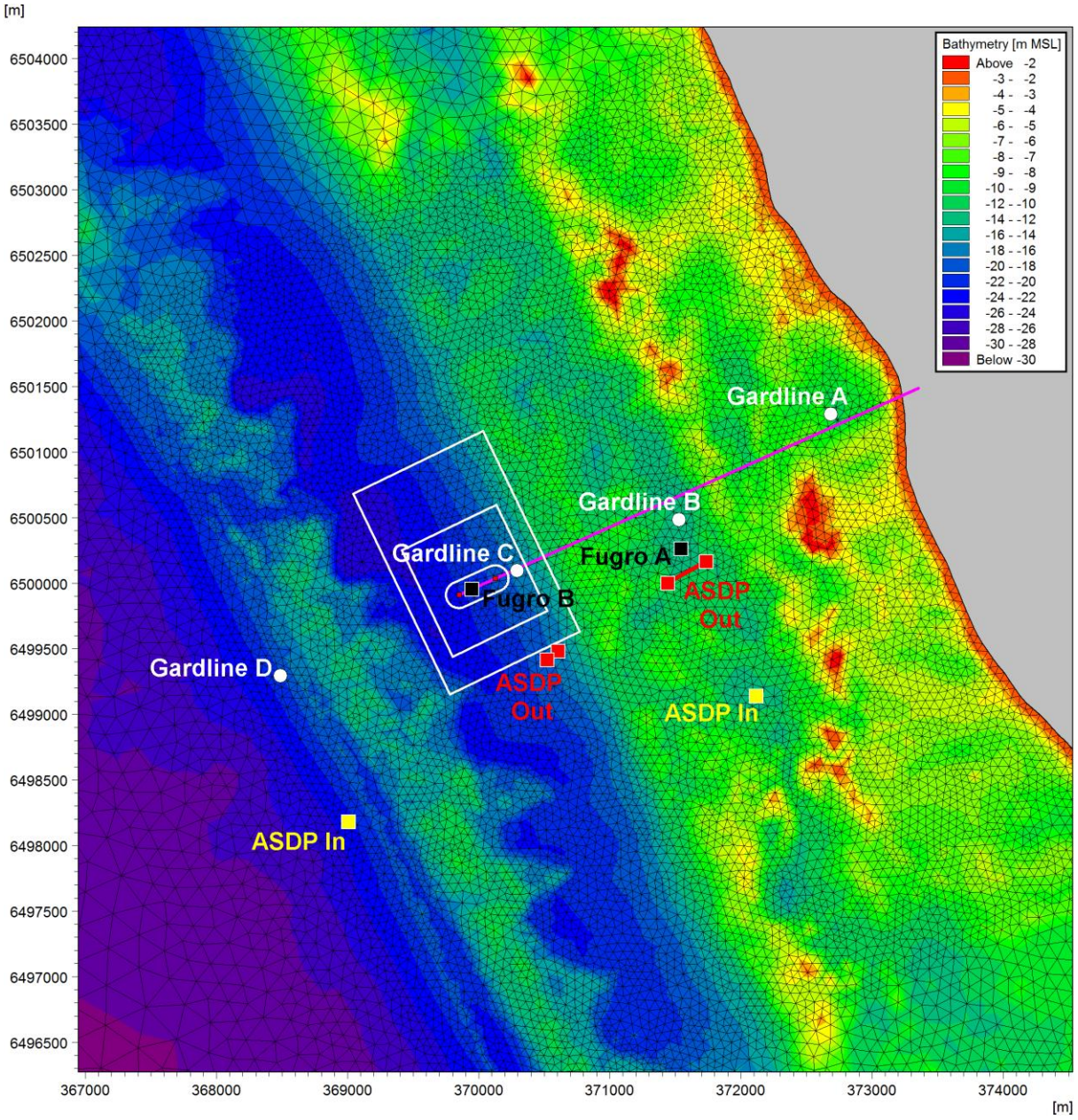

Figure 5-2 Unstructured mesh applied for the Local Wave Model and Local 3D Hydrodynamic Model (full area). White dots = Gardline AWACs, black squares = Fugro stations, magenta line = WWTP outfall pipe, yellow squares = candidate ASDP intakes, red squares = candidate ASDP outfalls.

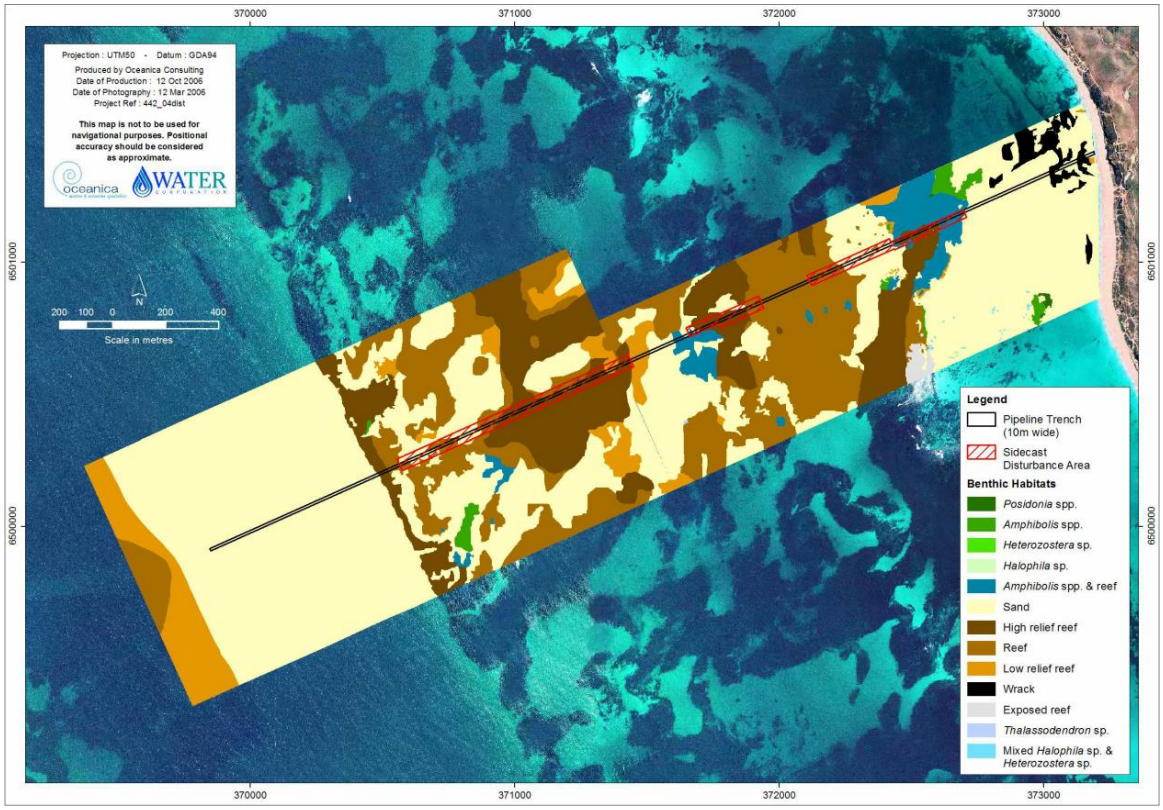

Figure 5-3 Reef seabed classicification performed in support of WWTP planning (Oceanica, 2006).

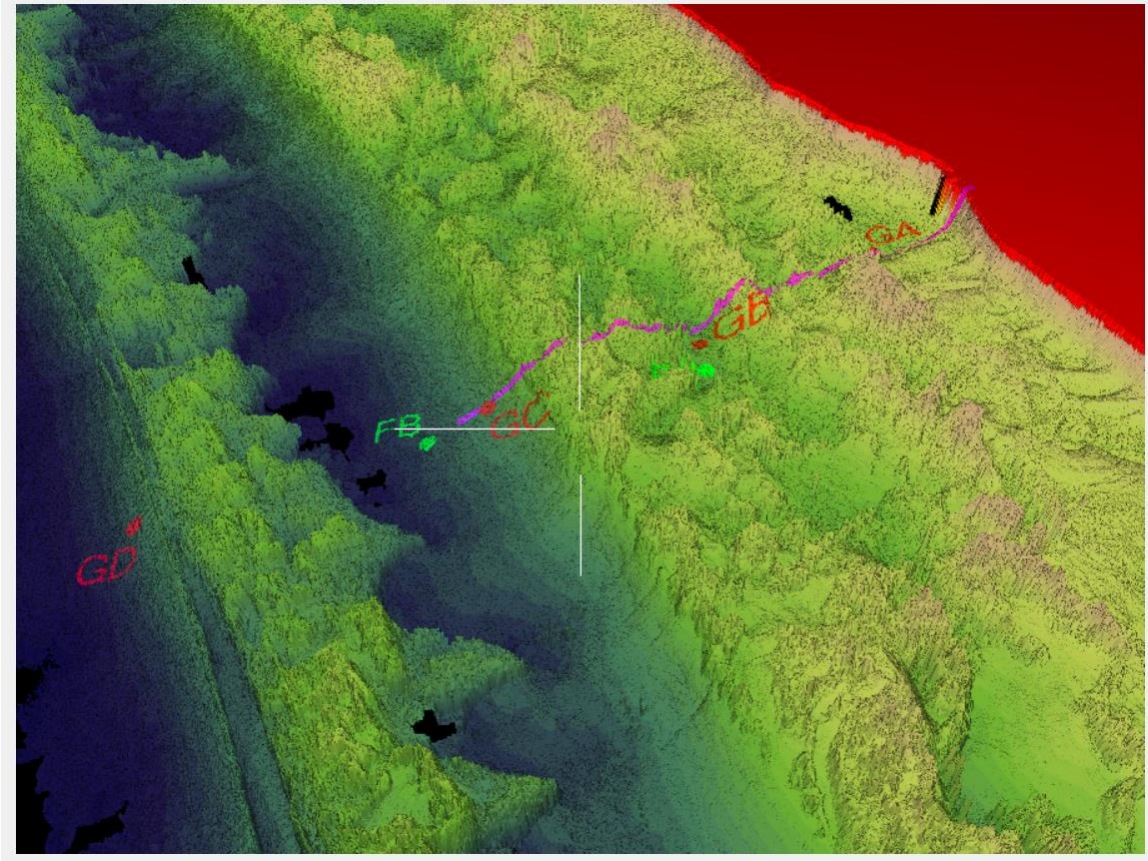

Figure 5-4 3D rendering of reef features around the WWTP outfall using 5m resolution DoT (2016) LIDAR.

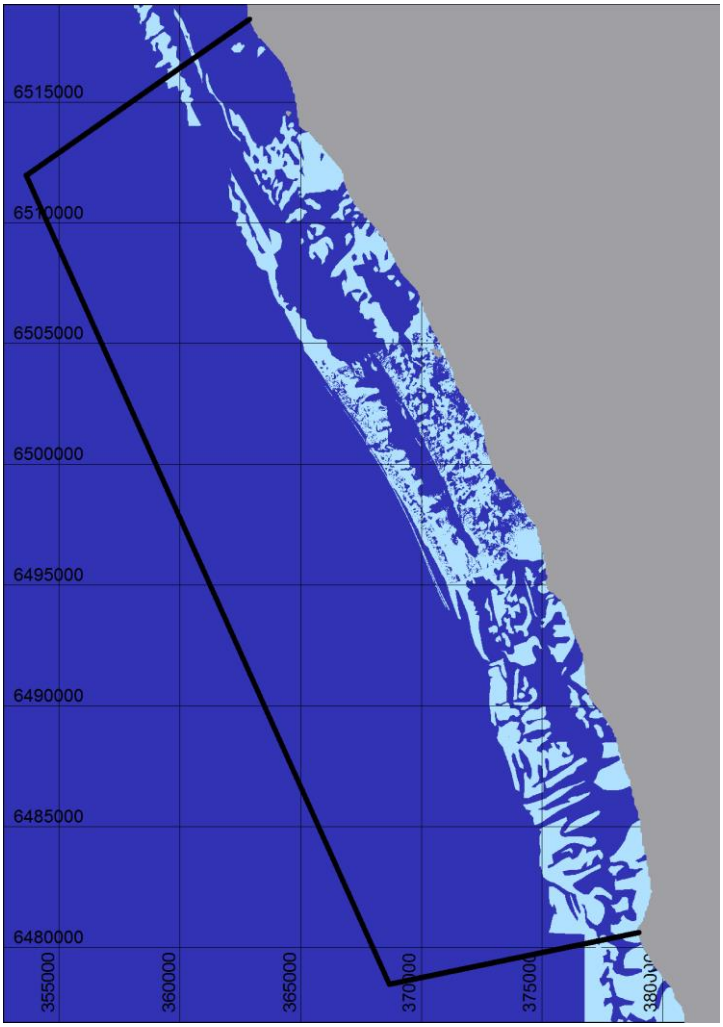

Figure 5-5 Baseline reef map (light blue = reef, dark blue = non-reef) generated for the project from a combination of a BMT reef classificaton map and visual image interpretation. Black line denotes location of Local Model.

5.5 Local Wave Model

5.5.1 Revised Wave Implementation Strategy

As noted in Section 2.2 and Figure 2-1, the original intent for the implementation of wave modelling for the project was for downscaling from global forcing in a manner analogous to that being performed for the hydrodynamics. Global and regional scale wave models were established via previous work for AMSA and others, and the regional model adapted for the present project. However, initial review of instrumentation and model testing for both local wave and flow models established several key facts for implementation:

- The complexity of the reef, in terms of geometry and roughness, means that the primary influence of waves is in terms of onshore transport in shallow areas of wave dissipation and offshore directed return flows in deeper areas which are channelised with a cross-shore orientation.

- Scattering and roughness induced by the reef means that longshore drift, in the classic sense, is not a major driver for nearshore circulation. Longshore directed

flows inshore are largely captured in the Local Hydrodynamic Model via wind forcing.

- Large reductions in wave energy occur across the reef profile even during moderate wave conditions. However, the effects of wave-driven currents on circulation are generally not noticeable even at the inshore instrumented locations unless wave heights approaching the reef are large, generally Hs > 1.5 to 2.0 m. For waves smaller than this threshold, the inclusion of wave-driven currents tends to induce bias in the modelled flows relative to observations.

- The effects of wave-driven currents are primarily felt at Gardline A, for large offshore waves, and primarily as offshore-directed return flow. Wave effects are smaller at Gardline B / Fugro A and negligible at Gardline C / Fugro C and at Gardline D.

- The universal inclusion of wave-driven currents leads to significant overpredictions of wave-induced currents unless extremely high bed roughness values are implemented to reduce their magnitude. However, such values tend to degrade the overall calibration performance of the Local 3D Hydrodynamic Model as tidal and other residual flows are overly dissipated as a consequence. This issue is partially mitigated through the implementation of wave-induced roughness over the reef in the Local 3D Hydrodynamic Model such that the effective roughness increases with the local wave conditions.

- Data provided from the AWAC instrument included bulk spectral values only, lacking directional spectra or a sea/swell split. This inherently limits the level of detail which is possible in the modelling of wave transformations approaching and over the reef.

5.5.2 Model Setup

Based on the above, the wave model provides a secondary forcing mechanism on the nearshore hydrodynamics, and flow results are improved if waves are fully excluded for much of the time. As such, a locally driven wave modelling solution was implemented whereby wave effects are selectively included in the Local Hydrodynamic Model only inshore of the WWTP Channel, and only when the incident measured wave height is Hs > 2m.

This approach is most practically achieved by forcing a quasi-stationary Local Wave Model directly by Alkimos measurements, thereby ensuring that the targeted wave condition can be readily imposed onto the reef when and where it is required with the above protocol. The calibration was executed with this approach, which is also viable for production so long as wave measurements at the site are available during the production periods. In the event that such data is not available during the required production periods, the Regional Wave Model would be required to supply the wave conditions incident to the reef.

The Local Wave Model is constructed upon the identical mesh applied for the Local 3D Hydrodynamic Model.

The model was calibrated using a setup which includes the outer reef and was forced by measured data from Gardline D. All wave transformation processes (breaking, bed friction) were disabled between the -20.7m contour and the offshore boundary, and bathymetry offshore was set to -20.7m. As such, no changes to the wave field occur between the offshore boundary and the Gardline D location, and the measured record is effectively applied as the boundary data for the model at the location of the -20.7m contour offshore of the outer reef.

Bed friction is applied in terms of a roughness map in which areas designated as “reef” in Figure 5-5 have been calibrated to provide the wave energy distribution as measured by the Gardline AWACs. The spatial distribution of energy dissipation over the reef then fuels wave-driven currents in the hydrodynamic model via radiation stress tensor fields. The final roughness map applied in the calibrated wave model is shown in Figure 5-6.

Table 5-1 Summary of Local MIKE21 SW spectral wave model configuration as applied for calibration.

Property	Local Wave Model
Model System	MIKE21FM SW
Nominal Mesh Resolution	750m → 50m
Coordinate System	MGA-50
Bathymetry	C-MAP, DoT LIDAR
Solver	Directionally decoupled parametric formulation
Directional Discretization	10°
Time step	Quasi-stationary
Boundary Conditions	Direct measurements from Gardline D AWAC
Met Forcing	Excluded
Bed Friction	Variable, based on simple reef classification map
Breaking	Battjes & Janssen (1978); γ_1=0.8, γ_2=α=1
Diffraction	Enabled
Water Level	Variable, based on Regional HD Model

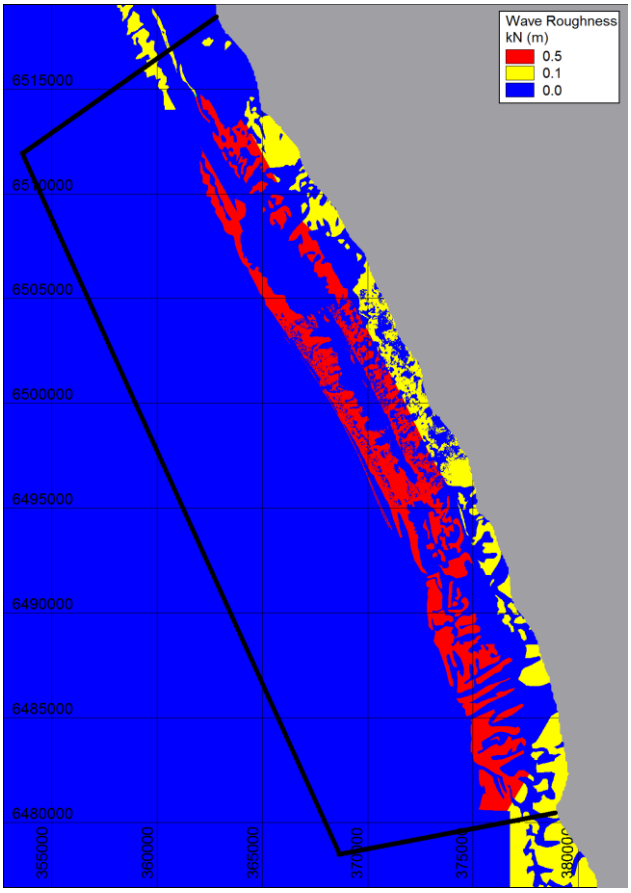

Figure 5-6 Roughness map applied in the final calibration of the Local Wave Model.

5.5.3 Calibration Results and Discussion

The Local Wave Model was calibrated during Deployment 1 of the Gardline AWACs over Apr-Jun 2017. Performance has been assessed in terms of time series comparisons at the four instruments as shown in Figure 5-6, where measurements from the DoT Rottnest buoy are also included for reference.

The comparisons between model and AWACs are seen to be extremely favourable for wave heights and periods, though Tp displays little modification within the study area for model or measurements. For directions the measurements show more scatter than the model, which is common. The mean wave directions at the inshore Gardline A station are particularly variable.

For additional perspective regarding the dominant wave mechanisms active over the reef, it is worthwhile to review the evolution of directional spreading from offshore to inshore as measured by the Gardline AWACs (Table 5-2). While directional spreading typically reduces (smaller DSD) due to refraction as waves propagate into shallower water towards shore when bathymetry is uncomplicated, the opposite is observed at Alkimos with values in the inner reef bearing little resemblance of the long-crested swell approaching offshore. This suggests that the wave energy is being strongly scattered due to the irregularity of the bathmetry. Such scattering reduces the amount and coherent directionality of wave energy dissipation that occurs over the reef. As such scattering is only partially captured in the model, this is one likely explanation for why wave-induced effects on mean flows tend to be overpredicted in the model. While the wave model reproduces the incremental reduction in wave height across the reef, this occurs in the model mainly through dissipation (which imparts energy into the mean current field) whereas a portion of this energy reduction in practice occurs through scattering.

Table 5-2 Measured directional spreading over Deployment from the four Gardline AWAC moorings, indicating strong scattering of waves over the inner reef.

Gardline AWAC Mooring (Deployment 1)	Measured Mean Directional Standard Deviation (DSD), °	Modelled Mean Directional Standard Deviation (DSD), °
D	19.6	18.9
C	20.5	26.8
B	25.0	33.1
A	38.0	32.3

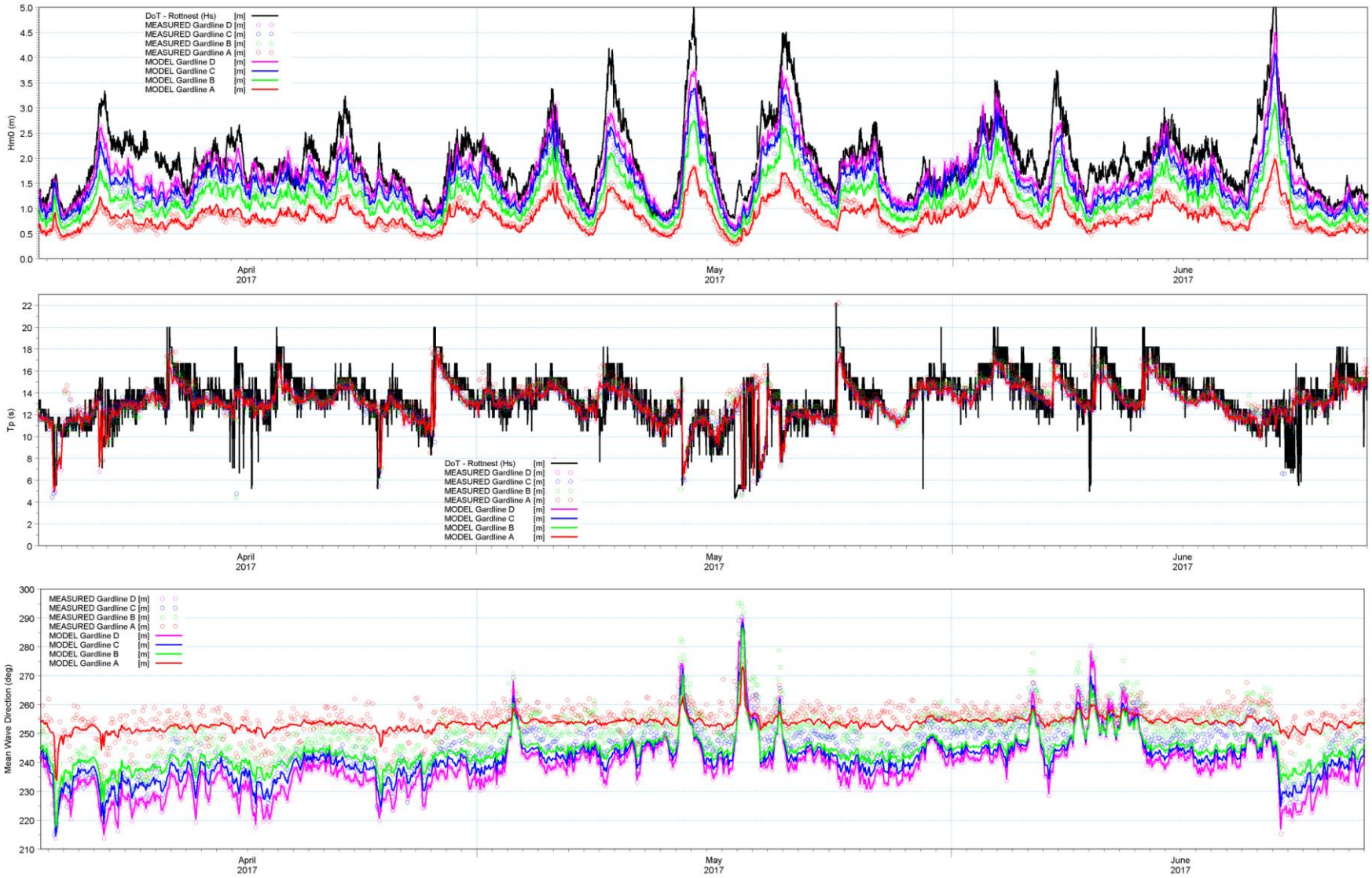

Figure 5-7 Calibration time series comparisons for the Local Wave Model at the Gardline AWAC moorings.

5.6 Local 3D Hydrodynamic Model

The Local 3D Hydrodynamic Model is forced by the combination of extracted boundary conditions from the Regional Hydrodynamic Model, measured wind records from Ocean Reef, and (when enabled) wave forcing from the Local Wave Model.

5.6.1 Model Setup

The spatial extent of the Local 3D Hydrodynamic Model is shown in Figure 5-1, with details shown in Figure 5-2.

The extent of the Local Hydrodynamic Model domain is approximately 40km in the longshore direction and 14km in the cross-shore direction. The offshore boundary terminates at about the -32m MSL depth contour. The nominal mesh resolution varies from 750m at the boundary down to 50m in a high resolution area centred around the Gardline AWAC validation stations as well as the WWTP outfall.

The arrangement of the innermost mesh resolution is tailored to both the model validation of ambient processes and the simulation of effluent plumes. Whilst reef features are present at scales below 50 metres, the key topographical features of relevance to plume dynamics (in particular flow pathways from the lagoon region to offshore) are captured by the 50m resolution. In addition, consideration was also made as to the coupling of the near-field with the far-field model for the plume scenarios. The most definitive evidence of the sufficiency of the mesh resolution is that the targeted near-field dilutions implemented into the far-field model (~1:30 and ~1:200 for the ASDP and WWTP respectively) in the test runs performed to date were reproduced accurately at the locations in the mesh where the sources were introduced, confirming that numerical dilution at the source locations does not occur and that mesh resolution is also adequate in this regard.

Basic details of the model construction are summarized below. Except where noted, the Local and Regional 3D Hydrodynamic Models may be assumed to be consistent in their construction:

- Constructed in in MGA-50 coordinates for ease of I/O with local geospatial data and to facilitate direct distance measurements when needed.
- Bathymetric data compiled in a manner fully consistent with that described for the Regional 3D Hydrodynamic Model.
- 13 sigma layers over the vertical, with additional resolution at both bottom (for ASDP plumes) and surface (for WWTP plumes), as shown in Table 5-3. The surface resolution is comparable to that applied in WP (2005) for the permitting of the WWTP.
- Boundary forcing is based on Flather boundary conditions, using water levels, and 2DV fields of velocity, salinity and temperature as extracted from the Regional 3D Hydrodynamic Model.
- Meteorological forcing is applied as hourly spatial CFSR wind as per Regional 3D Hydrodynamic Model.
- Spatially and temporally varying ambient salinity and temperature are included from the calibration simulations. A full heat exchange formulation is included in a manner consistent with the Regional 3D Model.

- Wave radiation stresses and wave-induced roughness are included inshore of the reef only, and only when Hs > 2m incident to the reef. As discussed in Section 5.5.1, the wave model provides a secondary forcing mechanism on the nearshore hydrodynamics, and flow results are improved if waves are fully excluded for much of the time. Wave effects are thus in practice included in the Local 3D Hydrodynamic Model for a minority of the time for most simulations. The Hs > 2m threshold is exceeded 23%, 55% and 15% of the time during the 2017 Autumn, Winter and Summer calibration/validation periods, respectively. The primary calibration simulations are executed without waves.

- Bed roughness is imposed in terms of an effective grain diameter for bedforms, which are input as a map to incorporate the significantly higher roughness over the reef. The final calibrated geometric grain size map is provided in Figure 5-9. Wave-induced roughness is applied by calculating the combined mean wave/current bed shear stress according to the parameterized method of Soulsby (1997), then calculating a modified roughness height which generates an equivalent bottom drag coefficient (Jones et al, 2014), in the manner shown in Figure 5-8.

Table 5-3 Vertical discretisation applied in Local 3D Hydrodynamic Model.

Layer # (from bottom)	Vertical Discretisation of σ-grid (% of water column)	Layer Thickness for Given Water Depth (m)		
		5m	10m	20m
13	5%	0.250	0.500	1.000
12	5%	0.250	0.500	1.000
11	5%	0.250	0.500	1.000
10	5%	0.250	0.500	1.000
9	10%	0.500	1.000	2.000
8	15%	0.750	1.500	3.000
7	15%	0.750	1.500	3.000
6	15%	0.750	1.500	3.000
5	10%	0.500	1.000	2.000
4	5%	0.250	0.500	1.000
3	5%	0.250	0.500	1.000
2	2.5%	0.125	0.250	0.500
1	2.5%	0.125	0.250	0.500

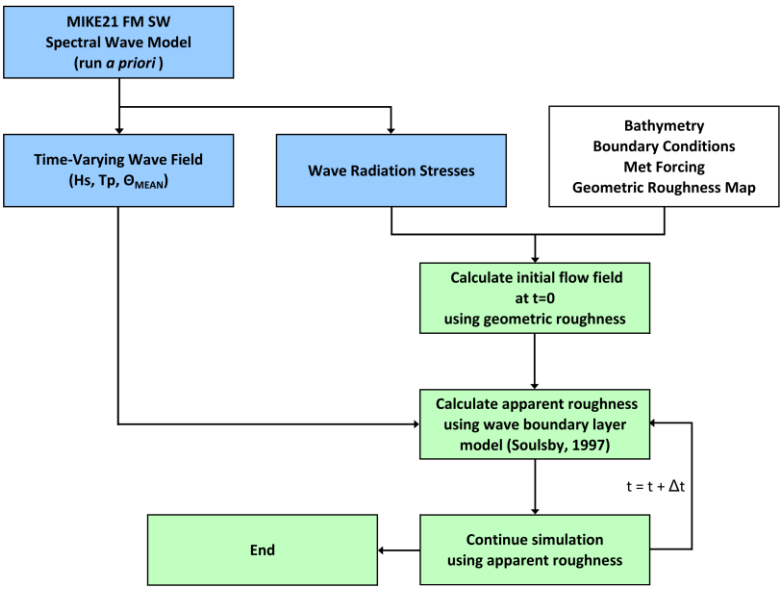

Figure 5-8 Flowchart showing the incorporation of wave-induced bed roughness into the Local 3D Hydrodynamic Model. Blue shaded boxes denote MIKE21 FM SW, green boxes MIKE3 FM HD.

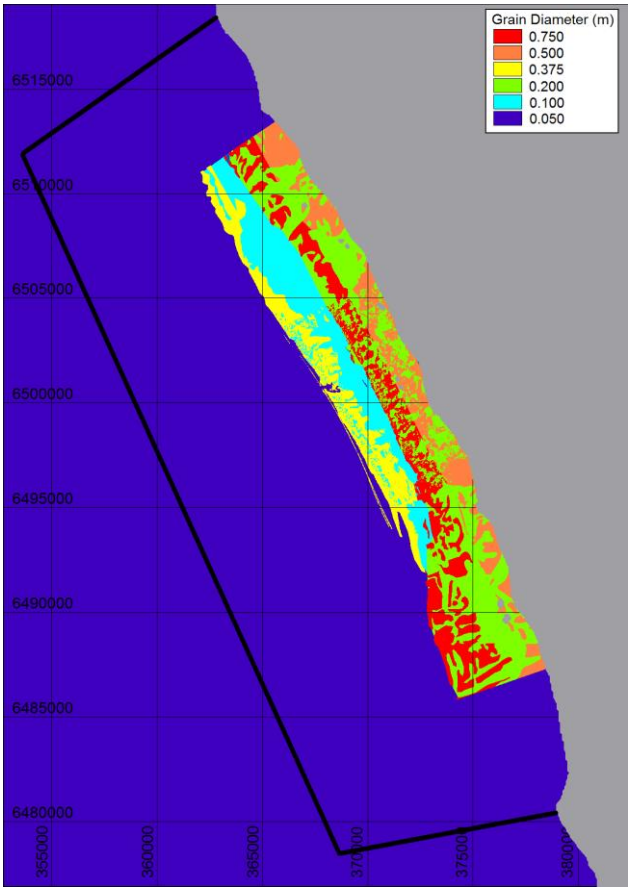

Figure 5-9 Geometric roughness (effective grainsize) map applied in the final calibration of the Local Hydrodynamic Model.

5.6.2 Calibration/Validation Results and Discussion

Calibration and validation graphics for the Local 3D Hydrodynamic Model are provided in thirteen appendices as described below.

Time series comparisons of water level, east and north current velocity components, as well as current speed and direction for depth-averaged currents and as near-surface and near-bottom currents, are provided in four appendices as follows:

- Appendix A1: Autumn 2017 Calibration
- Appendix A2: Autumn 2005 Validation
- Appendix A3: Winter 2017 Validation
- Appendix A4: Summer 2017 Validation

The upper pane of each plot includes a concise summary of the prevailing environmental forcing, including the wind speed (divided by 10 on right axis), the wind direction as arrows, the incident significant wave height as grey shading, and measured water level from the Hillarys ABSLMP site. Result graphics in the remaining panes are generated for sboth with and without the inclusion of wave forcing as indicated in the respective legends. Graphics in the remaining appendices are presented for the primary scenario (no waves) alone.

Current speed (u,v) scatter diagrams are similarly provided in the subsequent four appendices for depth-integrated, near-surface and near-bottom currents:

- Appendix B1: Autumn 2017 Calibration
- Appendix B2: Autumn 2005 Validation
- Appendix B3: Winter 2017 Validation
- Appendix B4: Summer 2017 Validation

Current speed Q-Q diagrams are similarly provided in the subsequent four appendices for depth-integrated, near-surface and near-bottom currents:

- Appendix C1: Autumn 2017 Calibration
- Appendix C2: Autumn 2005 Validation
- Appendix C3: Winter 2017 Validation
- Appendix C4: Summer 2017 Validation

The time series comparisons in Appendices A1 through A4 show that the model reproduces total water levels within the area of interest well, capturing modulations due to both tidal and nontidal mechanisms. For the Autumn 2005 validation period, no water levels were provided for this period from the project instruments, but the measured record from Hillarys ABSLMP station provides a basis for model comparison.

The current measurements generally exhibit far more noise than does the model. This is due in part to the inherent turbulence filtering of the model, and in part to the fact that differing sampling rates are being displayed (30min from model and 10min from data). However, the data inherently carries a large noise component. Many of the comparisons made here (as time series as well as scatter plots and Q-Q) would likely appear more favourable if the measured records were filtered. This is particularly true of bottom currents, which are weaker and for which the signal/noise ratio is inherently lower.

Cross-shore wave effects on the mean flow are captured at Gardline A, where large events during May generated offshore-directed return flows in the data during periods of weak winds where no other obvious forcing mechanism is present. The longshore components (which result from a combination of wave and wind forcing) tend to be underpredicted. A similar signal is also visible at Gardline B, though somewhat less distinctly. The inclusion of waves provides benefit to Gardline A and B for the 2017 Winter validation, while generating spurious flows at the outer stations. A strong wind/ and wave-driven event appears to have been recorded at Gardline B on 19 July, though the event was not seen at Gardline A or C. The model does not replicate this event.

The Autumn 2005 validation period is generally reproduced well by the model, though an apparent energetic event at the beginning of the surface Fugro A record is not captured by the model. The forcing for this event is not obvious, as both wind and waves were weak at the time. The measured directionality of the event is also curious, as the flow is directed toward southwest, which is counter to prevailing flow axes and is not present at all in the bottom instrument (see Figures B2-1a, B2-1b, B2-1c).

Current directionality, as indicated in the scatter diagrams in Appendices B1 – B4, are generally more favourable than was the case in Rev. A of this report. While some modelled distributions are somewhat more narrow than the measurements, this is attributable in part to instrument noise and the model reproduces the primary directional characteristics well. The complex directionality present at the near-bottom records at Gardline C and D are captured well.

In terms of current magnitude, it is clear that model carries a bias toward underprediction at Gardline A, a slight bias toward overprediction at Gardline B, and more stable agreement at the outer Gardline C and D stations. The inclusion of waves increases performance at Gardline A but weakens the agreement that outer stations.

Model skill values for current speeds during the calibration and validation periods are provided in Table 5-4 through Table 5-8. Indices provided include the root mean square error (RMSE), the mean absolute error (MAE), the index of agreement (IoA) per Willmott (1981), and the coefficient of determination (r^2). The RMSE and MAE (for which smaller values denote better performance) show a consistent trend toward yielding smaller values at the instruments lower in the water column and at the inshore locations, though this is primarily due to the magnitude of the current records themselves at those locations rather than on the model performance.

Model skill values for current speeds during the 2017 calibration period are provided in Table 5-4. Skill numbers for the present build of the model are mixed in relation to the model build reported in Rev. A of this report, with RMSE numbers for Gardline A and B increasing but those for Gardline C and D showing improvement.

RMSE values for surface and bottom current speeds during the Autumn 2005 validation period are provided in Table 5-5. These are calculated from the same measured/modelled subset as applied in WP(2005), and so is a direct comparison of model skill between the two studies. A direct comparison of the two models is provided in Table 5-6. DHI has a performance target to achieve a mean RMSE between the stations of less than 0.053, which was achieved the the Rev. A model (0.050) but not in the present build (0.057).

The IoA (which lies between 0 and 1, where larger values denote better performance) shows indistinct trends. For the Autumn 2005 validation period, the Fugro B comparison is notably better than Fugro A further inshore. For the Autumn 2017 period, the range of IoA values between the instruments is narrow, with Gardline C showing the highest values.

The r^2 values (which lie between 0 and 1, where larger values denote better performance) are generally low. While outright errors in modelled current magnitudes are certainly present, the low r^2 values are also affected by phase shifts (both leading and lagging) in

the model which is present when the model is otherwise reproducing the character of the observed flow behaviour reasonably well.

Table 5-4 Skill values from Local 3D Hydrodynamic Model for the Autumn 2017 calibration period.

Instrument and Elevation	RMSE (m/s)	MAE (m/s)	IOA	r^2
Gardline A – Depth Averaged	0.032	0.025	0.61	0.19
Gardline A – Upper (-2.1 m)	0.045	0.035	0.61	0.15
Gardline A – Lower (-8.1 m)	0.030	0.023	0.50	0.05
Gardline B – Depth Averaged	0.038	0.031	0.63	0.18
Gardline B – Upper (-3.3 m)	0.052	0.042	0.59	0.13
Gardline B – Lower (-11.3 m)	0.028	0.022	0.56	0.08
Gardline C – Depth Averaged	0.057	0.048	0.71	0.24
Gardline C – Upper (-4.5 m)	0.075	0.061	0.67	0.19
Gardline C – Lower (-16.5 m)	0.042	0.033	0.61	0.11
Gardline D – Depth Averaged	0.079	0.061	0.62	0.11
Gardline D – Upper (-4.3 m)	0.102	0.079	0.58	0.07
Gardline D – Lower (-19.3 m)	0.058	0.046	0.67	0.18

* Calculated over 16 Apr – 15 May 2017

Table 5-5 Skill values from Local 3D Hydrodynamic Model for the Autumn 2005 validation period.

Instrument and Elevation	RMSE (m/s)	MAE (m/s)	IOA	r^2
Fugro A – Depth Averaged	0.041	0.030	0.71	0.31
Fugro A – Upper (-3.0 m)	0.073	0.048	0.64	0.22
Fugro A – Lower (-9.0 m)	0.032	0.025	0.54	0.21
Fugro B – Depth Averaged	0.051	0.042	0.78	0.42
Fugro B – Upper (-3.5 m)	0.064	0.052	0.77	0.39
Fugro B – Lower (-15.5 m)	0.057	0.046	0.76	0.33

*[1] Calculated over 30 Apr – 28 May 2005

Table 5-6 Comparison of skill values (RMSE) for surface and bottom current speed from present model and from the model applied in the permitting of the Alkimos WWTP plant (WP, 2005). These values are calculated over the same duration as was used in WP (2005) and are directly comparable.

Instrument and Elevation	RMSE (m/s)*	
	WP (2005)	Present Model
Fugro A – Upper (-3.0 m)	0.086	0.073
Fugro A – Lower (-9.0 m)	0.025	0.032
Fugro B – Upper (-3.5 m)	0.096	0.064
Fugro B – Lower (-15.5 m)	0.058	0.057
Mean	0.066	0.057

*[1] Calculated over 30 Apr – 28 May 2005

Table 5-7 Skill values from Local 3D Hydrodynamic Model for the Winter 2017 validation period.

Instrument and Elevation	RMSE (m/s)	MAE (m/s)	IOA	r^2
Gardline A – Depth Averaged	0.032	0.023	0.60	0.03
Gardline A – Upper (-2.1 m)	0.044	0.034	0.59	0.04
Gardline A – Lower (-8.1 m)	0.024	0.019	0.64	0.03
Gardline B – Depth Averaged	0.048	0.037	0.63	0.03
Gardline B – Upper (-3.3 m)	0.063	0.049	0.56	0.02
Gardline B – Lower (-11.3 m)	0.033	0.026	0.63	0.02
Gardline C – Depth Averaged	0.075	0.061	0.64	0.03
Gardline C – Upper (-4.5 m)	0.089	0.072	0.61	0.02
Gardline C – Lower (-16.5 m)	0.040	0.032	0.72	0.02
Gardline D – Depth Averaged	0.084	0.069	0.60	0.01
Gardline D – Upper (-4.3 m)	0.103	0.083	0.62	0.02
Gardline D – Lower (-19.3 m)	0.053	0.043	0.63	0.01

* Calculated over 23 Jun – 22 Jul 2017

Table 5-8 Skill values from Local 3D Hydrodynamic Model for the Summer 2017 validation period. Gardline D measurements are unusable during this period.

Instrument and Elevation	RMSE (m/s)	MAE (m/s)	IOA	r^2
Gardline A – Depth Averaged	0.037	0.029	0.70	0.32
Gardline A – Upper (-2.1 m)	0.047	0.039	0.68	0.20
Gardline A – Lower (-8.1 m)	0.041	0.032	0.56	0.14
Gardline B – Depth Averaged	0.039	0.031	0.77	0.23
Gardline B – Upper (-3.3 m)	0.061	0.048	0.67	0.19
Gardline B – Lower (-11.3 m)	0.034	0.026	0.63	0.06
Gardline C – Depth Averaged	0.056	0.046	0.78	0.19
Gardline C – Upper (-4.5 m)	0.084	0.071	0.72	0.20
Gardline C – Lower (-16.5 m)	0.055	0.039	0.46	0.00
Gardline D – Depth Averaged	--	--	--	--
Gardline D – Upper (-4.3 m)	--	--	--	--
Gardline D – Lower (-19.3 m)	--	--	--	--

* Calculated over 17 Nov – 16 Dec 2017

Near-bottom water temperature timeseries plots are provided in Appendix D for the 2017 Autumn Calibration period, as well as 2017 Winter and Summer Validation periods. There are no available temperature records associated with the 2005 Fugro data. Temperature predictions in the model are seen to generally follow correct shorter-term trends in terms of temporal variations as well as spatially between stations. Persistent offsets of base temperature levels are present in the winter (model warmer than data) and summer (model

colder). The origin of these offsets lie primarily in the boundary data derived from the Regional 3D Model.

As a check of the predicted stratification in the area of interest, particularly the WWTP outfall, Figure 5-10 shows percentiles of the vertical density difference predicted in the three 2107 30 day simulation periods in relation to that observed by summer CTD profiles from previous years. The comparison shows that the level of stratification generated in the model varies, with the Winter and Summer simulations generating a similar distribution while the Autumn simulation generates a water column which is typically less stratified. Figure 5-11 shows a similar comparison, but where the model contribution originates from the 12-month pre-development simulation reported in DHI (2018). This figure also shows the largest stratification occurring in summer, though it also shows considerable scatter from month to month. For reasons already noted (Section 3.6), a direct comparison with the available CTD measurements is an imperfect comparison as the measurements derive from multiple years of a specific season, and also contain the contribution from the existing WWTP outfall.

Whilst further work is possible to improve the simulation of temperature, salinity and stratification, the extent to which this additional effort will improve calibration statistics is impossible to determine *a priori*. Uncertainties exist across numerous aspects of the calibration (eg bottom roughness, wave effects, stratification effects), as is typical, and prudent design, scenario testing and engineering judgement will be required, as is also typical, to handle these uncertainties and their impacts on site selection for the intake and outfall locations.

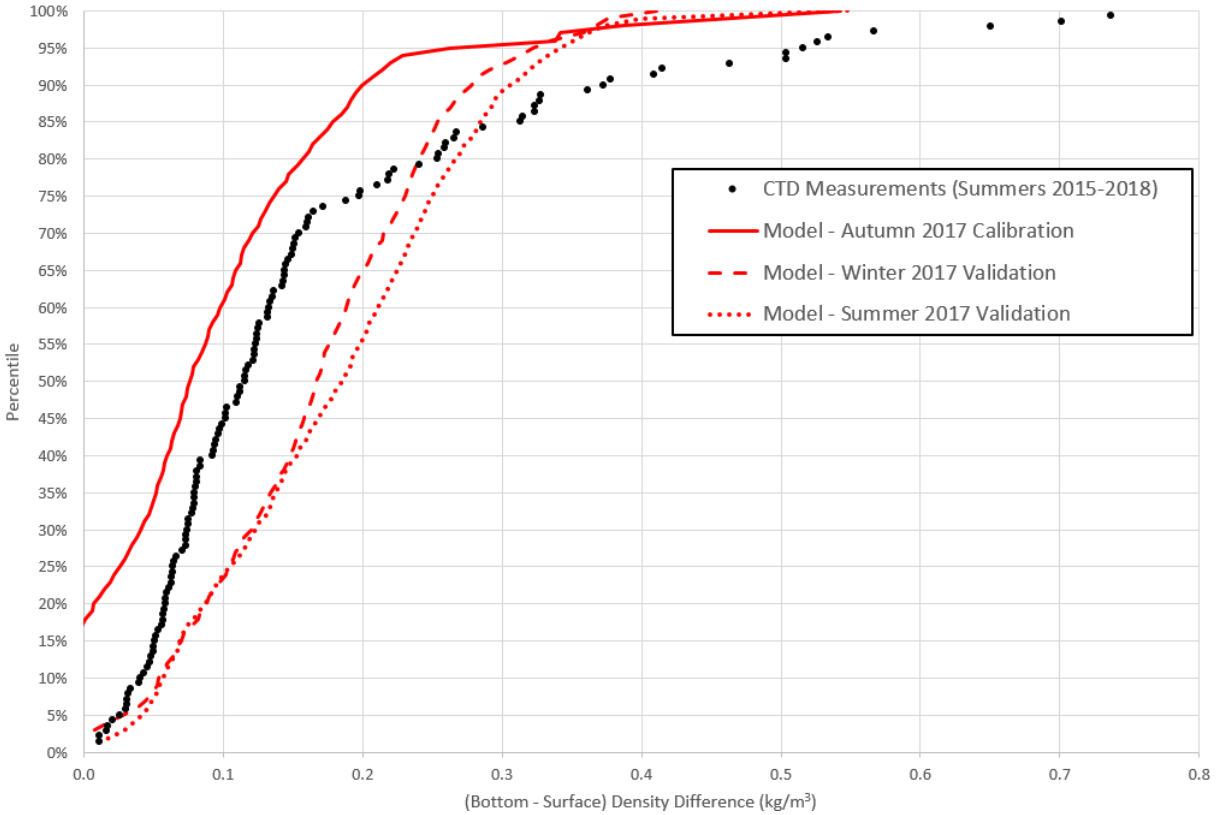

Figure 5-10 Measured and modelled vertical density differences at WWTP outfall. Measurements taken during successive summers over 2015-2018, while model results are extracted from three 30 day periods in 2017.

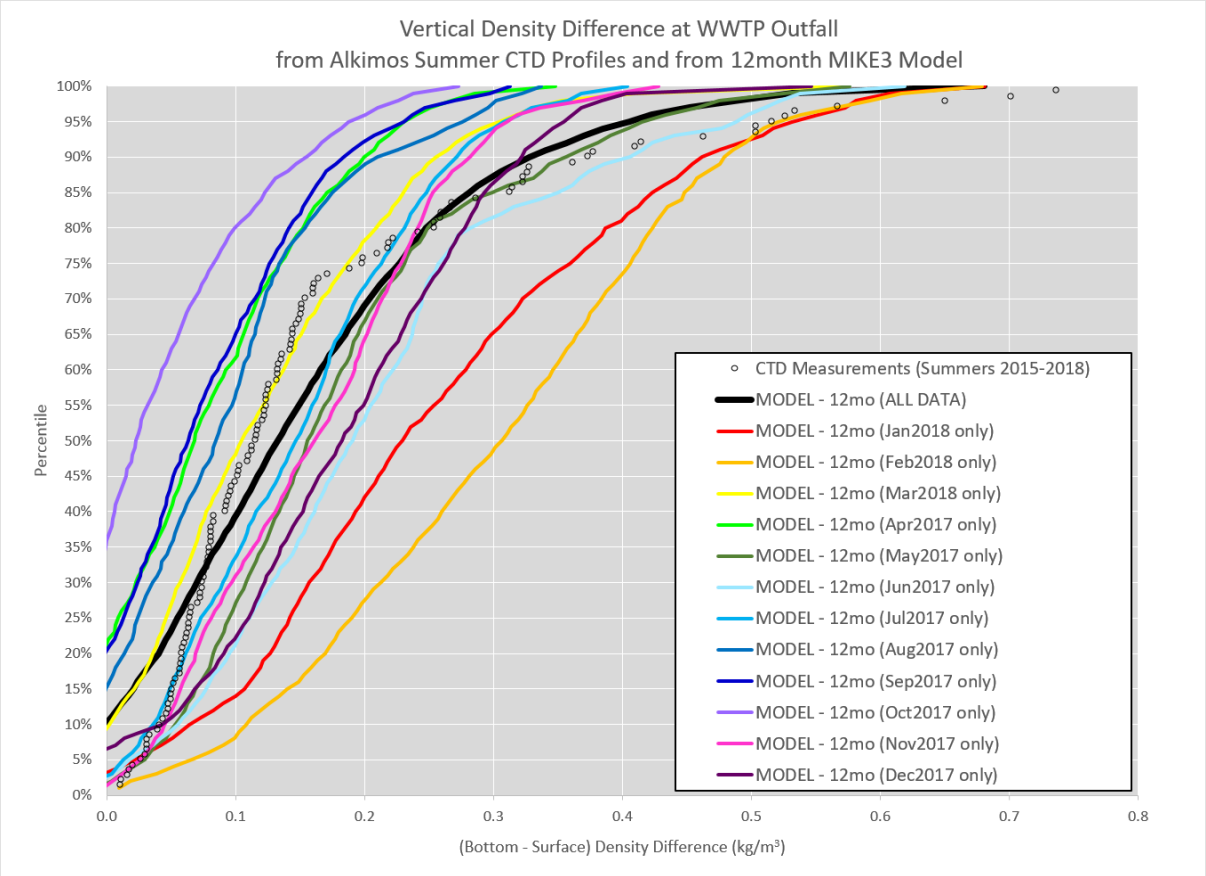

Figure 5-11 Measured and modelled vertical density differences at WWTP outfall. Measurements taken during successive summers over 2015-2018, while model results are extracted monthly from a pre-development MIKE3 simulation over March 2017 – Feb 2018 as reported in DHI (2018).

6 References

BoM (2018a): Surface wind records from Rottnest Island, Swanbourne, Ocean Reef and Hillarys, acquired from BoM by DHI under license.

BoM (2018b): “Australian Baseline Sea Level Monitoring Project Hourly Sea Level [ABSLMP] and Meteorological Data”. http://www.bom.gov.au/oceanography/projects/abslmp/data/index.shtml [last access May 2018], Australian Bureau of Meteorology.

Cheng, Y. and O.B. Andersen (2010): “Improvement in global ocean tide model in shallow water regions”. Poster, SV.1-68 45, OSTST, Lisbon, Oct.18-22.

CSIRO (2006): “Two-Rocks Moorings Data Report”, CSIRO Marine and Atmospheric Research Paper 005, Jan 2006.

DHI (2018): “Alkimos Hydrodynamic Modelling, Draft Scenarios Report”, Rev. A, Report prepared for Water Corporation, 21 December 2018.

DoT (2016): 5m gridded LIDAR data from 2016 survey, WA Dept of Transport. (Provided to DHI by DoT on 07 Jun 2018).

DoT (2009): 5m gridded LIDAR data from 2009 survey, WA Dept of Transport. (Provided to DHI by BMT 26 Sep 2017).

Fugro (2005): “Alkimos Current & Wave Measurement Study, 30 April 2005 to 26 June 2005”, Report prepared for Water Corporation, Fugro GEOS Ref. C10658/3710/R1, September 2005.

Gallop, S.L., F. Verspecht and C.B. Pattiaratchi (2012). Sea breezes drive currents on the inner continental shelf off southwest Western Australia. Ocean Dynamics. 62: 569-583.

HYCOM (2016): Data from HYCOM+NCODA Global 1/12° Analysis (GLBa0.08), www.hycom.org, HYCOM Consortium.

Jeppesen (2014): C-MAP Global Chart Database.

Jones, O., J.A. Zyserman and Y. Wu (2014):” Influence of apparent roughness on pipeline design conditions under combined waves and current”, Proceedings of the ASME 2014 33rd International Conference on Ocean, Offshore and Arctic Engineering,

Mihanovic, H., C. Pattiaratchi and F. Verspecht (2016). “Diurnal sea breezes force near-inertial waves along Rottnest Continental Shelf, Southwestern Australia”. Journal of Physical Oceanography. 46: 3487-3508.

MixZon (2015): "CORMIX User Manual - A Hydrodynamic Mixing Zone Model and Decision Support System for Pollutant Discharges into Surface Waters", MixZon Inc.

Oceanica (2006): “Alkimos BPPH Loss Assessment”, Memo prepared for Water Corporation, 12 Oct 2006.

RPS APASA (2016): “Ocean Reef Marina Development, Phase 2: Water Quality Modelling”, Report prepared for MP Rogers, Rev. 5, 01 Aug 2016.

Saha, S., et al. (2011, updated monthly): "NCEP Climate Forecast System Version 2 (CFSv2) Selected Hourly Time-Series Products". Research Data Archive at the National Center for Atmospheric Research, Computational and Information Systems Laboratory. http://dx.doi.org/10.5065/D6N877VB.

Soulsby, R. L. (1997): *Dynamics of Marine Sands: a Manual for Practical Applications*, Thomas Telford Publications, London.

UNESCO (2014): The GEBCO_2014 SID Grid, version 20141103, http://www.gebco.net.

Water Corporation (2018): "Alkimos SDP – Marine Modelling Guidance to Modelling Consultant, Technical Advice (Version 4)", Doc# 19411717v4, July 2018.

WP (2005): "Alkimos Wastewater Treatment Plant, Hydrodynamic Modelling of Outlet Discharge", Report prepared for Water Corporation, Worley Parsons ref. 302/08986/a04, 25 Oct 2005.

WP (2008): "Alkimos Outfall Dredge Management Plan, Hydrodynamic and Sediment Transport Modelling of Dredge Plume", Report prepared for Alkimos Alliance, Worley Parsons ref. 301012-00064/0, 28 Jun 2008.

APPENDIX A1

Local 3D Hydrodynamic Model Calibration - Time Series Plots

Autumn 2017

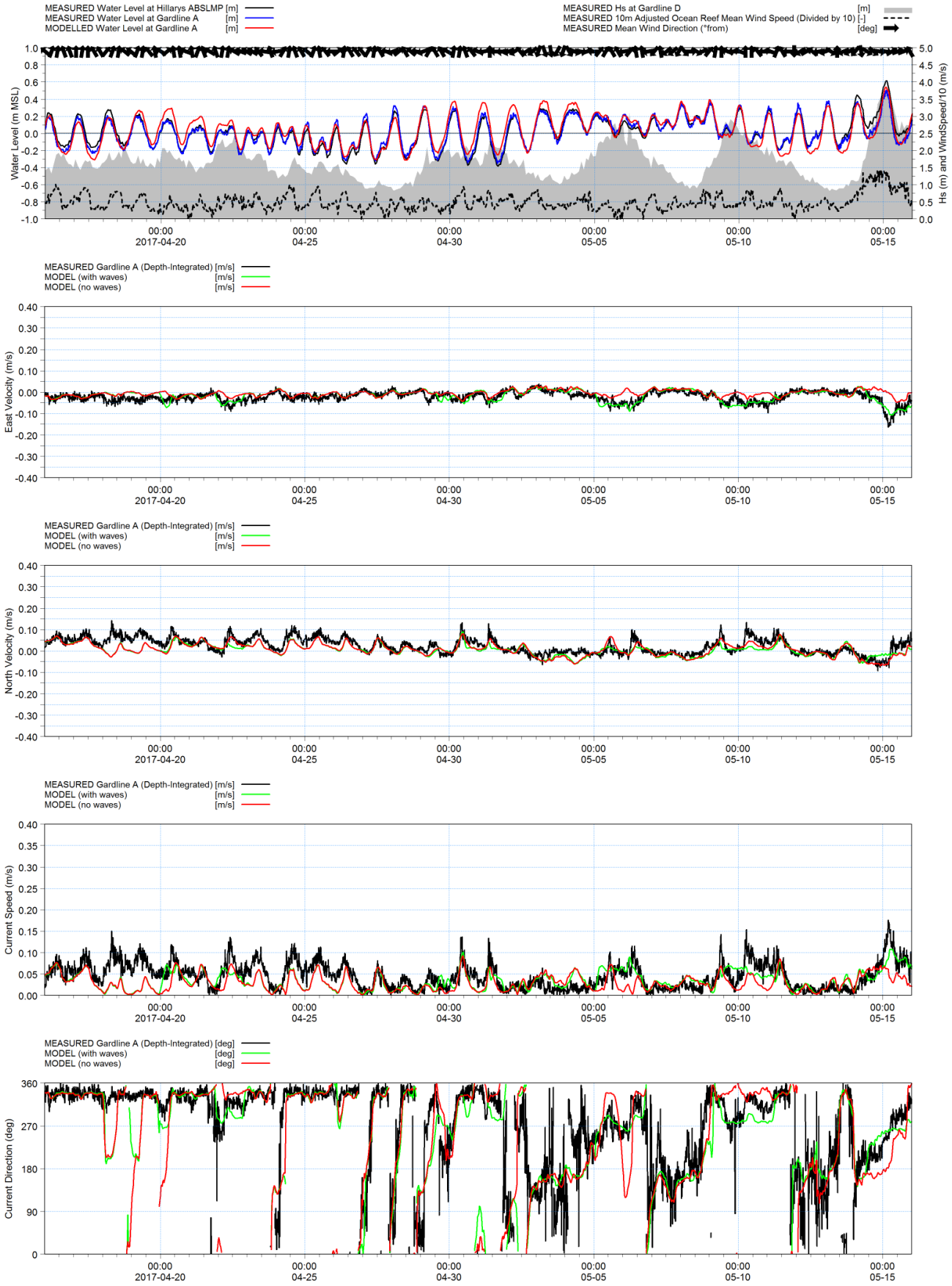

Figure A1-1a: Local 3D Model vs. Gardline A. Depth-integrated, Autumn 2017.

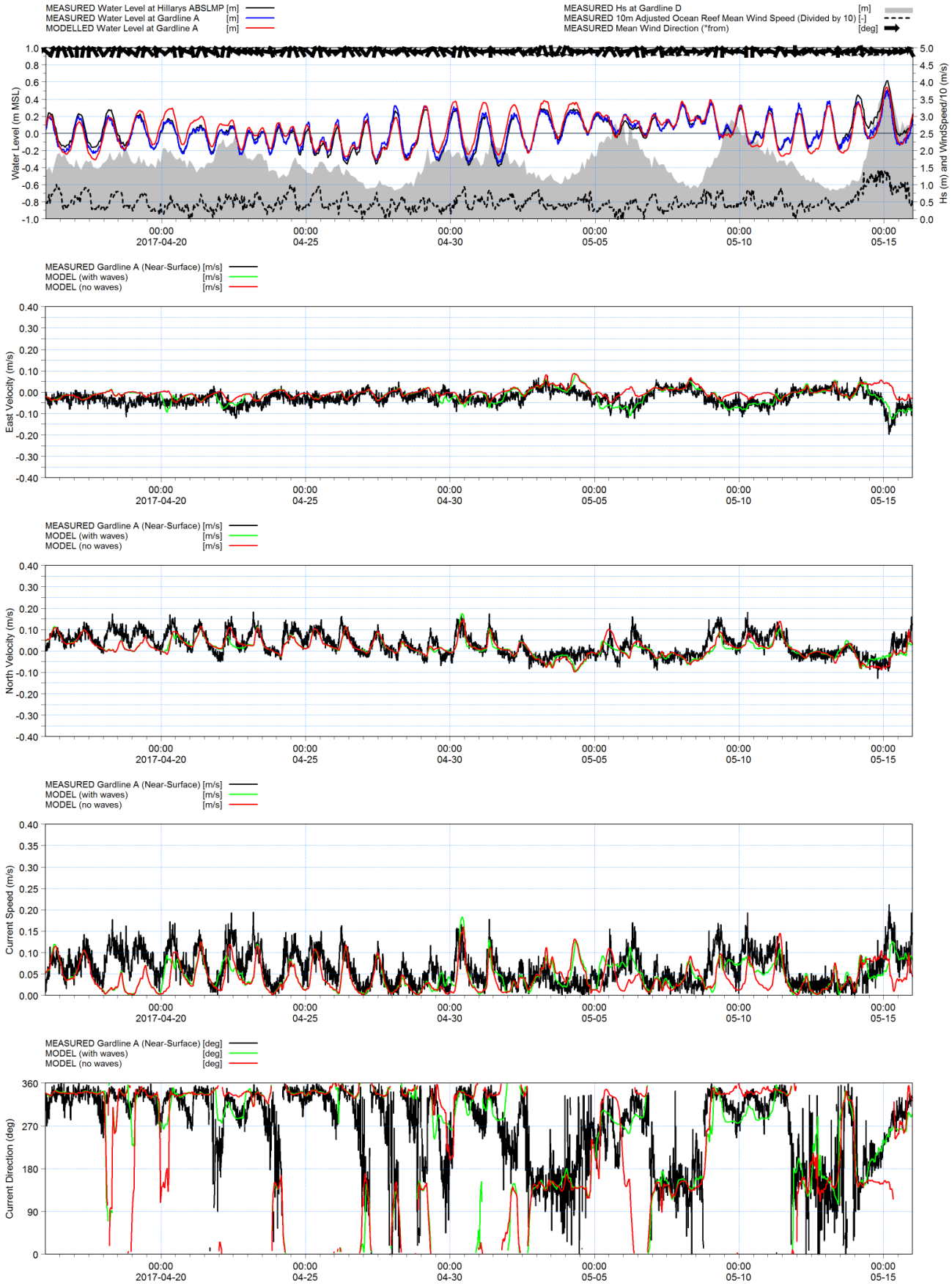

Figure A1-1b: Local 3D Model vs. Gardline A. Surface, Autumn 2017.

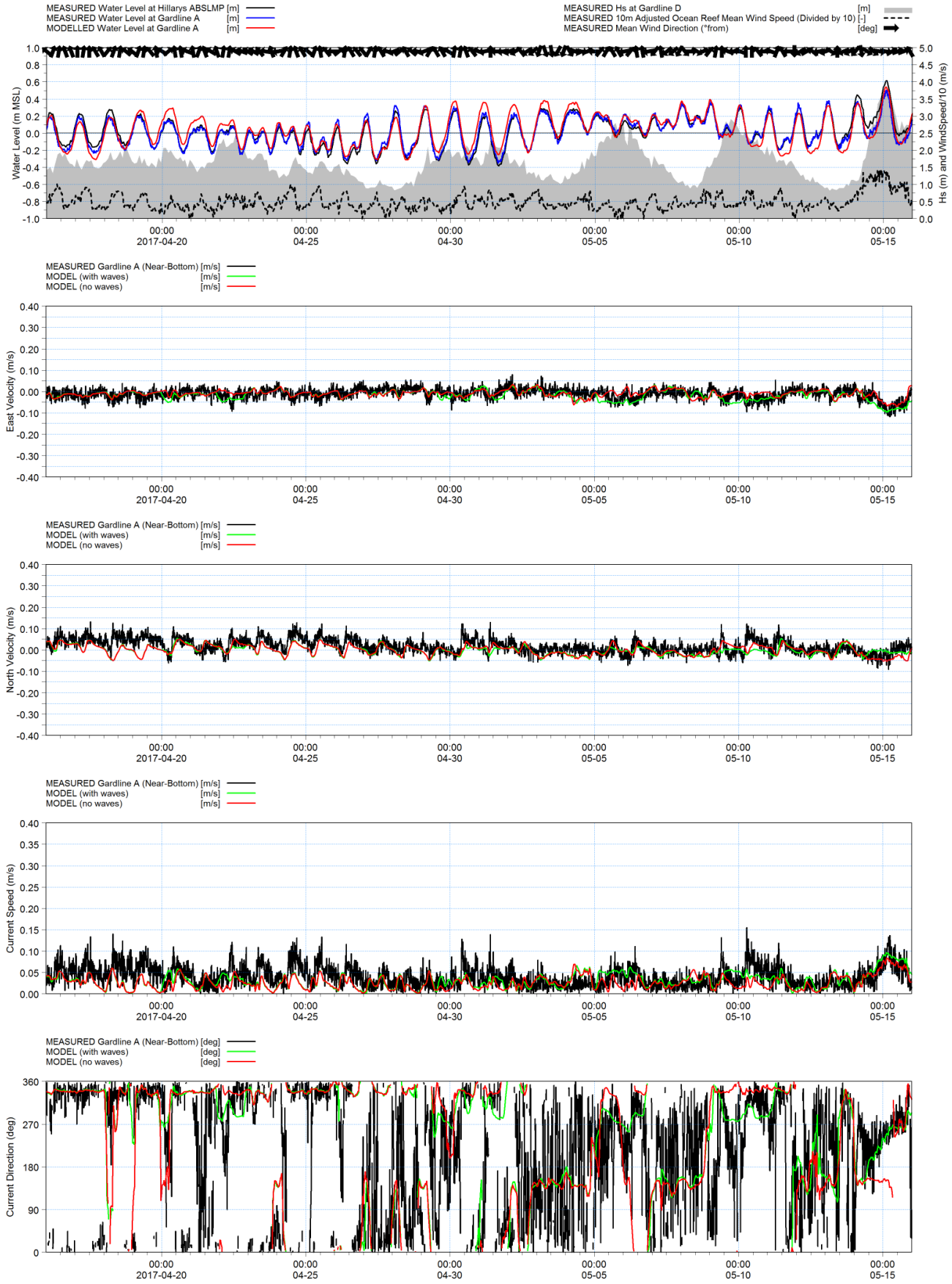

Figure A1-1c: Local 3D Hydrodynamic Model vs. Gardline A. Bottom, Autumn 2017.

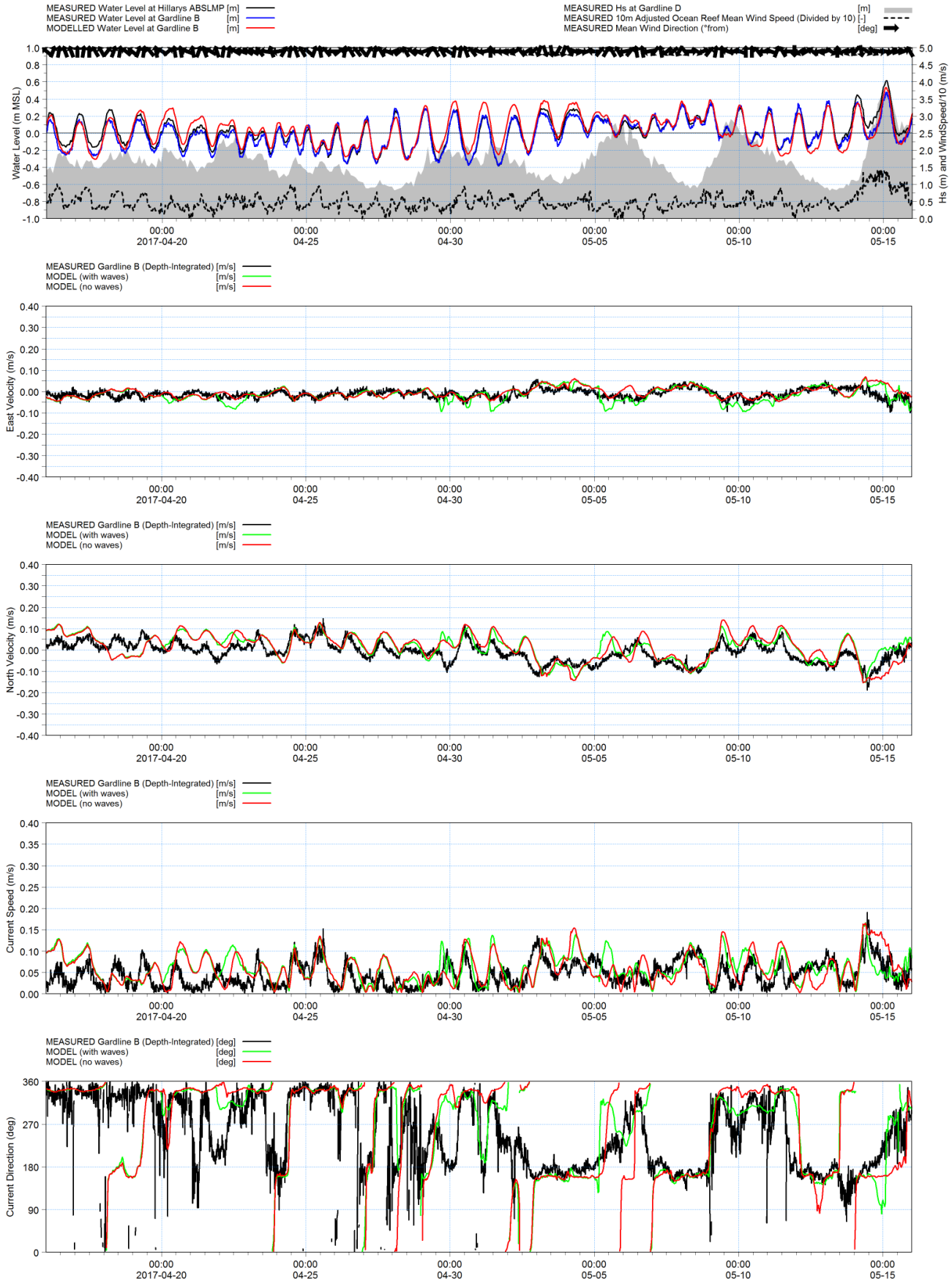

Figure A1-2a: Local 3D Model vs. Gardline B. Depth-integrated, Autumn 2017.

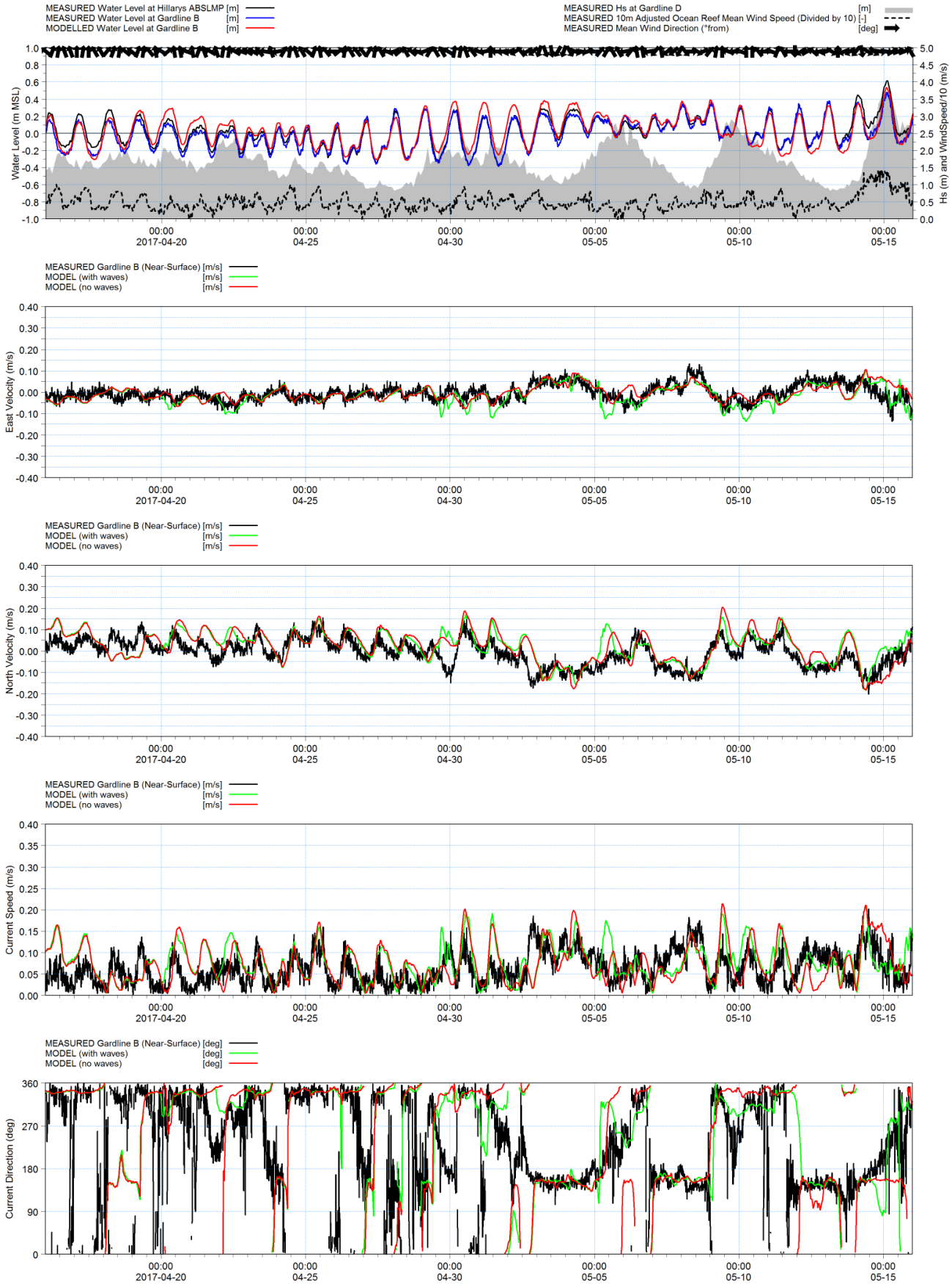

Figure A1-2b: Local 3D Hydrodynamic Model vs. Gardline B. Surface, Autumn 2017.

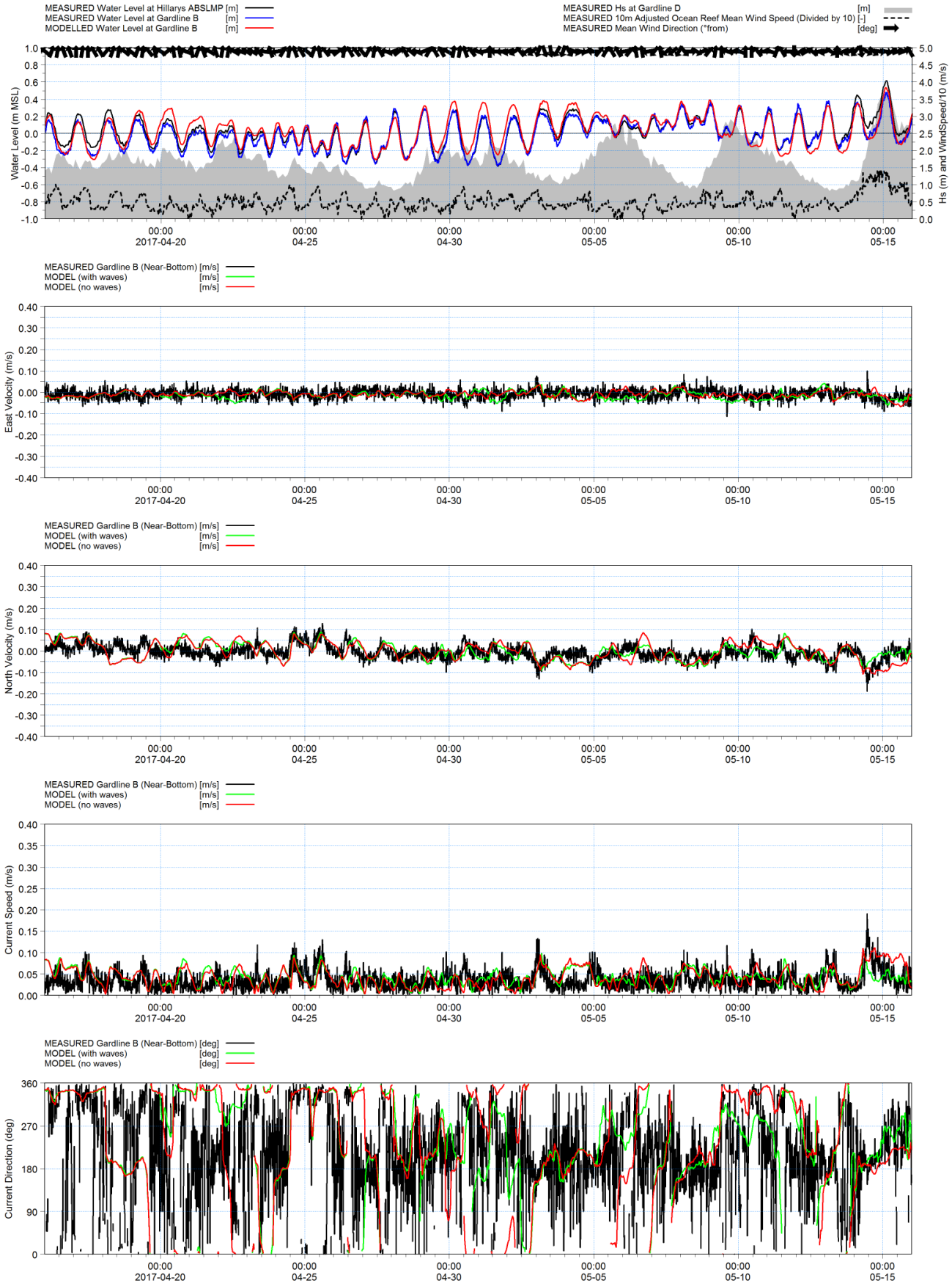

Figure A1-2c: Local 3D Hydrodynamic Model vs. Gardline B. Bottom, Autumn 2017.

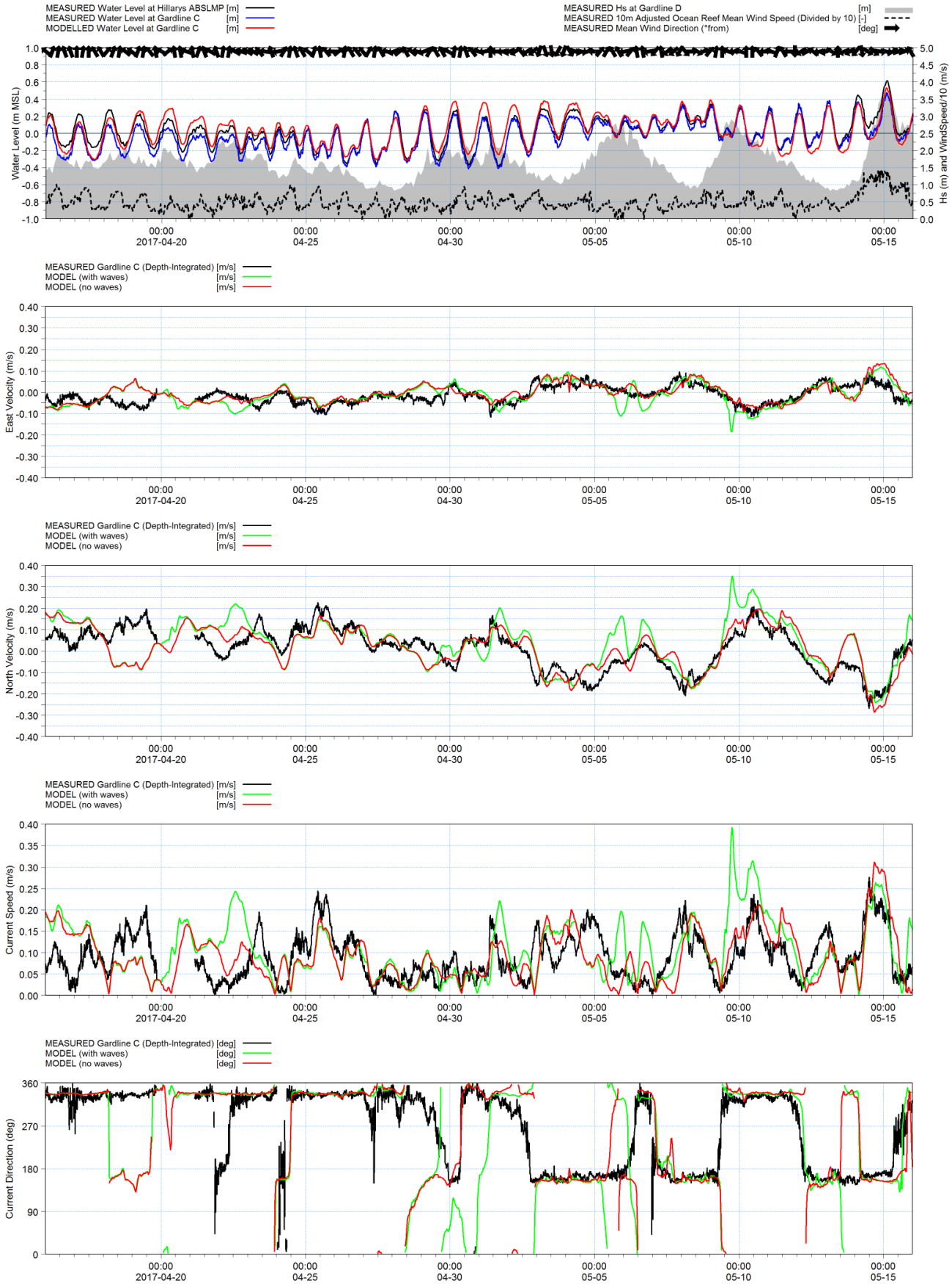

Figure A1-3a: Local 3D Hydrodynamic Model vs. Gardline C. Depth-integrated, Autumn 2017.

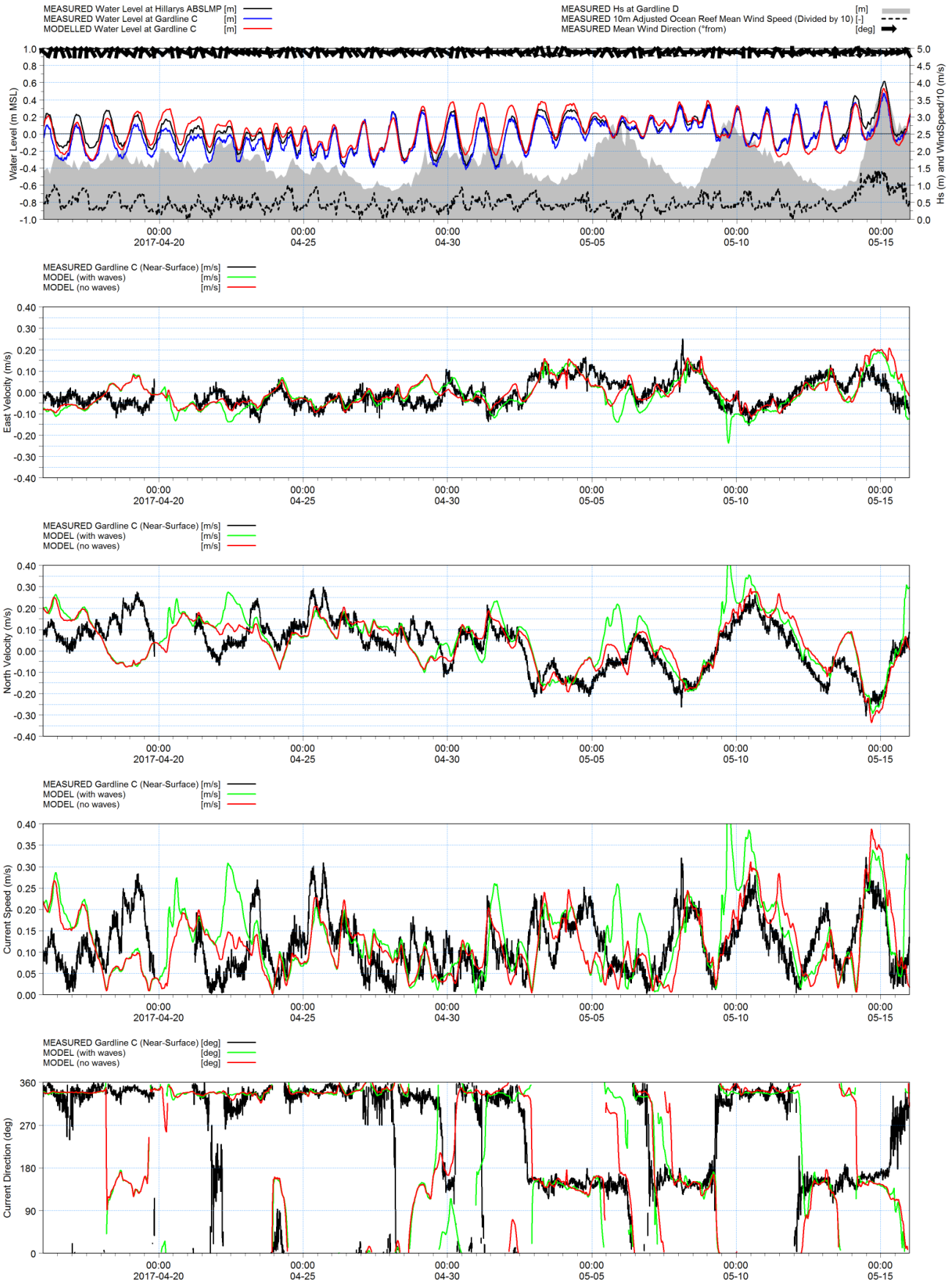

Figure A1-3b: Local 3D Hydrodynamic Model vs. Gardline C. Surface, Autumn 2017.

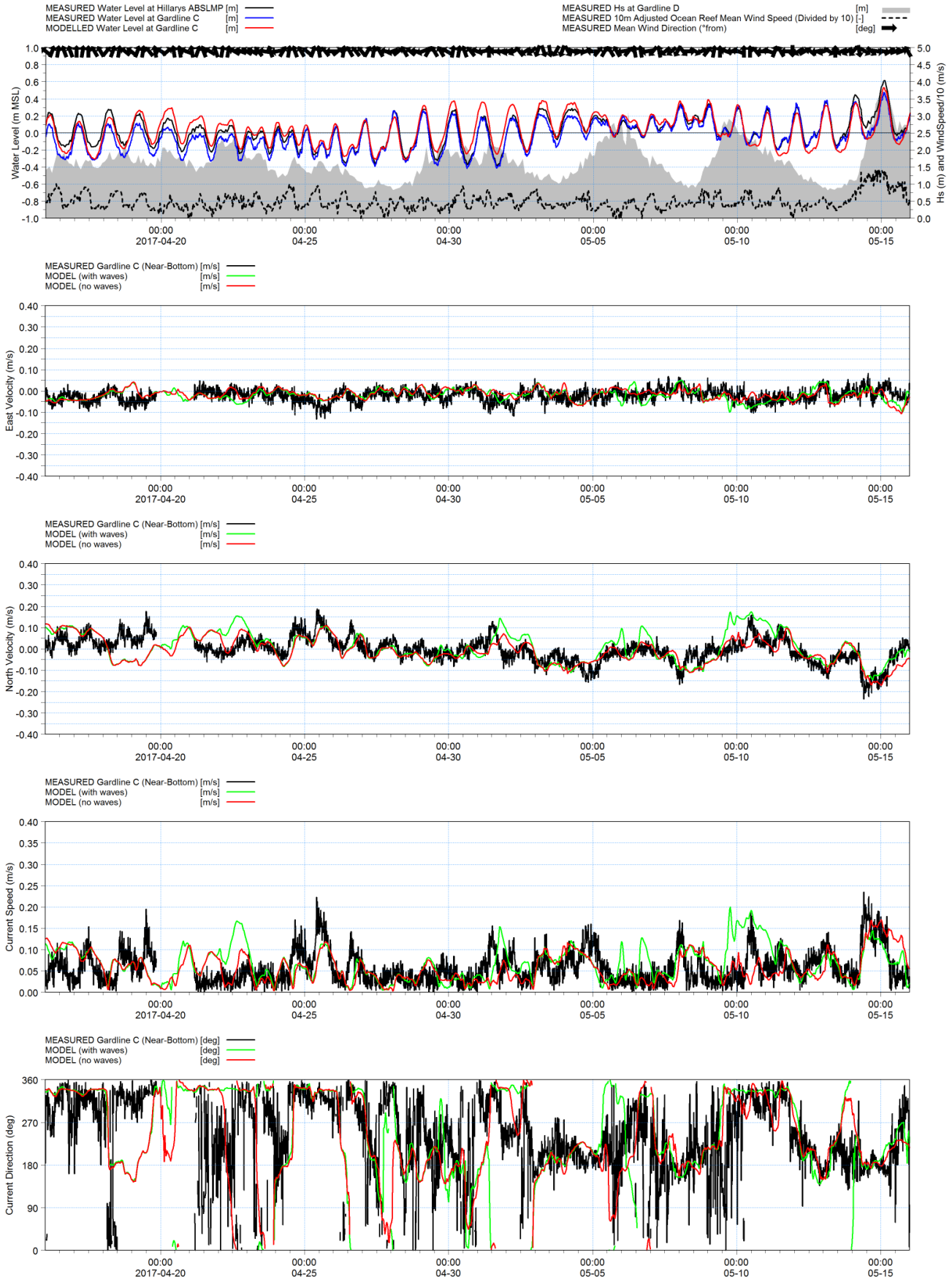

Figure A1-3c: Modelled vs. measured timeseries – Local 3D Hydrodynamic Model vs. Gardline C. Bottom.

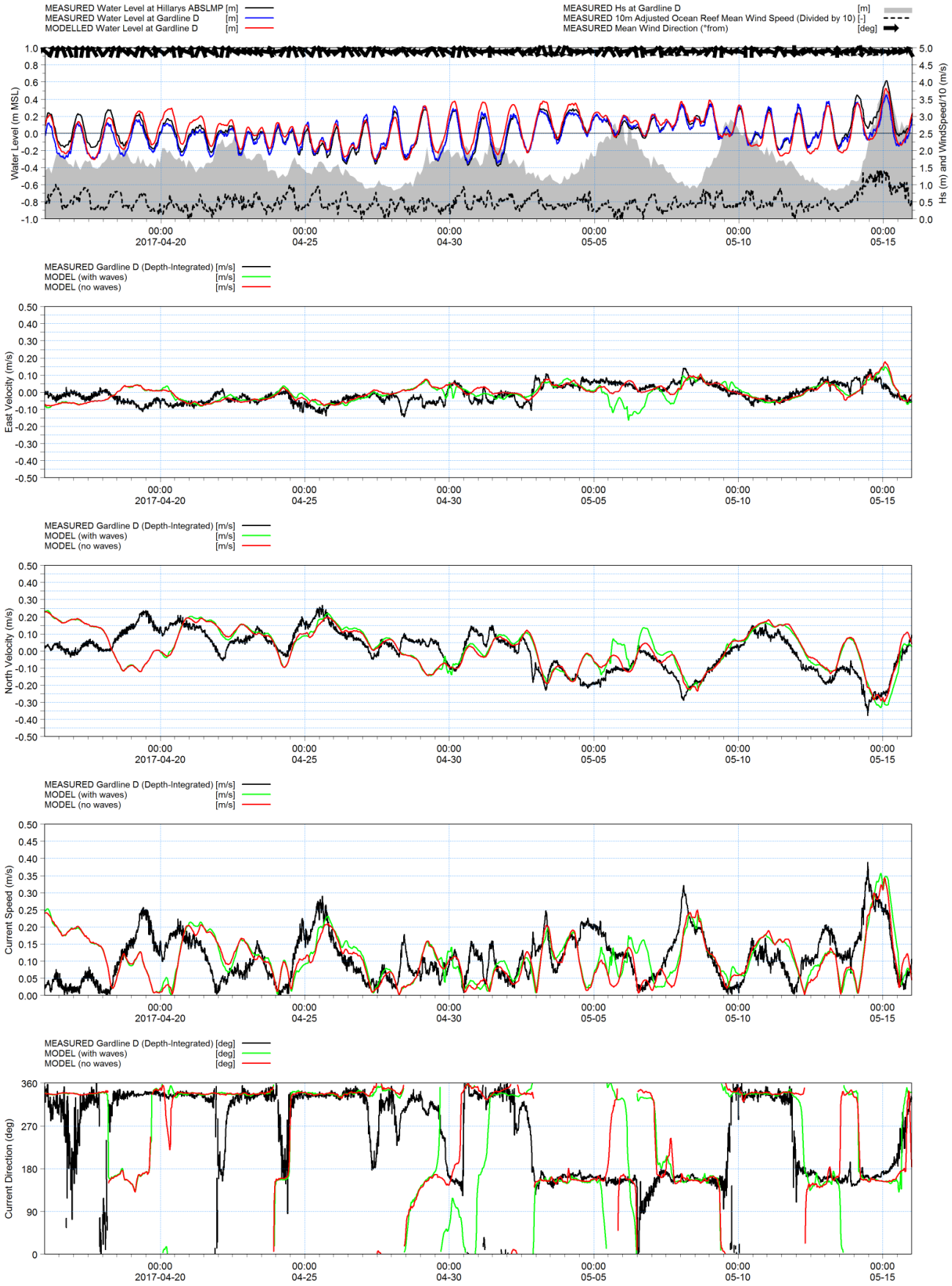

Figure A1-4a: Local 3D Hydrodynamic Model vs. Gardline D. Depth-integrated, Autumn 2017.

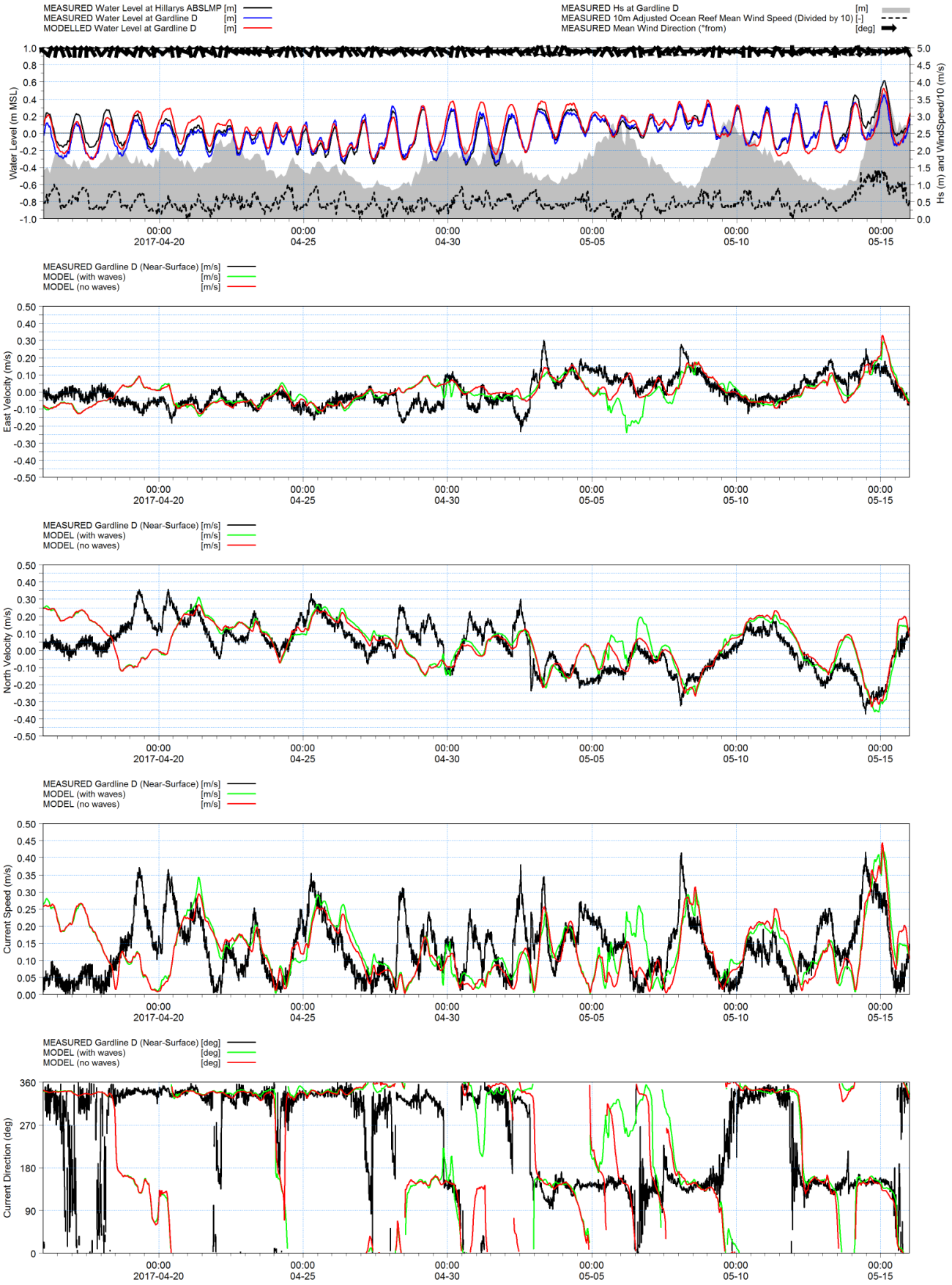

Figure A1-4b: Local 3D Hydrodynamic Model vs. Gardline D. Surface, Autumn 2017.

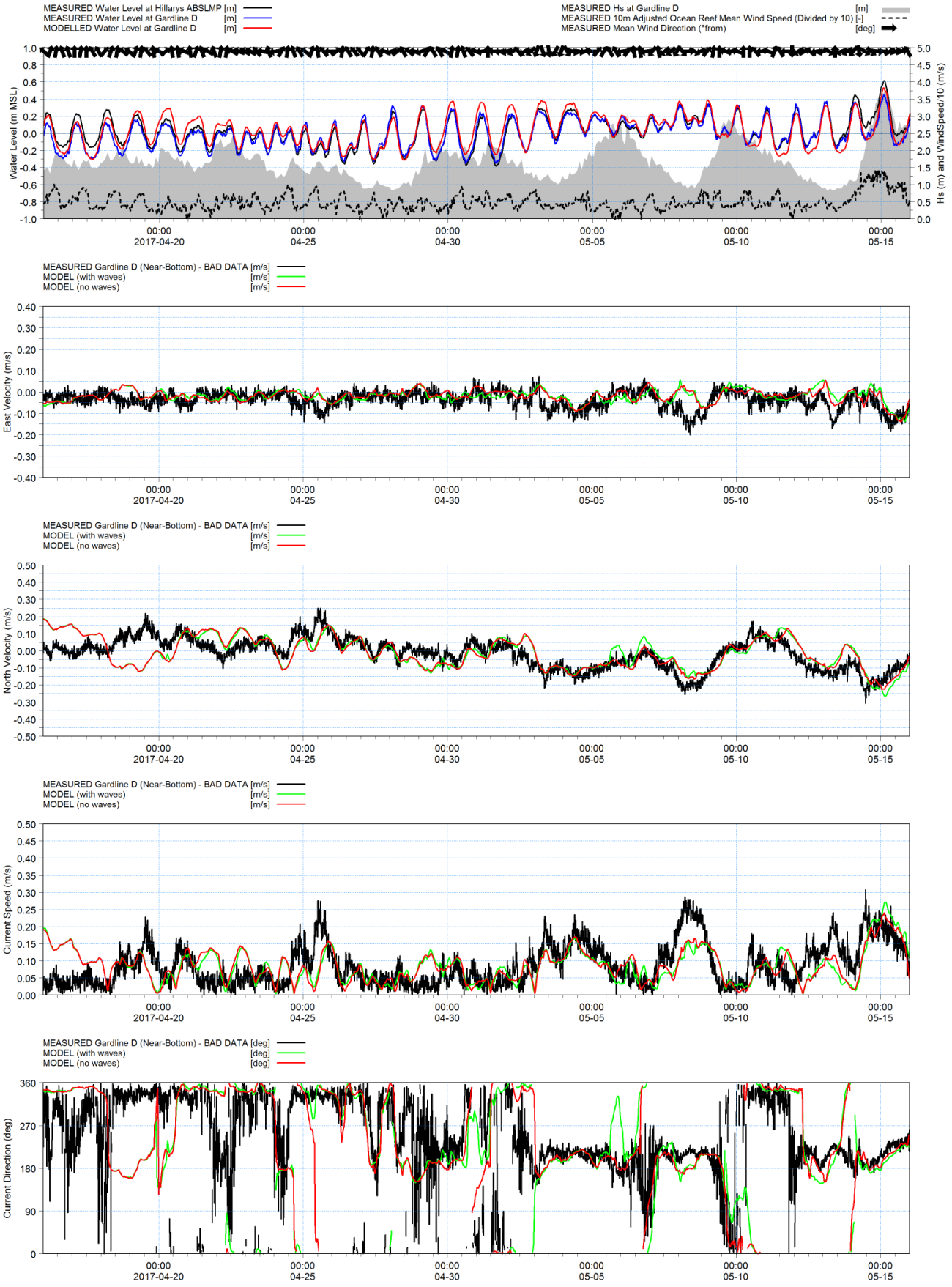

Figure A1-4c: Local 3D Hydrodynamic Model vs. Gardline D. Bottom, Autumn 2017.